CONCURRENT NEUROLOGICAL AND BEHAVIORAL ASSESSMENT OF NUMBER LINE ESTIMATION PERFORMANCE IN CHILDREN AND ADULTS

by

Joseph M. Baker

A dissertation submitted in partial fulfillment
of the requirements for the degree

of

DOCTOR OF PHILOSOPHY

in

Psychology

Approved:

Kerry E. Jordan, Ph.D. Major Professor	Jamison Fargo, Ph.D. Committee Member
Ronald Gillam, Ph.D. Committee Member	Patricia Moyer-Packenham, Ph.D. Committee Member
Timothy A. Shahan, Ph.D. Committee Member	Mark R. McLellan, Ph.D. Vice President for Research and Dean of the School of Graduate Studies

UTAH STATE UNIVERSITY
Logan, Utah

2013

Copyright © Joseph M. Baker 2013

All Rights Reserved

ABSTRACT

Concurrent Neurological and Behavioral Assessment of Number Line Estimation Performance in Children and Adults

by

Joseph M. Baker, Doctor of Philosophy

Utah State University, 2013

Major Professor: Kerry E. Jordan, Ph.D.
Department: Psychology

Children who struggle to learn math are often identified by their poor performance on common math learning activities, such as number line estimations. While such behavioral assessments are useful in the classroom, naturalistic neuroimaging of children engaged in real-world math learning activities has the potential to identify concurrent behavioral and neurological correlates to poor math performance. Such correlates may help pinpoint effective teaching strategies for atypical learners, and may highlight instructional methods that elicit typical neurological response patterns to such activities. For example, multisensory stimulation that contains information about number enhances infants' and preschool children's behavioral performance on many numerical tasks and has been shown to elicit neural activation in areas related to number processing and decision-making. Thus, when applied to math teaching tools, multisensory stimulation may provide a platform through which both behavioral and neural math-related processes may be enhanced.

Common approaches to neuroimaging of math processing lack ecological validity and are often not analogous to real-world learning activities. However, because of its liberal tolerance of movement, near-infrared spectroscopy (NIRS) provides an ideal platform for such studies. Here, NIRS is used to provide the first concurrent examination of neurological and behavioral data from number line estimation performance within children and adults. Moreover, in an effort to observe the behavioral and neurological benefits to number line estimations that may arise from multisensory stimulation, differential feedback (i.e., visual, auditory, or audiovisual) about estimation performance is provided throughout a portion of the task.

Results suggest behavioral and neural performance is enhanced by feedback. Moreover, significant effects of age suggest young children show greater neurological response to feedback, and increase in task difficulty resulted in decreased behavioral performance and increased neurological activation associated with mathematical processing. Thus, typical math learners effectively recruit areas of the brain known to process number when math activities become increasingly difficult. Data inform understanding typical behavioral and neural responses to real-world math learning tasks, and may prove useful in triangulating signatures of atypical math learning. Moreover, results demonstrate the utility of NIRS as a platform to provide simultaneous neurological and behavioral data during naturalistic math learning activities.

(161 pages)

PUBLIC ABSTRACT

Concurrent Neurological and Behavioral Assessment of Number Line Estimation Performance in Children and Adults

by

Joseph M. Baker, Doctor of Philosophy

Utah State University, 2013

Understanding the brain's response to common math-learning activities may help improve math education. For example, by imaging the brains of typically developing children and adults throughout a number line estimation task, it is possible to establish a baseline of what "typical" brains do in such situations. Thus, comparisons may be made to determine the degree to which brain functioning differs between typical and atypical math learners. Moreover, by identifying methods that may increase the brain's response to real-world math activities, it may be possible to improve the math learning process for typical and atypical learners alike.

Brain imaging devices such as fMRI are not well suited for real-world math learning tasks because they require participants to lay prone within the device and to minimize movement. Therefore, the tasks that participants complete are not always analogous to real-world math tasks, and often do not provide information about real-world math processing. Because of its liberal tolerance of movement and high temporal resolution, a brain-imaging technology known as near-infrared spectroscopy (NIRS) represents an ideal platform to make such assessments. Here, NIRS is used to assess

concurrent behavioral and neural responses to a common math-learning activity in which behavioral performance has previously been shown to correlate significantly with success in mathematics: the number line task. Also, by providing different types of performance feedback (i.e., visual, auditory, or audiovisual) throughout a portion of the task, we are able to determine whether feedback influences estimation performance as well as neurological responses.

The results of this study demonstrated that both behavioral and neurological responses are enhanced following feedback, and that such neurological responses are greatest in young children. Furthermore, we demonstrated that when number line estimations become more difficult, typically developing children increase activation in areas of the brain that are known to process number and math calculations. In sum, this study provided evidence regarding how typically developing children and adults process number line estimations. In addition, this is the first study to demonstrate such patterns of activation during a number line task, further justifying the use of NIRS in conducting brain imaging assessments of real-world math learning tasks.

ACKNOWLEDGMENTS

To begin, I would like to thank my family. I could never imagine reaching such an important milestone in my life without their support. Joy, I love you so much and I thank you for being such a wonderful partner. I look forward to our life together. Dad, thank you for teaching me the value in hard work and keeping my "nose to the grindstone." Mom, I will forever cherish the constant love and support you have always provided. Sarah, I cannot imagine having a stronger and more supportive sister. Gunner, you have such a wonderful family around you.... I cannot wait to read your dissertation one day! Peggy and Greg, I love you both very much and I thank you for being such a positive source in Joy's and my life.

I will never forget my time in Logan, and in large part that is because of the great friends that I have had the pleasure of making part of my life. Colin, party later? And remember...fear is the mind killer! Adam, do not ever lose your pep and vibrant attitude. Andy, I will never have a better hug. Eric, your homebrew was always fantastic. Nick, Anyang! And to anyone else who I am missing, I have really enjoyed knowing you all and I wish everyone the very best.

Finally, there are so many fantastic professors at USU who I have had the pleasure of working with and learning from. Thank you Jamison, Patricia, and Tim for being such great committee members. Ron, you were absolutely instrumental in beginning my career in cognitive neuroimaging, and for that I will always be grateful.

Kerry, thank you for being a fantastic advisor and for teaching me all that you have. I have learned more from you than I can express.

Joseph M. Baker

CONTENTS

Page

LIST OF TABLES

Table Page

LIST OF FIGURES

CHAPTER I

INTRODUCTION

Investigating the development of human numerical knowledge can potentially transform instructional practices in mathematics. For example, multisensory numerical information enhances infants' and preschool children's representation of number (Jordan & Baker, 2011), and may also enhance the effectiveness of teaching tools. Moreover, assessment of concurrent behavioral and neural responses to real-world math learning activities is vital to understanding the signatures of effective math learning, and may also prove useful in informing instructional practices as well as triangulating signatures of atypical math learning. Emergent neuroimaging technologies such as near-infrared spectroscopy (NIRS), which because of its liberal tolerance of movement and high temporal resolution now enable researchers to assess such concurrent responses in naturalistic learning environments. This project thus combined the use of multisensory numerical information and NIRS in order to observe concurrent behavioral and neural activation patterns in young children and adults throughout a math-learning activity commonly used in the classroom: the number line task.

Children's ability to accurately estimate number line proportions (e.g., 15 out of 100) correlates significantly with success on standardized assessments of math achievement (Siegler & Booth, 2004). As number lines represent a common math-learning activity, much effort has been made to facilitate accurate number line estimation performance throughout instruction (Opfer & Seigler, 2007; Siegler & Booth, 2004; Thompson & Opfer, 2010). In practice, number line estimations are made by identifying

the point on a line that identifies a target values within a given scale. For example, a teacher may provide a student with a line that represents 1,000, and ask him to identify where 150 goes. In this case, each point from 0 to 1,000 can be represented on the line, such that each value is equidistant from the next. When a child's estimation locations are plotted as a function of the actual location of a value within the scale, a linear function indicates that the child accurately represents the spatial distribution of values along the number line. Alternatively, a nonlinear (e.g., logarithmic) function indicates that the child does not comprehend the spatial distribution of values within the scale (see Figure 1). A common problem that leads to inaccurate number line estimations is misunderstanding this number-to-scale relationship as the two values increase proportionately in magnitude (e.g., 15:100 :: 150:1000). Therefore, identifying methods that effectively highlight the

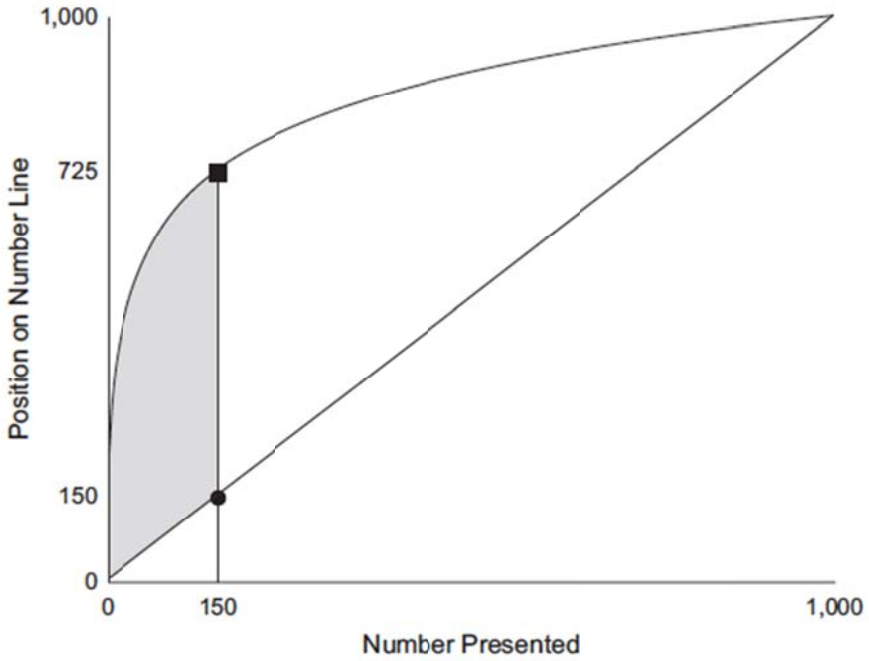

Note. Overestimation of numbers near the low end of the scale yields a logarithmic response function.

Figure 1. Linear and logarithmic number line estimation functions.

number-to-scale relationship across increasingly larger scales has been the focus of many efforts that intend to improve this ability in children (Opfer & Seigler, 2007; Siegler & Booth, 2004; Thompson & Opfer, 2010).

One approach that remains untested insofar as improving number line estimation accuracy, but which has proven successful in enhancing representations and discriminations of many continuous quantities is intersensory redundancy (Bahrick & Lickliter, 2000). The term "intersensory redundancy" describes the temporally and spatially synchronous presentation of information about a property across two or more sensory modalities. For example, when a child watches a ball bounce on the ground, he is receiving information about the number of bounces visually (i.e., watching the bounces) and auditorily (hearing the bounce off of the ground) simultaneously in time and space. In this case the visual and auditory information are said to be redundant because they are both providing identical information about number. It is hypothesized that intersensory redundancy selectively recruits attention to bimodally specified stimulus properties (e.g., number, tempo, rhythm, etc.), which enhances psychophysical discrimination of these amodal properties at the expense of modality-specific properties (e.g., orientation, color, pitch, etc.; Bahrick & Lickliter, 2000; Lewkowicz, 2004; Lewkowicz & Kraebel, 2004; Raposo, Sheppard, Schrater, & Churchland, 2012). Conversely, information experienced in one sensory modality alone selectively recruits attention to modality-specific properties of events (at the expense of bimodally specified properties; Bahrick & Lickliter, 2000; Bahrick, Lickliter, & Flom, 2004).

Intersensory redundancy presented in such common media as board games may play a role in improving children's number line estimations (Ramani & Siegler, 2008;

Siegler & Ramani, 2008). For example, in the board game "Chutes and Ladders," the number in a given square on the board coincides with the number of movements required to reach it, the number of words the child will say and hear as he moves across the board, the distance of the square from the origin, and the time it takes for the child to reach his destination on the board (Siegler & Mu, 2008). This redundant quantitative information may contribute to the subsequent improvement in children's number line estimation and magnitude comparisons (Ramani & Siegler, 2008; Siegler & Ramani, 2008).

Based on these findings, it is possible that providing redundant multisensory feedback within a typical number line estimation task (e.g., through audio-visual correspondence of estimation locations on the line) will improve children's number line estimations to a greater degree than unisensory feedback. For example, if each point on a visual line coincides with a tone of a particular intensity (i.e., volume), such that the intensity increases linearly as one travels from left to right across the number line, each spatial location is then represented both visually and auditorily. Thus, feedback about estimation performance provided in this manner may be more effective at enhancing future estimations than either visual or auditory feedback presented in isolation. That is, synchronous audio-visual feedback about proportion may selectively recruit attention to the spatial relationship between number and scale, and may thus enhance future estimations. This finding may have far reaching implications for mathematics instruction: as virtual mathematics teaching tools become ever more present in today's classroom (Cannon, Heal, Dorward, Duffin, & Edwards, 2010; Moyer-Packenham & Westenskow, in press), substituting the already commonly used visual number line teaching tool with a computerized version that provides redundant multisensory feedback may enhance

children's proportional judgment abilities (i.e., number line estimation accuracy) and may thus improve their mathematics learning experience. Moreover, taken together with recent neurological evidence that identifies locational differences in processing of number related stimuli between different aged children (i.e., second and third graders) (Rosenberg-Lee, Barth, & Menon, 2011) as well as neurological plasticity that results from disparate instruction methods (Delazer et al., 2005), it is possible that children of different ages and who received different feedback will display divergent cortical-level processing.

For example, given the same math problem, second-grade children have been shown to elicit greater working memory processes compared to their third-grade counterparts, while third-grade children elicited greater intraparietal activity (Rosenberg-Lee et al., 2011). Ostensibly, this difference arises due to superior math performance in the third compared to second-grade children, and thus a greater reliance on working memory for second-grade children. These working memory processes manifest largely, although not exclusively, as activity in the prefrontal cortex (PFC), whereas efficient processing of number and number-related processes, including navigation of the mental number line (Hubbard, Piazza, Pinel, & Dehaene, 2005), occurs primarily in the intraparietal regions (i.e., parietal lobe) of the brain (Dehaene, Piazza, Pinel, & Cohen, 2003). Therefore, third-grade children process math problems more "efficiently," insofar as the neural regions recruited, than second-grade children. Similar locational "shifts" in neurological activity (i.e., plasticity) between the frontal and parietal lobes of the brain have been shown to occur as a result of both the difficulty of a given mathematics operation (Delazer et al., 2003; Rosenberg-Lee et al., 2011) and instruction type for

solving a mathematics operation (Delazer et al., 2005). While it remains untested, I hypothesize that similar changes in neurological activity will occur when second- and third-grade children and adults perform number line estimations across increasingly larger scales. For example, I predict that third-grade children will easily estimate values within a small scale (e.g., 100), and will thus engage relatively little working memory processes. As this scale increases (e.g., 100,000), so too will their reliance on working memory processes, which will be observable by NIRS as an increase in PFC activation. Behaviorally, this increased activation in the PFC will be accompanied by greater error in the children's number line estimations. Furthermore, I hypothesize that similar effects will occur within adults while they engage in estimation within extremely large estimation scales (e.g., billion and quadrillion).

While previous literature suggests that adults accurately estimate number line locations across all scales, extant pilot data suggest that estimations on extremely large scales made under time pressure elicit errors that increase in magnitude and variability as the scale increases. Similar to children, I hypothesize that adults will recruit greater PFC activity throughout extremely large scale estimations, while greater intraparietal activation will be observed throughout smaller scale estimations. Finally, I hypothesize that redundant intersensory feedback (i.e., correction of initially inaccurate estimations through both visual and auditory stimulation) about estimation performance will enhance estimation accuracy and facilitate functional changes in neurological activation patterns such that estimations will be accomplished more efficiently, and will thus recruit intraparietal regions to a greater degree following multisensory feedback. Conversely, I predict that unisensory feedback will enhance number line estimation performance to a

lesser degree than multisensory feedback, and thus greater amounts of hemodynamic activity in the PFC will be observed as scales increase relative to multisensory feedback.

Improving Number Line Estimations

Children's representation of number is a hotly debated topic. Behavioral evidence from number line estimation tasks, in which children estimate the position of a number on a line of a given scale (e.g., 15 out of 100), indicates that children may rely on approximate logarithmic representations of number early on in development then come to rely more heavily on accurate linear representations of number as they develop and gain experience throughout the educational process (Booth & Siegler, 2006; Laski & Siegler, 2007; Siegler & Booth, 2004; Siegler & Opfer, 2003). Booth and Siegler argued that this pattern of behavior as indicative of an overall shift in children's internal representation of number throughout development. Evidence for representational shift accounts come from the number line estimations of children across increasingly larger scales—estimations on small scales (e.g., 15 out of 100) are accurate and fall on a perfect diagonal slope such that $y = x$. However, as the scale is increased proportionately (e.g., 150 out of 1,000), children tend to overestimate the correct location of estimations within the scale such that a logarithmic function is apparent when their estimations are plotted (see Figure 1). This linear-to-log shift that results from scale increases is thought to represent children's reliance on an intuitive logarithmic internal number line to estimate on unfamiliar scales (Dehaene, Izard, Spelke, & Pica, 2008). As children gain greater experience with increasingly larger scales their estimations become more linear, thus providing evidence that their internal representation of number becomes more linear with development. The

theory of poverty of input describes this tendency directly (Dehaene & Mehler, 1992). In short, this theory predicts that lack of experience is the sole reason that estimations are inaccurate, and once sufficient input about a scale is acquired estimations become accurate.

Variations on theories that posit multiple representations have also suggested that children may concurrently possess a variety of approaches (i.e., strategies, rules, or representations) that compete with one another for use when solving problems such as number line estimations (Opfer & Siegler, 2007; Siegler, 1996). As children develop they learn the appropriateness of each approach for each type of problem and begin to choose the most appropriate approach most often. As a result of this learning process the child's numerical performance improves (i.e., becomes more linear). However, if a child fails to learn the appropriateness of one approach over another, his performance will not change, leading to older children and adults sometimes continuing to use approaches that are typical of young children (i.e., logarithmic estimations).

Opponents of the representational shift hypothesis argue that improvements in number line estimations are instead attributed to enhanced judgments of proportion, as opposed to alterations in internal representations of number (Barth & Paladino, 2011; Ni, 2000). In short, while number and number line estimations are similar insofar as both involve numerical representations, number line estimations are essentially judgments of proportion because any such estimation cannot be made for a given digit without constraining it in proportion to a given scale (Barth & Paladino, 2011). Therefore, number line estimations may become more accurate with development, but this does not imply a shift in internal representations of number so much as greater proportional

estimation abilities. However, behavioral and neurological data alike link judgments of both number and proportion together during number line estimations (Hubbard et al., 2005).

No matter the exact nature of internal representations of number line estimations, the fact is that accurate performance correlates highly with performance in mathematics (Booth & Siegler 2006, 2008; Siegler & Booth, 2004). Facilitating accurate number line estimations has thus long been a priority for educators and psychologists alike. Often, children's inaccurate (i.e., logarithmic) number line estimations arise from a lack of understanding about the number-to-scale relationship as the two increase proportionately. That is, children may not understand that the point on a line at which 15 out of 100 lies is the same point at which 150 out of 1,000 lies, and so on. A firm understanding of this relationship as demonstrated by accurate number line estimations translates to a better understanding of the structure of our decimal system in general, which is important when engaging in mathematics. Therefore, highlighting this scalar relationship between number and scale is both important and difficult. Many techniques have been developed to highlight this relationship across scales, including progressive alignment (Gentner, Lowensterin, & Hung, 2007; Kotovsky & Gentner, 1996; Thompson & Opfer, 2010) and analogy (Opfer & Siegler, 2007). Progressive alignment allows children to make similarity comparisons over concrete, perceptual similarities such as monotonic increases in size across differently shaped stimuli, which facilitates their ability to notice higher order relational commonalities across stimuli that possess fewer surface-level features in common (Kotovsky & Getner, 1996). Similarly, analogies (e.g., loaf of bread : single slice of bread :: lemon : _____?) have been used to highlight consistencies across

disparate stimuli in the hopes that the connections between dissimilar objects will generalize to tasks such as number line estimations across scales (Abdellatif, Cummings, & Maddux, 2008). Alternatively, proportional judgment accounts posit that providing children with "landmarks," such as where 15 out of 100 would fall on a given line, allows them to readjust their estimations relative to the landmark and thus brings them closer to linearity (Barth & Paladino, 2011).

For the present proposal, the exact mechanisms underlying children's improvement in number line estimations across scales (e.g., shift in numerical representation vs. proportional judgment enhancement) is not of immediate importance. As discussed below, representations of both number and proportions are linked because of overlapping parietal circuits for representation of magnitudes such as number and attention to external space (Hubbard et al., 2005). Given this neurological overlap, I hypothesize that intersensory redundancy, which enhances the processing of number and other magnitudes will similarly enhance number line estimations.

Neural Correlates of Numerical and Spatial Representations

A wealth of neurological evidence implicates the intraparietal regions of the brain as being involved in both number and spatial processing (Hubbard et al., 2005). Individual circuits have been identified for many types of numerical processing. For example, patients suffering trauma to the inferior intraparietal region often demonstrate selective impairment in representing numerical quantities. Lesions in this region within the language dominant left hemisphere often cause number processing deficits ranging from impairment of numerical comprehension, production, and calculation (Cipolotti,

Butterworth, & Denes, 1991) to calculation specific impairments (Dehaene & Cohen, 1997; Takayama, Sugishita, Akiguchi, & Kimura, 1994; Warrington, 1982). Importantly, these patients generally remain capable of identifying non-numerical ordinal relationships (e.g., correctly ordering the days of the week) and bisecting non-numerical stimuli (e.g., "What day is between Monday and Wednesday?"). This double dissociation between order and number meaning suggests that the two are separable and processed at least semi-independently (Turconi, 2002).

Similarly, children with developmental dyscalculia, a condition that affects approximately 5% of children who exhibit normal intelligence but present a specific and persistent difficulty with calculation and mental arithmetic, possess various structural and functional alterations in the left intraparietal sulcus (IPS) and the PFC (Isaacs, Edmonds, Lucas, & Gadian, 2001). Children with dyscalculia have less grey matter in the left IPS, tend to have less right-parietal grey matter, and have grey matter abnormalities in regions of the PFC (Rotzer et al., 2008). Furthermore, a functional neuroimaging study of developmental dyscalculia found that children with dyscalculia did not have abnormalities in brain activation during number-comparison or calculation, but did show lower overall activation during approximate calculation in regions of the PFC and IPS (Kucian et al., 2006). Astonishingly, Cohen-Kadosh and colleagues (2007) found that virtually and temporarily lesioning the right parietal cortex in healthy adults by means of transcranial magnetic stimulation significantly impaired automatic number processing, implicating the right IPS as the region that is crucial for the automatic activation of numerical magnitude.

Single-cell recording studies in the brains of nonhuman primates have also

directly implicated the IPS and PFC in numerical representations (Nieder, Freedman, & Miller, 2002; Nieder & Miller, 2004). Specific populations of neurons in both locations preferentially fire during the presentation of a particular numerosity. These number-specific cells effectively represent cardinal values, or specific places on the 'mental number line' (Dehaene, 2011). Moreover, Tudusciuc and Neider (2007) demonstrated that length and numerosity were similarly encoded by functionally overlapping groups of parietal neurons, and that the activity of populations of quantity selective neurons contained accurate information about both continuous and discrete quantity. These findings have major implications for our ability to perform mathematics, as they provide evidence of biological structures that bridge the gap between analog and discrete representations of number, both of which are integral in performing mathematics (Feigenson, Dehaene, & Spelke, 2004).

Neuroimaging studies provide perhaps the largest body of evidence to implicate the intraparietal regions in numerical processing. A review of fMRI studies investigating number-related processes reveals a tripartite organization of neural regions involved in numerical processing, including the IPS, the angular gyrus (AG), and the posterior superior parietal systems (Dehaene et al., 2003). The latter two areas are thought to be associated with broader functions than mere calculation (language-related processing and attentional processes, respectively). However, the IPS has been shown to be specifically responsive to number-related processes including mental arithmetic (Burbaud et al., 1999; Chochon, Cohen, van de Moortele, & Dehaene, 1999; Dehaene, Spelke, Pinel, Stanescu, & Tsivkin, 1999; Lee, 2000; Menon, Rivera, White, Glover, & Reiss, 2000; Pesenti, Thioux, Seron, & De Volder, 2000; Simon, Cohen, Mangin, Le Bihan, &

Dehane, 2002), number comparisons (Chochon et al., 1999; Cohen & Dehaene, 1996; Dehaene, 1996; Langdon & Warrington, 1997; Le Clec'H et al., 2000; Pesenti et al., 2000; Pineal, Dehaene, Riveiere, & Le Bihan, 2001; Rosselli & Ardila, 1989; Seymour, Reuter-Lorenz, & Gazzaniga, 1994; Thioux, Pesenti, De Volder, & Seron, 2002), category specific representation and processing of number (Dehaene, 1995; Le Clec'H et al., 2000; Pesenti et al., 2000; Thioux et al., 2002), parametric modulation of number (Dehaene, 1996; Kiefer & Dehaene, 1997; Piazza, Mechelli, Butterworth, & Price, 2002a; Piazza, Mechelli, Price, & Butterworth, 2002b; Pinel et al., 2001; Stanescu-Cosson et al., 2000), and unconscious quantity processing (Dehaene, 1992, 1997; Dehaene, Dehaene-Lambertz, & Cohen, 1998; Dehaene & Marques, 2002; Naccache & Dehaene, 2001). Moreover, responses in the parietal cortex are greater for numerical value than for other stimulus dimensions (Castelli, Glaser, & Butterworth, 2006; Dehaene & Cohen, 1997; Eger, Sterzer, Russ, Giraud, & Kleinschmidt, 2003; Naccache & Dehaene, 2001; Piazza, Izard, Pinel, Le Bihan, & Dehaene, 2004; Pinel, Piazza, Le Bihan, & Dehaene, 2004). However, as noted below, the intraparietal regions of the brain are also responsive to other continuous properties outside of number, such as size and luminance (Cohen-Kadosh, Cohen-Kadosh, & Henik, 2008; Pinel et al., 2004).

Importantly, activity in the IPS adheres to psychophysical predictions seen in number-related behaviors such those predicted by Weber's Law (Cantlon et al., 2009). For example, discrimination of numerical representations in the parietal cortex, at the neural level, is ratio dependent (Nieder, Diester, & Tudusciuc, 2006; Nieder & Miller, 2004; Piazza et al., 2004; Pinel et al., 2001, 2004). Numerical ratio effects manifest as increased blood-oxygen-level-dependent (BOLD) contrasts to numerical values at fine

relative to crude ratios (Cantlon et al., 2009). In other words, greater hemodynamic fluctuations in oxygen levels occur in response to large compared to small ratios indicating greater mental activity as the ratio between stimuli approaches 1:1. This effect holds for numerical values presented in various notations including Arabic numerals, number words, and arrays of dots (Cohen-Kadosh et al., 2007; Piazza, Pinel, Le Bihan, & Dehaene, 2007), as well as for mathematic fractions (Jacob, Vallentin, & Neider, 2012). Each of these studies has identified a numerical ratio effect in BOLD activity during passive viewing of numerical stimuli without an explicit behavioral task. Furthermore, single-cell recording of number neurons in nonhuman primates has demonstrated that logarithmic plotting of the neurons' activation assumes a Gaussian distribution about the numerical input, which is predicted by a logarithmic account (Nieder & Miller, 2004). These results support the assertion that the mental number line is logarithmic, which is predicted by Weber's Law (Dehaene et al., 2003).

Internal representations of number are thought to maintain a distinct spatial organization that is determined by the culture in which an individual develops. While studying the Mundurucu, an Amazonian indigene group with a reduced numerical lexicon and little or no formal education, Dehaene and colleagues (2008) demonstrated that Mundurucu adults mapped symbolic and nonsymbolic number onto a logarithmic scale, while Western adults mapped small or symbolic numbers linearly and non-symbolic numbers logarithmically. These findings suggest that the mapping of numbers onto space may be a universal practice and that this initial intuition of number is logarithmic. Moreover, these findings suggest that the concept of a linear number line may be a cultural invention that fails to develop in the absence of formal education (Dehaene et al.,

2008). The assertion that humans possess a mental number line is supported by many behavioral studies that demonstrate various numerical-spatial interactions (Calabria & Rossetti, 2005; Dehaene, Bossini, & Giraux, 1993; Denys et al., 2004; Fias, Brysbaert, Geypens, & D'ydewalle, 1996; Fias, Lauwereyns, & Lammertyn, 2001; Fischer, 2001; Fischer, Castel, Dodd, & Pratt, 2003; Hubbard et al., 2005; Lammertyn, Fias, & Lauwereyns, 2002), and was first proclaimed by Sir Francis Galton who documented that to most people, numbers seemed to occupy very precise locations in space (Galton, 1880a, 1880b). Furthermore, neurological evidence in nonhuman primates implicates the IPS in various types of spatial cognition as well (Hubbard et al., 2005). Intraparietal regions including the lateral (Astafiev et al., 2003; Ben Hamed, Duhamel, Bremmer, & Graf, 2001; Medendorp, Goltz, Crawford, & Vilis, 2005; Sereno, Pitzalis, & Martinex, 2001), ventral-intraparietal (Bremmer, Schlack, Duhamel, Graf, & Fink, 2001a), and anterior-intraparietal regions (Binkofski et al., 1998; Bonda, Petrides, Frey, & Evans, 1995; Buccino et al., 2001; Chao & Martin, 2000; Culham et al., 2003; Grefkes, Weiss, Zilles, & Fink, 2002; Muhlau et al., 2005; Shikata et al., 2003) are directly involved in processing of events in space. The lateral-intraparietal region is active during saccadic eye movements and is thought to play a role in actively attending to peripheral targets (Astafiev et al., 2003). The ventral-intraparietal region responds selectively to motion in space within any sensory modality (Bremmer et al., 2001b), and the anterior-intraparietal region is involved in fine motor movements and grasping in space (Binkofski et al., 1998; Culham et al., 2003; Shikata et al., 2003). This overlap of neural structures related to processing of both number and space is thought to account for the behavioral interactions between representations of number and space (Hubbard et al., 2005; Walsh, 2003).

The lateral intraparietal region has been implicated in mediating shifts in attention across the mental number line as well as the external world (Hubbard et al., 2005). Direct involvement of the lateral-intraparietal region in both numerical and spatial cognition could explain many of the numerical-spatial interactions cited above, and provides a feasible biological bridge between number and spatial representations that number line estimations require. For example, the spatial-numerical association of response codes (SNARC) effect refers to the common finding that subjects respond more quickly to larger numbers if the response is on the right side of space, and to the left for smaller numbers, which indicates automatic spatial-numerical associations. Interestingly, the lateral-intraparietal region remains active even when attempts are made to disrupt the SNARC effect, such as by crossing hands. For example, Dehaene and colleagues (1993) required one group of subjects to use their right hands to respond to small values, and left hands to respond to large values. A reversal of the SNARC effect in this condition could indicate a dependence of the effect on the hand performing the response, thereby suggesting a hemispheric dominance effect. However, subjects in this condition demonstrated standard SNARC effects, thus indicting that the interaction between numerical magnitude and left-right spatial coordinates occurs at the level of a more abstract representation of the left-right axis. These findings have led many to theorize that consultation of the mental number line is akin to viewing a physical number line on paper. That is, we maintain an "eye-centered" spatial representation in the lateral-intraparietal region that is unaffected by attempts to disrupt the effect (Dehaene et al., 1993). Taken together, the neurological evidence described above highlights the important role that the intraparietal regions of the brain play in representing number and

space. As described below these same regions are highly involved in processing of crossmodal (i.e., intersensory) stimuli (Lewkowicz & Ghazanfar, 2009), and ultimately help give rise to humans' ability to perform symbolic mathematics (Rosenberg-Lee et al., 2011).

Finally, recent evidence has demonstrated that neurological processing of fractions and proportions is accomplished within many of the same PFC and intraparietal areas in which whole numbers are processed. By habituating participants to a constant fraction, Jacob and colleagues (2012) identified significant increases in neural activity within the PFC and intraparietal regions when deviant fractions were displayed. Moreover, this increase in activity escalated in proportion to the numerical distance between the constant and deviant fractions, indicating adherence to Weber's Law (Jacob & Neider, 2009; Jacob et al., 2012). Thus, the same regions that are involved in numerical, mathematical, and spatial processing are also implicated in processing of fractions.

How Intersensory Redundancy Enhances Psychophysical Sensitivity

Importantly, the neurological correlates described above coincide with psychophysical predictions such as Weber's Law: discrimination of two continuous quantities is dependent on the ratio between them, such that as this ratio approaches 1:1 discrimination suffers. Nieder and Miller (2004) demonstrated that both behavioral and neurological representations of number in the PFC of rhesus monkeys are best described by nonlinearly compressed scaling of numerical information, as postulated by Weber's Law. In short, activity of a number specific neuron is highest for the number to which it

is tuned and decreases in activity as the numerical input becomes more distant from the tuned value (Cordes, Gelman, & Gallistel, 2001). The behavioral sensitivity of an organism (i.e., its ability to discriminate disparate quantities) is driven by the accuracy (i.e., lack of scalar variance) of its psychophysical representations.

This relationship between psychophysical sensitivity and discrimination accuracy is not trivial. For example, Halberda, Mazzocco, and Feigenson (2008) identified a significant correlation between approximate number discrimination and math achievement. Fourteen-year-old children's discrimination performance on an approximate number discrimination task correlated with standardized mathematics test scores as far back as kindergarten, and was not driven by differences in other cognitive and performance factors (Halberda et al., 2008). The authors argue that individual differences in approximate number discrimination acuity might give rise to individual differences in math ability. Importantly, this finding has recently been extended to college-entrance examination scores (Libertus, Odic, & Halberda, 2012). Similarly, Siegler and Booth (2004) identified a significant correlation between individual differences in number line estimations and math achievement scores in 6- to 8-year-old children. The correlation between psychophysical sensitivity and academic performance is very important and while any possible causal relationship between these correlations remains unidentified, it is clear that greater accuracy in discrimination of continuous quantities is positively correlated with performance in school mathematics. Importantly, we know from studies of intersensory redundancy that the way in which information about continuous quantities is presented can change discrimination performance.

Discrimination of many analog properties is enhanced by the way in which

information about the property is provided. The intersensory redundancy hypothesis (Bahrick & Lickliter, 2000) describes the tendency for discriminations of analog properties to be enhanced following synchronous and redundant sources of information about the property from different modalities (Bahrick, Flom, & Lickliter, 2002; Flom & Bahrick, 2007; Lewkowicz & Lickliter, 1994). For example, 5-month-old infants are able to differentiate between two complex rhythms when they are presented bimodally, but not unimodally (Bahrick et al., 2002). Similarly intersensory redundancy in the form of synchronized vocalizations and object motion facilitates learning of arbitrary speech-object relations in 7-month-old infants, which is not facilitated by unisensory stimulation (Gogate & Bahrick, 1998). In relation to numerical processing, intersensory redundancy, and even *intra*sensory redundancy to some extent, enhances 6-month-old infants' numerical discrimination abilities to levels typically not seen until 9 months of age. That is, synchronous audiovisual information about number allows infants to successfully discriminate a 2:3 (e.g., 8 vs. 12) ratio of ball bounces, whereas unisensory information limits them to 1:2 (e.g., 8 vs. 16) ratio discriminations (Jordan, Suanda, & Brannon, 2008). Concerning intrasensory redundancy, recent data suggest that multiple sources of information from within the same sensory modality, such as dual visual cues to stimulus change in the form of proportionately identical changes in number and size, have been shown to enhance discrimination abilities in 6-month-old infants (Baker & Jordan, in press). Infants were capable of discriminating a 2:3 difference in the number of bounces of a ball when the number change coincided with a 2:3 change in the size of the ball. Moreover, pre-school aged children in a numerical delayed match to sample task in which they receive multiple unisensory (audio or visual) and multisensory (audiovisual)

trials perform more accurately and demonstrate more linear representations on multisensory compared to unisensory trials (Jordan & Baker, 2011).

What are the mechanisms that underlie benefits to discrimination by multisensory stimulation? The enhancing effects described by the intersensory redundancy hypothesis are thought to arise from an attraction to multisensory stimuli that contributes in critical ways to perceptual development (Lewkowicz & Ghazanfar, 2009). Because our environment is wrought with multiple stimuli, many of which occur in concert and potentially provide a good deal of information (e.g., the sound of the car approaching along with its increasing retinal image size), our ability to integrate diverse multisensory perceptual attributes is crucial to our ability to extract coherent meanings from ubiquitous communicative signals. In general, there are two theoretical points of view that explain organisms' attraction to multisensory stimulation. The progressive framework theories suggest that organisms are either born with, or develop shortly after birth, the ability to perceive as a coherent whole multiple sensory cues that occur together in time. These theories posit that the large amounts of information inherent in multisensory cues attract infants' attention, and that our ability to perceive and extract information from these sources develops progressively throughout the first year of life. As infants age they come to rely less on low-level attributes of multisensory stimuli, such as synchrony, and begin to attend to higher-level multisensory cues such as facial expressions and affect (Lewkowicz & Ghazanfar, 2009).

While behavioral evidence consistent with the progressive framework theory has been found, emerging neurological evidence suggests that a separate *regressive* action may be occurring. Perceptual narrowing describes the tendency for organisms to begin

life with the ability to perceive and discriminate between a wide range of stimuli (e.g., vowels and consonants, faces, music, etc.), and slowly lose those abilities throughout development until only the most relevant stimuli (e.g., vowels and consonants from the infant's native language, faces of similar ethnicity, culturally relevant music, etc.) in the infant's environment are readily perceived and discriminated. This phenomenon of perceptual narrowing has been demonstrated for many stimuli, both unisensory (Best, McRoberts, LaFleur, & Silver-Isenstadt, 1995; Cheour et al., 1998; Chiroro & Valentine, 1995; Hannon & Trehub, 2005a, 2005b; Kelly et al., 2007, 2009; Kuhl, Williams, Lacerda, Stevens, & Lindblom, 1992; Kuhl, Tsao, & Liu, 2003; Pascalis, de Haan, & Nelson, 2002; Pascalis et al., 2005; Quinn et al., 2008; Sangrigoli, & de Schonen, 2004; Weikum et al., 2007; Werker & Tees, 1984), and importantly, multisensory (Lewkowicz & Ghazanfar, 2006; Lewkowicz, Leo, & Simion, 2010; Lewkowicz, Sowinksi, & Place, 2008; Lewkowicz & Turkewitz, 1980; Pons, Lewkowicz, Soto-Faraco, & Sebastian-Galles, 2009; Poulin-Dubois, Serbin, Kenyon, & Derbyshire, 1994) in nature. In short, perceptual narrowing is thought to occur because of strengthening of synaptic connections within neuronal circuits that are most active in the infants' perceptual environment throughout development.

The neurological underpinnings of multisensory processing are far from straightforward, although much effort has been made to understand the pathways and interactions amongst neuronal areas in relation to multisensory perception. Among the neurological areas most highly implicated in sensory convergence are the superior temporal sulcus (STS), the IPS, and the anterior cingulate (AC; Calvert, 2001). Furthermore, multisensory integrative cells, whose firing rate increases multiplicatively

when two or more sensory cues from different modalities appear in close temporal and spatial proximity, have been identified in many species including cats (Wallace, Meredith, & Stein, 1992; Wilkinson, Meredith, & Stein, 1996), rats (Barth, Goldberg, Brett, & Di, 1995), and monkeys (Duhamel, Colby, & Goldberg, 1991; Graziano & Gross, 1998; Mistlin & Perrett, 1990), indicating that similar biological processing of multisensory stimuli occurs in a diverse range of organisms. However, despite the presence of multisensory integrative cells, entire neural areas, rather than any individual site seem to be involved in the matching and integration of crossmodal inputs. For example, the STS is heavily implicated in the integration of complex featural information, particularly during the perception of audiovisual speech (Banati, Goerres, Tjoa, Aggleton, & Grasby, 2000; Callan, Callan, Kroos, & Vatlklotis-Bateson, 2001; Calvert, 2001; Calvert, Campbell, & Brammer, 2000; Raij, Utela, & Hari, 2001). The IPS appears to be specialized for synthesizing crossmodal spatial coordinate cues and mediating crossmodal links in attention (Banati et al., 2000; Bushara, Grafman, & Hallett, 2001; Bushara et al., 1999; Callan et al., 2001; Calvert, 2001; Eimer, 1999; Lewis, Beauchamp, & DeYoe, 2000; Macaluso, Frith, & Driver, 2000). Detection of temporal coincidences between crossmodal stimuli appears to be mediated in part by the predominantly subcortical posterior insula (Banati et al., 2000; Bushara et al. 2001; Calvert, 2001; Hadjikhani & Roland, 1998; Lewis et al., 2000). The involvement of the frontal cortex in multisensory integration is less understood, but seems to be involved in integrating newly acquired crossmodal associations, such that frontal areas may be recruited when associations between crossmodal cues are essentially arbitrary (Banati et al., 2000; Bushara et al., 2001; Callan et al., 2001; Calvert, 2001; Calvert et al., 2000;

Giard & Peronnet, 1999; Gonzalo, Shallice, & Dolan, 2000; Lewis et al., 2000; Raij et al., 2000).

These findings serve to underscore the fact that the brains of many organisms are specially equipped to handle multisensory information and that processing of this information is not relegated to any one area. Moreover, these findings further implicate the intraparietal and prefrontal regions as being directly involved in the processing of number, space, and now multisensory integration, each of which is integral to the current proposal. Concerning my hypothesized interaction between intersensory redundancy and number line estimations, these commonalities among neural regions are very important. Namely, number line estimations require a combination of numerical and spatial representations. Next, intersensory redundancy provides multisensory information that increases the salience of redundant quantitative properties. Because each of these properties (number and space) are processed at least in part in the intraparietal regions, it is possible that enhancing performance of any one process subserved by the intraparietal region by way of intersensory redundancy may enhance other processes (i.e., number and space) that the region is also responsible for processing, through overlapping circuitry. This claim is strengthened by behavioral evidence demonstrating enhanced discrimination of number and other continuous properties, which are also processed within the intraparietal regions of the brain, following intersensorily redundant stimulus presentation.

Neurological Plasticity of Number Processing

Neurological patterns in response to number and other quantitative stimuli are not

fixed. Much variation in these patterns occurs throughout development. For example, 3-month-old infants demonstrate similar scalp voltage topographies in response to numerical stimuli as adults and 4-year-old children, but differ slightly in the regions of activation when they are viewing changes in number (Izard, Dehaene-Labertz & Dehaene, 2008). By the age of 4, children exhibit a number-selective response in parietal cortex to numerical values expressed nonsymbolically (Cantlon, Brannon, Carter, & Pelphrey, 2006), and by the age of 5 children demonstrate neurological activity that is modulated by the difference between numerical values for Arabic numerals and arrays of dots (Temple & Posner, 1998). Similarly, Rosenberg-Lee and colleagues (2011) identified a significant shift in neurological processing of numerical stimuli within intelligence-matched children between grades 2 and 3. When asked to solve simple and complex two-operand addition problems that were age-matched for difficulty, second-grade children demonstrated greater reliance on the PFC compared to third-grade students. Conversely, with development came a global shift in activation towards the intraparietal region. Given the reliance on this region in numerical processing in adults, these data serve to implicate these years of schooling as a time in which this frontal-to-parietal shift may occur in response to simple mathematics problems. Moreover, similar developmental shifts towards a greater reliance on intraparietal regions have also been shown across a diverse range of ages and mathematical problem types such as subtraction and multiplication of single digits (Kawashima et al., 2004), approximate addition (Kucian, von Aster, Loenneker, Dietrich, & Martin, 2008), and mixed addition and subtraction problems (Rivera, Reiss, Eckert, & Menon, 2005). It is unknown if similar neurological patterns are present in second- and third-grade children when they are

engaged in number line estimations. However, given the similarities insofar as use of numerical representation and working memory processes between number line estimations and the math problems used in these studies it is possible that analogous neurological activity patterns when solving both problem types may be observed.

Moreover, both instruction type and method of presentation of numerical stimuli affect neurological response patterns. Delazer and colleagues (2005) trained adults to solve one set of math problems with a "training by drill" method (i.e., rote learning the result of two-operand problems), and a second set with a "training by strategy" method (i.e., applying an instructed algorithm to two-operand problems). The results demonstrated significantly greater reliance on the PFC for the drill method, whereas activity in the strategy method was primarily allocated to the intraparietal regions, indicating that the type of instruction modulates intraparietal activation during mathematical processing. Moreover, Delazer and colleagues identified a positive relationship between PFC activity and reaction time. The authors argue that greater use of the PFC during mathematical calculations is indicative of greater cognitive effort needed to solve the problems. Conversely, effective training methods, and hence dominant intraparietal activity throughout calculations and faster reaction times, are indicative of less cognitive effort. This conclusion also holds for a second study, which indicates that parietal activation is greater following processing of trained versus untrained multiplication problems, whereas the reverse is true for PFC activity (Delazer et al., 2003). These results indicate that, while it is possible to solve math problems when activity is primarily relegated to the PFC, less cognitive effort is expended when processing of mathematical information is relegated to the intraparietal region. Thus, it is

important to identify instructional strategies and methods that facilitate processing in the intraparietal region of the brain.

It remains to be seen if intersensory redundancy will facilitate differential frontal and parietal changes in neural activation. Therefore, imaging the brains of children and adults performing number line estimations will serve a dual role: I will be able to identify whether such neurological activation changes occur across age and scales when performing number line estimations, as well as determine the effect of intersensory redundancy on number line accuracy and its neurological correlates. Given previous findings demonstrating frontal-to-parietal shifts in neural activation between second- and third-grade aged children engaged in other numerical processes, it is predicted that I will observe similar hemodynamic fluctuations here. Also, recent pilot data demonstrating that adult's number line estimation errors positively correlate with rises in very large scales (e.g., billion and quadrillion) indicate that adults and children may be similar in their estimation abilities. As a result similar neurological patterns between the two age groups in response to both rises in scale and intersensory feedback may be present.

The Present Study

Number line estimations are an important indicator of children's understanding of number. Those children who perform accurately on number line estimations have a better understanding of the spatial distribution of number along their mental number line, and perform better in school mathematics than children who estimate poorly (Booth & Siegler, 2006; Siegler & Booth 2004). Because of this, much effort has been made to facilitate accurate number line estimation performance in children (see Thompson &

Opfer, 2010). Of those methods that have yet to be applied to this domain is intersensory redundancy, which posits that multiple synchronous sources of information presented across two or more sensory modalities enhance representations of amodal properties such as number.

Given the overlap in neurological processing of number and space, both of which are necessary to make accurate number line estimations, it is possible that intersensory redundancy may enhance number line estimations as well. That is, providing synchronous multisensory (e.g., audiovisual) information about the correct location of a target number on a virtual number line may make the positional relationship of numbers both within and across scales more salient. Here, three experiments will be conducted to test the effect of intersensory redundancy on number line estimation accuracy and response time across scales, as well as to contrast this effect across age. Behaviorally, I hypothesize that the enhancing effects of intersensory redundancy will manifest as greater accuracy and faster response times across all scales and age groups for number line estimations following multisensory feedback compared to unisensory (audio or visual) feedback. Also, it is likely that significant age effects will be observed, such that third-grade children will outperform second-grade children across all scales. Similarly, I expect to identify a significant effect of scale, such that all age groups will perform less accurately and will respond more slowly as scales rise in magnitude. Moreover, by recording neurological activation patterns throughout each estimation by way of NIRS, I will be capable of identifying changes in neural activation patterns that may occur in response to number line estimations across scales. These differences in activation patterns may be present across ages, scales, and following multisensory compared to unisensory

number line stimulation.

Based on extant pilot data that demonstrate significant behavioral differences in adult number line estimations within the task proposed below, Experiment 1 will test whether significant activation changes are present as adults complete a speeded number line task across large scales (e.g., billion and quadrillion). Next, Experiment 2 will test this effect using smaller, more age appropriate scales (e.g., hundred and hundred thousand) in second- and third-grade children, aged 7-9. Previous studies have identified this age range as being crucial in the development of accurate linear representations of number (Siegler, 1996) as well as implicating this developmental stage as a time during which large neurological shifts occur during numerical problem-solving (Rosenberg-Lee et al., 2011). I hypothesize that increases in scale for both adults and children will result in greater error in number line estimations as well as increased neurological activity in the PFC. Similarly, I hypothesize that a significant decrease in PFC activation will occur following the feedback phase of the task. Furthermore, I hypothesize that adult and child number line estimation accuracy will be significantly enhanced following multisensory compared to unisensory estimation feedback. Neurologically, multisensory feedback will facilitate greater reliance on, and hence greater hemodynamic activity in the parietal lobe throughout estimations across all scales. Finally, Experiment 3 will directly compare children's' and adults' neurological responses to their respective number line estimation tasks. Such comparisons will allow identification of the degree to which children and adults differ in response to number line estimations across age-appropriate scales.

CHAPTER II

EXPERIMENT 1

The Effect of Intersensory Redundancy on Number Line Estimation Accuracy and Hemodynamic Response Patterns in Adults

Extant studies of number line estimation performance in adults demonstrate that they are accurate in their estimations across many scale magnitudes (Booth & Siegler, 2006, 2008; Siegler & Booth, 2004; Thompson & Opfer, 2010). However, as noted by Siegler and Booth, this consistency might not hold true if adults are required to make estimates on extremely large scales, and if their time to make such estimates were limited. Moreover, as the poverty of input theory (Dehaene & Mehler, 1992) suggested, estimations within scales with which adults tend to have little experience (e.g., billion, quadrillion) may reveal estimation performance that mirrors that of children on smaller scales. Should adults demonstrate similar estimation performance as children under these conditions, it is reasonable to suspect that similar neurological response patterns would also exist. That is, estimations on unfamiliar scales may elicit differential amounts of pre-frontal activation as working memory and problem solving processes are evoked to assist in the estimation process. Conversely, on relatively smaller scales such as those used in past studies (Booth & Siegler, 2006, 2008; Siegler & Booth, 2004; Thompson & Opfer, 2010) adults are likely capable of making accurate estimations without the use of extensive working memory processes. Thus, neural activation during number line estimations on small scales may be relegated to the intraparietal regions of adult brains. Moreover, it is feasible that intersensory redundancy will enhance adults' number line

estimation accuracy on large-scale estimations as well as facilitate greater activation in the intraparietal regions as the number line scale increases.

Participants

In all, 27 (female = 15, mean age = 19 years, range = 18-26 years) right-handed adults were recruited for participation in this study by way of SONA participant recruitment services and were given partial course credit for their participation. All adult participants were typically developing, did not have a diagnosis of a learning disability, had normal hearing, normal or corrected to normal vision, and were native English speakers.

Setting and Apparatus

All experimental sessions were conducted in the Utah State University NIRS Laboratory, housed within the Emma Eccles Early Childhood Educational Research Center. All trials occurred on a PC desktop computer running Windows XP®, and were presented by E-Prime Stimulus Presentation Software (Schneider, Eschman, & Zuccolotto, 2002a 2002b). Along with an accurate record of number line estimation response time and accuracy, E-Prime also provided accurate stimulus timing throughout the task, which is necessary in order to accurately map NIRS data onto real-time events (e.g., number line estimation trials) experienced by the participant throughout the task (see Appendix A for exact trial structure). The screen resolution was set to 1020 x 1280 pixels.

To assess changes in the cortical concentration of oxygenated hemoglobin

(O_2Hb), NIRS was used (see Hoshi, 2003; Obrig & Villringer, 2003 for review). Data were recorded with a continuous wave system (ETG 4000, Hitachi Medical Co., Japan; see Plichta et al., 2006 for detailed description) using two 3x5 optode probe sets, each with 22 data-recording channels (7 photo detectors and 8 light emitters; see Figure 2). The interoptode distance was 30mm and the sampling rate was set to 10Hz. The probe sets were attached to participants' heads by a simple elastic-band cap (see Figure 2) that allowed for firm yet comfortable placement of each optode.

Localization of NIRS Probe Sets and Functional Regions of Interest

Probe set localization was determined prior to each scan based on physical measurements of each participant's head and corresponding international 10-20 system locations (see Okamoto et al., 2004). The international 10-20 system was initially developed to ensure the standardized reproducibility of EEG optobe locations across participants whose heads differ in size, and is now frequently used for the same standardization purpose across many other neuroimaging techniques including NIRS

Note. The numbers within the white boxes indicate channel numbers and locations.

Figure 2. Probe set placement and channel locations.

(Niedermeyer, & da Silva, 2004; Okamoto et al., 2004). The system is based on the relationship between head size and specific neurological landmarks. Head size is determined by measuring the actual distance between the nasion (i.e., the depressed area between the eyes) and the inion (i.e., the lowest point of the skull from the back of the head, normally indicated by a prominent bump). The "10" and "20" refer to the fact that the actual distances between each neurological landmark are either 10% or 20% of the total nasion-to-inion distance.

For probe set 1, the middle optode on the first row of the set was placed directly over Fpz (i.e., 10% of nasion-to-inion distance above the nasion, directly on the midline of the head, which marks the frontopolar midpoint of the pre-frontal cortex. For probe set 2, the middle optode in the second row of the set was placed directly over Pz (i.e., 70% of nasion-to-inion distance from nasion), which marks the midpoint of the parietal cortex (see Figure 2).

All functional regions of interest (fROI) used throughout the analyses were identified *a priori* based on previous fMRI studies of math processing in children and adults (see Arsalidou & Taylor, 2011; Delazer et al., 2005; Rosenberg-Lee et al., 2011) and were localized for each participant based on their correspondence to the Montreal Neurological Institute (MNI) standardized neurological coordinate system (Okamoto et al., 2004). MNI coordinates of NIRS observation channels were obtained immediately after each scan session through measurements made by a 3D magnetic space digitizer (FASTRAK, Polhemus, Cochester, VT), which provides an accurate measurement of the NIRS optode positions and thus each observation channel, within a real-world coordinate system (Singh, Okamoto, Dan, Jurcak, & Dan, 2005). Following these measurements,

anatomical labels of the neural regions convolved within each NIRS observation channel were obtained and were used to identify the NIRS observation channels that constitute each fROI. Because of its low spatial resolution, a measurable amount of overlap between neighboring neural locations was present within each NIRS observation channel. In order to reduce the inclusion of channels with such overlap within each fROI, an inclusion criterion of >25% overlap with the anatomical location of interest was imposed when identifying the channels that constitute an fROI.

See Appendices C and D for schematics of the fROIs within the frontal and parietal probe sets, respectively. In the prefrontal cortex, fROIs included the medial PFC (channels 7, 11, 12, 16), and the left dorsolateral PFC (channels: 6, 10, 11, 15, 19, and 20; Delazer et al., 2005; Rosenberg-Lee et al., 2011). In the parietal cortex, fROIs included the left intraparietal sulcus (channels 28, 32, 33, and 37), the left angular gyrus (channels 32 and 36), the right intraparietal sulcus (channels 30, 34, 35, and 39), and the right angular gyrus (channels: 13 and 18; Arsalidou & Taylor, 2011; Delazer et al., 2005; Rosenberg-Lee et al., 2011). Because spatial resolution of NIRS is poor with a nonoverlapping geometric arrangement of optodes (e.g., no better than the emitter-detector distance of 30mm) and no anatomical image was taken, the non-ROI was limited to channels outside each ROI and were thus excluded from further analyses.

Experimental Design and Procedure

A mixed block and event-related design was employed. All participants experienced three distinct experimental blocks, each consisting of 30 number line estimation trials, in a set order (see Appendix A for adult trial structure). As one purpose

of the current study was to assess the effect of condition-relevant feedback on number line estimations, each block was named based on its position relative to the feedback portion of the task (i.e., block two). That is, block one was "prefeedback," block two was "feedback," and block three was "postfeedback." The estimation trials within each block (described in detail below) were randomized prior to data collection. Each participant was then exposed to the same randomized trial structure, thus resulting in pseudo-randomness. In this manner, neurological responses related to each scale magnitude "event" (i.e., trial) throughout the task could be captured in isolation, without being predictably related to the previous or following trial magnitudes. Thus, the presentation method throughout each block is said to be 'event-related'. The predefined trial onsets and their respective durations reported in Appendix A were thus used to define the GLM design matrix (i.e., X_n) for which the corresponding parameter matrix (i.e., β_n) was estimated (see NIRS Data Analysis and Outcomes section below for further explanation of the GLM design matrix).

The experiment began and ended with a 30 second rest period in which each participant was asked to close his/her eyes and clear his/her mind. Similarly, each experimental block was separated by identical 30-second rest periods, after which a "ding" sound was presented so that the participants knew when to open their eyes and prepare for the next phase of the task. Within each experimental block the participants completed 15 trials of both scales (i.e., billion and quadrillion), totaling 90 trials (15 trials x 2 scales = 30 trials per block x 3 blocks = 90 total trials). Within blocks one and three, the duration of each trial was exactly seven seconds. This duration was raised to nine seconds in block two to account for the feedback that was given during the final two

seconds of each trial.

See Figure 3 for trial structure schematic. Each trial contained four distinct sections: First, a brief ITI was presented that ranged between two, four, six, or eight seconds. Each ITI was presented an equal number of times ($\bar{x}$ = 5s), and appeared simply as a '+' in the center of the computer screen for its duration. Next, the *estimation statement* (e.g., "Out of **scale**, show me **value**") was presented for 3 seconds. The "scale" and "value" within the estimation statement were presented as words, rather than Arabic numerals (e.g., "Out of **one billion**, show me **twenty million"**). Each value was limited to a three-word description plus its scale (e.g., "six hundred thirty trillion"; see Appendix E for exact numbers used). Therefore, each target value in the estimation statement contained no more than four words. In order to maintain consistency across scales and blocks, the same numerical values were used throughout each block of the task, and only differed by the magnitude of their scale (e.g., "six hundred thirty trillion" and "six hundred thirty million" appeared in each block). In this manner, it was possible to assess estimation inaccuracies that arise strictly because of an increase in numerical magnitude, while all other factors are held constant. After three seconds the estimation statement disappeared and was replaced by the *response line*, which was simply a blank line on which the participant clicked his/her mouse on the location marking his/her estimation point. The response line was exactly 1,000 pixels in length and was flagged on each end with short vertical lines that denoted its end points. The response line always appeared in the center of the computer screen and was the only object on the screen throughout the participants' estimation. Each participant was given up to three seconds to respond on the

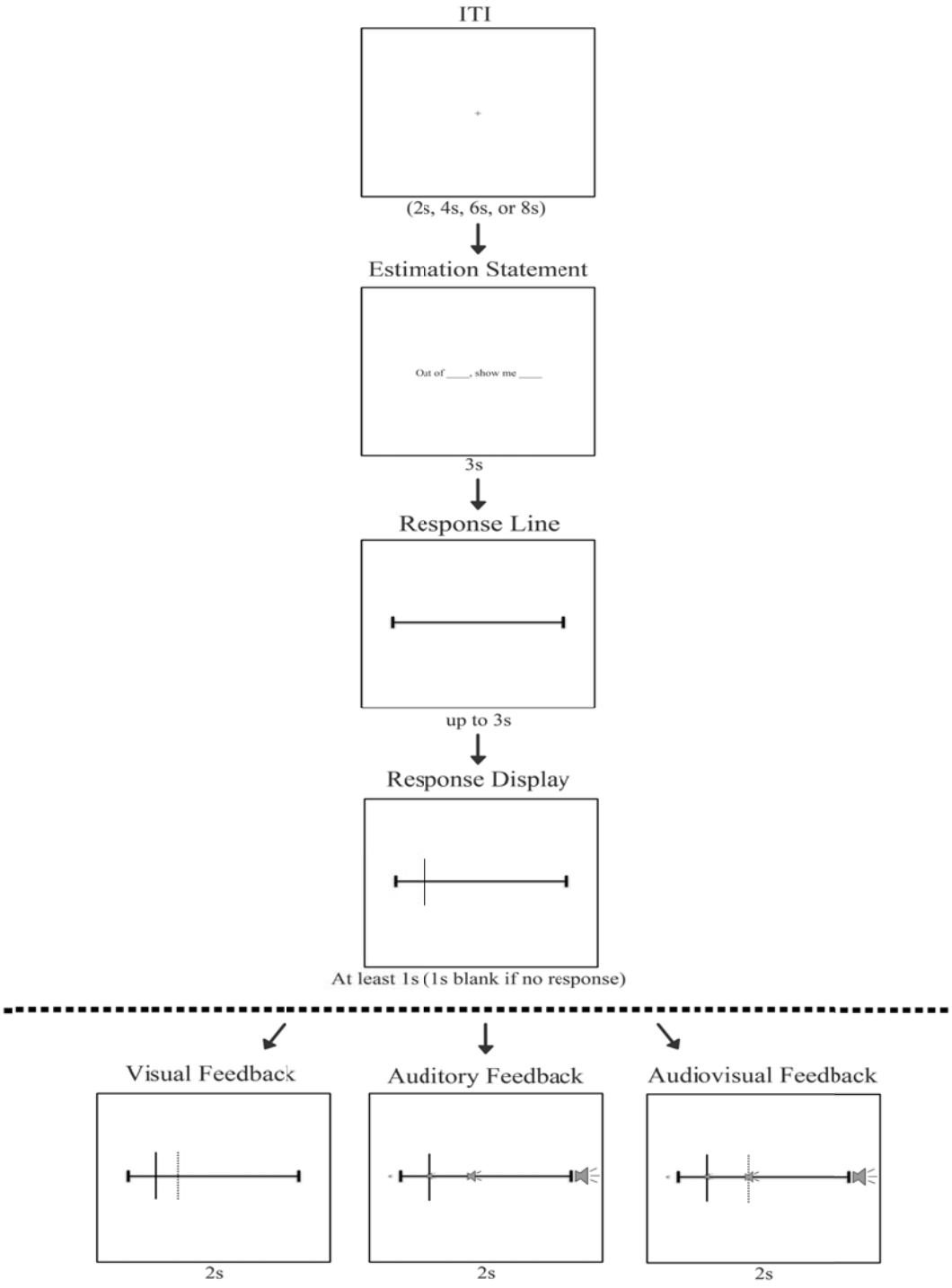

Note. Pre- and postfeedback trial structure is represented within the vertical portion of the figure, above the dashed line. Condition relevant feedback, provided in block 2 of the task, is represented within the horizontal portion at the bottom, below the dashed line.

Figure 3. Trial structure schematic.

response line.[1] Immediately upon the participant's response the *response display* (i.e., a blue vertical "hash mark") appeared on the location of the participant's mouse click. This response display remained visible for at least one second; however, its total presentation duration was allowed to vary depending on the speed of the participant's response, so that a total trial duration of seven seconds could be maintained. For example, if a participant responded exactly 1 second after the onset of the response line, the response display must have remained visible for 3 seconds in order to maintain a seven second trial duration (e.g., 3 second estimation statement presentation + 1 second response time + 3 second response display time = 7 total seconds). However, if a subject responded exactly 2 seconds after the onset of the response line, the response display must have remained visible for 2 seconds in order to maintain a seven second trial duration (e.g., 3 second estimation statement presentation + 2 second response time + 2 second response display time = 7 seconds). Finally, if the participant failed to respond on the response line within three seconds after the offset of the estimation statement, the response line remained blank for one additional second (e.g., 3 second estimation statement presentation + 3 second response time opportunity + 1 second blank response line = 7 seconds), and the trials moved forward as programmed. Participants were not able to adjust their estimates after their initial estimation.

This trial structure was maintained throughout each block of the task. However, within the feedback block, an extra two seconds of condition relevant feedback (i.e., visual, auditory, audiovisual) was presented immediately after the 7-second trial length.

[1] In order to reduce the tendency for participants to leave their cursor on a predetermined point on the line in between trials, the program automatically reset the cursor position between trials.

Thus, all trials within the feedback block lasted a total of 9 seconds. Each feedback type is described below.

Visual Feedback

Visual feedback was provided by a vertical red "hash mark" placed on the trial's correct value-to-scale location on the response line. As the purpose of the feedback was to provide the participants with information that allows them to compare their own estimation location relative to the correct location on the line, their own blue response display remained visible throughout the feedback portion of each trial. Therefore, their own estimation location and the correct location could be observed simultaneously throughout the two seconds of feedback within each trial. On trials in which the participant provided no response, the feedback display appeared alone on the response line for two seconds.

Auditory Feedback

Auditory feedback was provided as a pair of tones that varied in loudness depending on the spatial relationship on the response line between the participant's estimation response (tone 1: participant's response tone), and the correct value-to-scale location (tone 2: correct response tone). Throughout the feedback block of this condition, the participant's response display was accompanied by a pure tone (3000Hz) whose volume was position dependent. Specifically, a quiet-to-loud volume orientation was mapped onto the left-to-right physical orientation of the response line: The decibel level on the far left side of the line was approximately 10dB, while the far right side of the line was approximately 100dbB. Thus, a point on the left side of the response line coincided

with a tone that was quieter than a tone that coincided with a point on the right side of the line. Throughout the 2-second-feedback portion of each trial, a second tone was presented whose volume represented the correct value-to-scale location on the line. However, as humans' psychophysical discrimination of volume change is not linear, this volume orientation was scaled, using Steven's Power Law, so that a one-unit spatial change in left-to-right location on the line resulted in a one-unit psychophysical increase in the volume of the tone. The general form of the Steven's power law ($\psi(I) = kI^a$) defines the relationship between the physical magnitude of a stimulus and its perceived intensity (Stevens, 1957). According to this power function, I is the magnitude of a stimulus, $\psi(I)$ is the psychophysical function relating to the physical magnitude of the sensation evoked by the stimulus, a is an exponent that depends on the type of stimulation, and k is a proportionality constant that depends on the type of stimulation and the units used. An exponent of 1 indicates that the perceived intensity of a stimulus coincides directly with its physical magnitude. According to Stevens, the exponent associated with perception of volume change is .67, suggesting that a greater than 1 unit increase in the physical magnitude of a tone is needed to perceive a one unit increase in perception of volume. Thus, solving for I (i.e., physical magnitude of the tone at each point along the line) within Stevens' power function allowed for an estimation of successive volume increases across each physical unit of the line that would more accurately approach perceptual linearity. Therefore, participants were able to compare the accuracy of their estimations based on the magnitude of volume difference between their response tones and the correct location tones.

Audiovisual Feedback

The audiovisual feedback condition provided a combination of both the visual and auditory feedback simultaneously. That is, similar to the auditory feedback condition, a position-dependent response tone (e.g., tone 1) accompanied the participants' response display on the response line. Next, similar to the visual feedback condition, a red "hash mark" was presented in the correct value-to-scale location. However, in the audiovisual feedback condition, the red "hash mark" was also accompanied by a correct response tone (e.g., tone 2) whose volume also indicated the correct value-to-scale location. Therefore, participants received simultaneous audiovisual information about their estimation locations as well as the correct locations of the estimation values, and were thus able to use this combined sensory information to inform future estimations.

Practice Trial

Immediately prior to beginning the task, each participant engaged in a practice session that introduced him or her to the task, as well as to the condition relevant feedback that they would experience. Participants were first shown an example estimation statement, in which a target and scale that were not used throughout the task were displayed (e.g., "Out of one hundred, show me twenty"). It was explained to the participant that he or she would have exactly three seconds to read this sentence before making his or her estimation. Next, participants were shown a blank estimation response line. The experimenter highlighted for the participant the end points of the line and described that the line was intended to represent the scale that was read in the prior estimation statement. The participant was then instructed to click on the line in the

location that represented “twenty out of one hundred.” This resulted in the blue response display being shown. As this section of the practice was completely experimenter driven (i.e., not automatically timed, as throughout the task), it was possible to make sure the participant understood how each trial would progress. Next, each participant underwent at least five practice trials that were structured and timed exactly like the trials they experienced throughout the task, except that the scale magnitudes used were smaller than those used throughout the task. These practice trials allowed the participant to become familiar with the pacing of each trial, while not being exposed to the scale magnitudes that were to be used throughout the task.

Next, each participant was introduced to his or her condition-relevant feedback. First, a series of animations demonstrated the type of feedback that would be received. These animations were identical across each feedback condition, and only varied insofar as the type of feedback they produced. As with the initial practice section above, this section was experimenter driven so that participants understood the feedback that they would receive. If the participant expressed confusion, the feedback instructions were repeated. Following this introduction, each participant then underwent an additional 5 feedback trials that progressed in the same manner as throughout the task. Following these practice trials, the NIRS cap was placed on the participant’s head, and the task moved forward as programmed.

Behavioral Data Analysis and Outcomes

In order to examine the accuracy of numerical estimates across each experimental block, we first converted a participant’s estimation point to a numerical value by taking

the proportion of the line indicated by the participant (i.e., linear distance from "0" mark to the participant's estimation point, divided by the total length of the line) and then multiplied this proportion by the scale value. Next, the percent absolute error (PAE) of each estimate (0-100%) was calculated by dividing the mean absolute difference between each estimated value and the actual value, divided by the total scale. Finally, accuracy scores were computed by subtracting percent absolute error from 100% (see Thompson & Opfer, 2010 for review; see Table 1 for accuracy means and standard deviations). These accuracy scores were then subjected to repeated measures analysis of variance (ANOVA) as follows.

See Figure 4 for adults' block x scale performance. First, a 3 (block) x 2 (scale) x 3 (feedback condition) repeated measures ANOVA of adults' number line estimation accuracy identified a significant main effect of block, $F(1.4, 36.41) = 35.68$, $MSE =$

Table 1

Adults' Estimation Accuracy Means and Standard Deviations

	Prefeedback		Feedback		Postfeedback	
Variable	Mean	*SD*	Mean	*SD*	Mean	*SD*
Auditory						
One billion	89.040	15.487	91.735	10.683	93.375	7.942
One quadrillion	89.899	10.749	91.179	12.360	91.859	10.608
Visual						
One billion	92.096	8.613	95.455	7.141	95.093	4.822
One quadrillion	91.882	9.456	94.650	6.662	95.834	5.009
Audiovisual						
One billion	91.939	8.762	95.597	4.296	95.179	7.821
One quadrillion	89.934	10.160	94.891	7.000	95.702	4.185
Combined						
One billion	91.025	10.954	94.262	7.373	94.549	6.862
One quadrillion	90.572	10.122	93.573	8.674	94.465	6.601

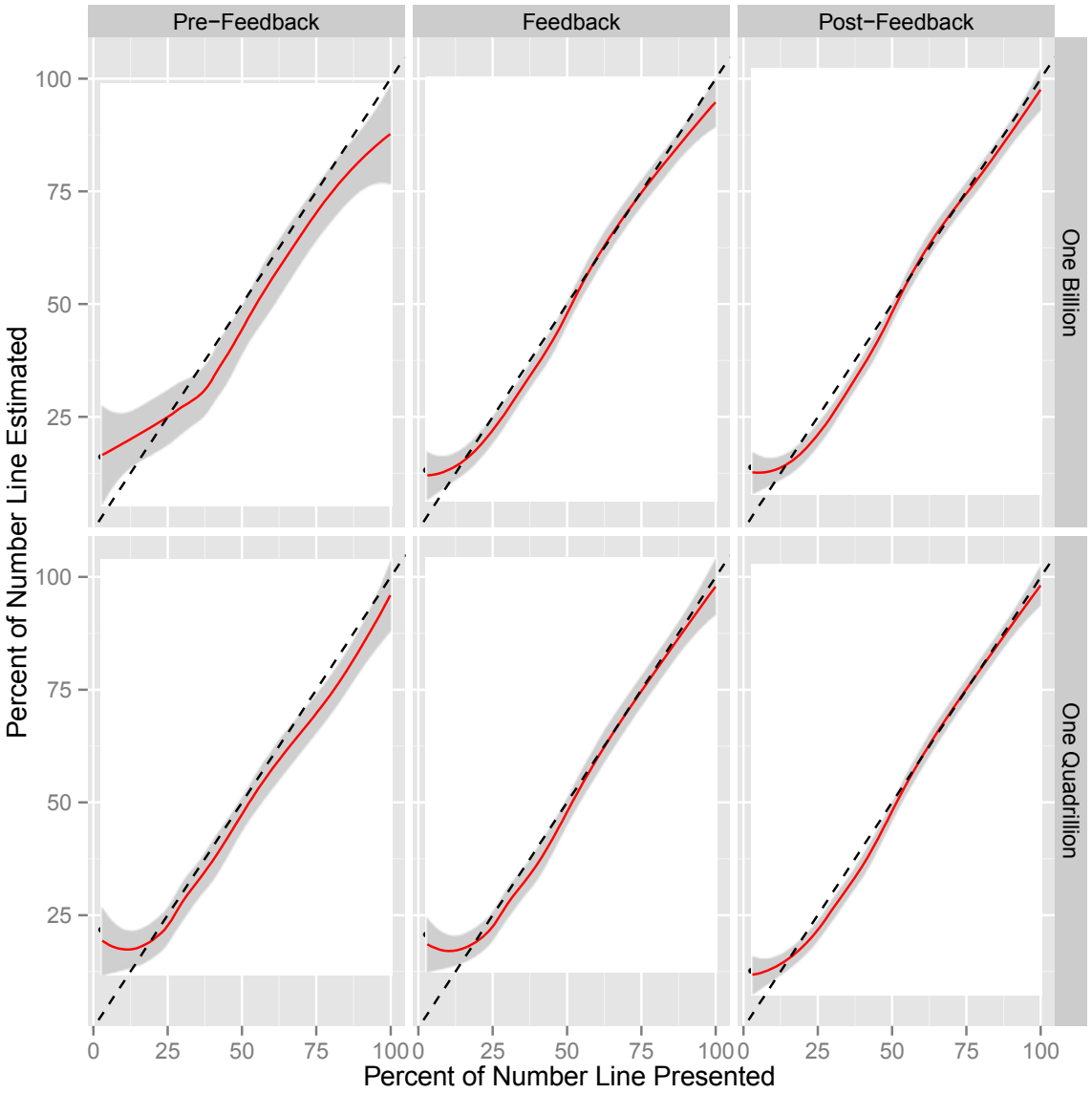

Note. Perfect performance is seen within each subplot by the checkered line with an intercept of 0 and a slope of 1. Each dot represents the average estimation location (y-axis) for each estimation value (x-axis) within each block x scale condition. A trend line has been overlaid to highlight the average overall performance and standard error (shaded area surrounding each trend line) within each condition. A trend line that lies below the perfect performance line indicates a tendency to underestimate the correct location on the line.

Figure 4. Adult's block x scale estimation performance.

305.68, *H-F p*< .001, partial η^2= .598; indicating that estimations became more accurate as participants progressed across blocks. No other main effects or interactions were significant (see Table 2 for breakdown of accuracy comparisons). Individual pairwise comparisons with Bonferroni adjustments identified significant differences in accuracy between the prefeedback and feedback conditions ($p < .001$), and between the pre- and postfeedback conditions ($p < .001$). The pairwise comparison between the feedback and postfeedback condition approached significance ($p = .07$).

See Figure 5 for response time performance and Table 3 for response time means and standard deviations. An identical 3 x 2 x 3 repeated measures ANOVA of response times identified a significant main effect of scale, $F(1, 48) = 5.15$, $MSE = 42186.62$, *H-F* $p = .033$, *partial* $\eta^2 = .177$; driven by faster reaction times for small compared to large scales. Similarly to the analysis of accuracy, the main effect of block was also significant for response time, $F(1.95, 48) = 16.65$, $MSE = 460879.37$, *H-F* $p < .001$, *partial* $\eta^2 = .410$; indicating that participants' response times decreased as they progressed through

Table 2

Breakdown of Adults' Estimation Accuracy Comparisons

Variable	*df*	Sum of squares	Mean square	*F* ratio	*p* value	Partial eta-squared
Block	1.444	4.38.386	303.662	35.682	.000[1]	.598
Block x condition	2.887	26.708	9.248	1.087	.366	.083
Scale	1	6.159	6.159	.540	.470	.022
Scale x condition	2	3.093	1.546	.136	.874	.011
Block x scale	1.514	2.725	1.800	.319	.668	.013
Block x scale x condition	3.028	32.853	10.851	1.924	.143	.138
Condition	2	281.829	140.915	1.784	.189	.129

[1] Estimation accuracy increased from pre- to postfeedback.

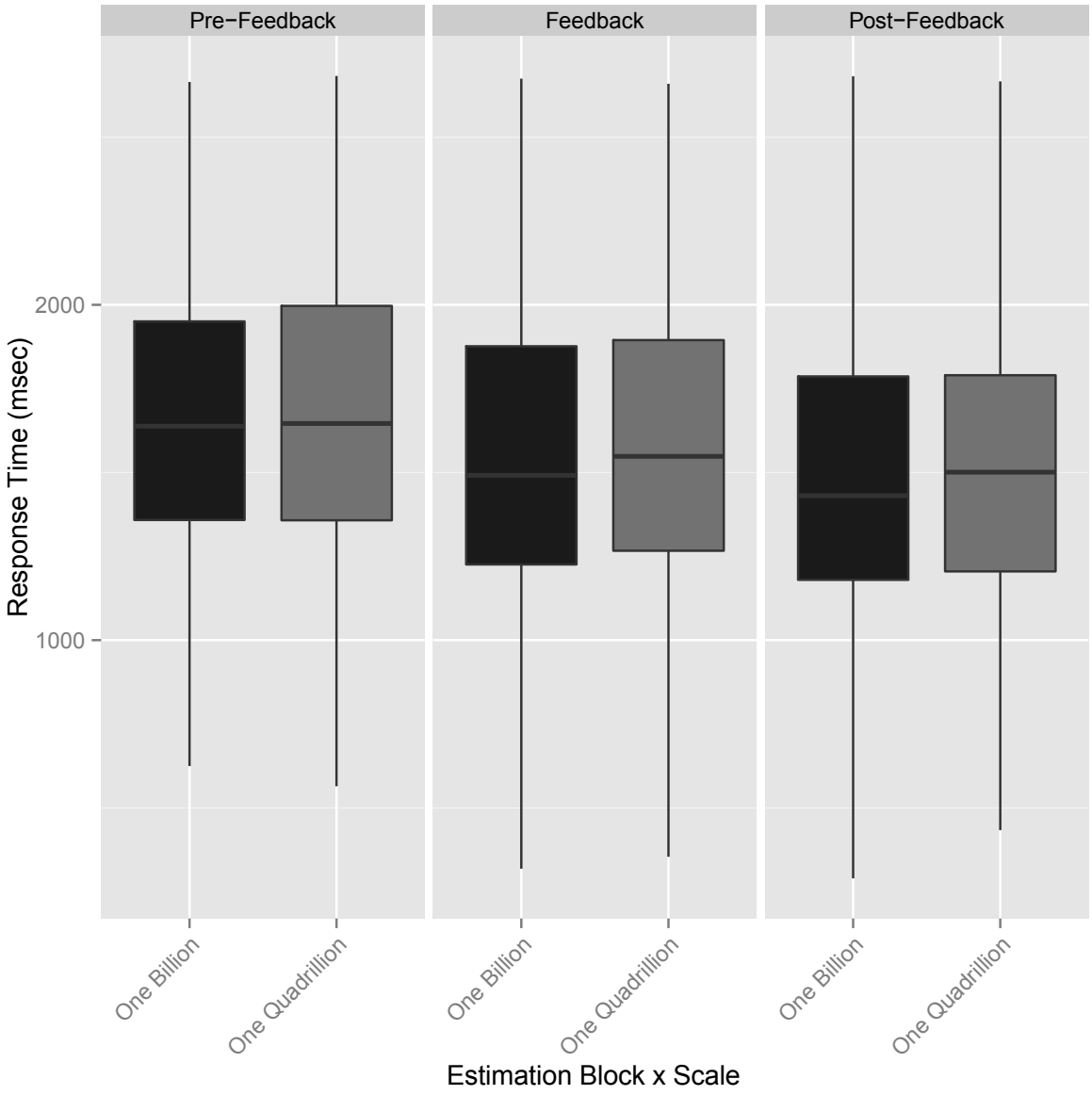

Note. The bold line in the middle of each boxplot represents the median response time for each scale. Seventy-five percent of response time values fall below the top line of each box, while 25% fall below the bottom line of each box. The lines extending from each box (e.g., whiskers) provide an indicator of the range of values along the y-axis. Black boxes represent small-scale estimations.

Figure 5. Adults' estimation response times across each block x scale condition.

Table 3

Adults' Response Time Means and Standard Deviations

	Prefeedback		Feedback		Postfeedback	
Variable	Mean	*SD*	Mean	*SD*	Mean	*SD*
Auditory						
One billion	1675.281	493.539	1486.872	427.872	1408.591	442.169
One quadrillion	1645.795	417.244	1542.800	413.203	1477.852	451.142
Visual						
One billion	1765.184	402.700	1734.391	427.848	1639.842	432.329
One quadrillion	1793.211	417.629	1746.429	436.094	1639.438	391.955
Audiovisual						
One billion	1590.805	397.869	1444.425	382.453	1437.970	415.752
One quadrillion	1644.132	417.086	1487.400	395.065	1476.879	470.191
Combined						
One billion	1677.090	431.369	1555.229	412.724	1495.468	430.083
One quadrillion	1694.379	417.320	1592.210	414.787	1531.390	437.763

the task. No other main effects or interactions were significant (see Table 4 for breakdown of response time comparisons). Moreover, response times within the prefeedback condition were significantly longer than those of the feedback condition (p = .003), and those of the postfeedback condition ($p < .001$). Similar to the effects seen in the analyses of accuracy, the response time difference between the feedback and postfeedback conditions approached significance (p = .09).

Next, in order to identify whether a linear or logarithmic function best fit the correlation between estimation accuracy and scale across each experimental condition, a combination of linear and non-linear regression analyses were conducted for each scale x block pair. The R^2 value provided following each of these analyses were compared, and the higher of the two values was considered to be the better fit. Consistent with previous

Table 4

Breakdown of Adults' Response Time Comparisons

Variable	*df*	Sum of squares	Mean square	*F* ratio	*p* value	Partial eta-squared
Block	1.954	900507.984	460879.174	16.647	.000[1]	.410
Block x condition	3.908	90539.640	23169.063	.837	.506	.065
Scale	1	42186.624	42186.624	5.148	.033[2]	.177
Scale x condition	2	7739.591	3869.795	.472	.629	.038
Block x scale	2	2011.290	1005.645	.130	.878	.005
Block x scale x condition	4	17820.587	4455.147	.576	.682	.046
Condition	2	1395728.215	697864.108	1.996	.158	.142

[1]Response times decreased from pre- to postfeedback.
[2]Response times were significantly faster for small- compared to large-scale trials.

studies (Siegler & Opfer, 2003; Thompson & Opfer, 2008, 2010), median values were used to reduce the impact of outliers at the group level (although similar logarithmic and linear fits were obtained with mean values). Across each scale x block pair, adults' estimation accuracy was better fit by linear than logarithmic functions (small scale x prefeedback: linear R^2= .97 > logarithmic R^2= .78; small scale x feedback: linear R^2= .99 > logarithmic R^2= .85; small scale x postfeedback: linear R^2= .99 > logarithmic R^2= .86; large scale x prefeedback: linear R^2= .97 > logarithmic R^2= .76; large scale x feedback: linear R^2= .97 > logarithmic R^2= .77; large scale x postfeedback: linear R^2= .99 > logarithmic R^2= .87).

NIRS Data Analysis and Outcomes

Each treatment of NIRS data reported below was conducted with NIRS-SPM NIRS analysis package (Ye, Tak, Jang, Jung, & Jang, 2009) for Matlab®. Initially, the modified Beers-Lambert law was used to convert raw optical density data recorded by the

ETG 4000 device into units of volume, which provide an indicator of oxygenated (O_2Hb) and deoxygenated (O_2Hr) hemoglobin concentration levels within the blood of the cortex at each observation. Previous research has found oxygenated hemoglobin to be a more informative marker of cognitive processing compared to deoxygenated hemoglobin (e.g., Baird et al., 2002; Bortfeld, Fava, & Boas 2009; Grossmann et al., 2008; Minagawa-Kawai, Mori, Hebden, & Dupoux, 2008; Peña et al., 2003; Wilcox, Bortfeld, Woods, Wruck, & Boas, 2008; Wilcox et al., 2009). Therefore, only oxygenated hemoglobin data was used throughout the following analyses. Next, because several physiological processes (e.g., respiration, blood-pressure changes, heartbeat, etc.) are known to produce structured "noise" within the data (i.e., autocorrelation) a precoloring treatment was performed, through which such temporal correlations are "swamped" by an imposed 4s Gaussian temporal correlation structure and are thus effectively reduced (Worsely & Friston, 1995). As opposed to prewhitening treatments, which have been developed in order to account for autocorrelation in fMRI data, the precoloring method has been shown to be more appropriate for NIRS data (Ye et al., 2009). Furthermore, O_2Hb data were highpass-filtered with a cutoff of 128s using a set of discrete cosine transform (DCT) functions to remove low frequency noise in the data (Ye et al., 2009).

Next, these treated data were analyzed using a procedure developed by Plichta, Heinzel, Ehlis, Pauli, and Fallgatter (2007). This approach follows typical fMRI analyses of the hemodynamic response function (HRF) and is based on the general linear model (GLM). The GLM approach has been extensively described in fMRI literature (see Bullmore et al., 1996; Friston, Holmes, Worsley, & Poline, 1995; Worsley & Friston, 1995). Briefly described by Plichta and colleagues (2007), "The data matrix **Y** of order

(TxC) containing the functional NIRS time series *T* of each channel *C* is predicted by **X** consisting of a set of reasonable hemodynamic response functions (HRFs) which are convolved with the event sequence (the order of **X** is (TxM) where *M* is the number of modeled effects)" (p. 627). Thus, the functional data can be modeled as:

$$\boldsymbol{Y} = \boldsymbol{X\beta} + \varepsilon$$

where **X** is the design matrix and **β** is the parameter matrix. The error matrix Ɛ defines the variation in **Y** that is not accounted for by **β.** In the simplest case, each column *M* of matrix **X** contains the predicted hemodynamic response for one experimental condition over time (*T*). A total of six levels of the **X** and **β** variables, each corresponding to a specific estimation scale and experimental block, were used in the present experiment. In this manner, the functional data for the present experiment where modeled as

$$\boldsymbol{Y} = \boldsymbol{X_1\beta_1} + \boldsymbol{X_2\beta_2} + \boldsymbol{X_3\beta_3} + \boldsymbol{X_4\beta_4} + \boldsymbol{X_5\beta_5} + \boldsymbol{X_6\beta_6} + \varepsilon$$

That is, $\mathbf{X_1}$ always represented the small-scale estimations within the prefeedback block of the task, whereas $\mathbf{X_2}$ always represented the large-scale estimations within the prefeedback block, and so on. Each variable (i.e., **X**) was defined by the seconds within each scan that related to each trial type and block respectively (see Appendix A). For example, for each adult participant, a prefeedback small-scale estimation trial (i.e., $\mathbf{X_1}$) occurred at exactly 43, 58, 73, 97, 130, 204, 215, 228, 243, 254, 263, 274, 313, and 337 seconds into the scan, and each of these trials lasted exactly 7 seconds. Therefore, the hemoglobin oxygenation values (i.e., HbO) within these time periods of the scan occurred as the participant was directly engaged in a prefeedback small-scale estimation, and were thus entered into the linear regression model in order to estimate the standardized beta weight corresponding to, in this case, $\mathbf{X_1}$. Given an observation rate of

10Hz, and 15 trials per level of **X** each lasting 7 seconds, a total of 1,050 HbO values were used to estimate the beta values for the pre- and postfeedback conditions (i.e., $\mathbf{X_1}$, $\mathbf{X_2}$, $\mathbf{X_5}$, and $\mathbf{X_6}$). The number of observations used to calculate the beta values for the feedback conditions (i.e., $\mathbf{X_3}$ and $\mathbf{X_4}$) was increased to 1,350 due to the extra 2 seconds provided for feedback. This procedure was repeated for each **X** variable.

In this manner the **β**-weights quantify the contribution of a predictor (e.g., HRF) for explaining the functional time series **Y** and serve as the parameter set for subsequent hypothesis testing. In practice, positive HbO **β**-weights indicate neural activation, as increases in HbO are expected throughout periods of high cognitive expenditure (Plichta et al., 2007). ANOVA or paired-sample *t* tests may be applied to group level beta estimates in order to test within- and between-group comparisons and interactions (Plichta et al., 2007). Following the GLM analysis, the resulting **β**-weights of HbO for all fROIs were subjected to a 3 (block) x 2 (scale) x 3 (feedback condition) repeated measures ANOVA (Köchel et al., 2011). See Table 5 for adult fROI beta means and standard deviations

Prefrontal fROI Analyses

See Figure 6 for adult prefrontal fROI activation patterns. Each fROI within the prefrontal cortex reacted similarly throughout the task (see Tables 6 and 7 for breakdown of adult PFC beta value comparisons). A significant effect of scale was present within each fROI (medial PFC: $F(1, 24)= 9.39$, $MSE= .003$, $H\text{-}F\ p= .005$, $partial\ \eta^2= .281$; left dorsolateral PFC: $F(1, 24)= 13.69$, $MSE= .005$, $H\text{-}F\ p= .001$, $partial\ \eta^2= .363$), indicating that neural activation in the prefrontal cortex is greater for small compared to large scale

Table 5

Adults' fROI Beta Means and Standard Deviations

		Frontal ROIs				Parietal ROIs							
		Medial PFC		Left DLPFC		Left IPS		Left AG		Right IPS		Right AG	
Variable	Size	Beta	*SD*	Beta	*SD*	Beta	*SD*	Beta	*SD*	Beta	*SD*	Beta	*SD*
Auditory													
Prefeedback	Small	-.056	.041	-.049	.037	-.055	.044	-.072	.053	-.033	.059	-.046	.079
	Large	-.061	.275	-.0555	.024	-.067	.042	-.075	.063	-.039	.052	-.056	.071
Feedback	Small	-.045	.038	-.046	.056	-.047	.041	-.061	.057	-.030	.062	-.023	.058
	Large	-.055	.046	-.063	.075	-.076	.041	-.095	.052	-.056	.048	-.053	.048
Postfeedback	Small	-.005	.036	-.009	.031	.047	.087	.000	.081	.019	.058	-.005	.067
	Large	-.019	.035	-.025	.069	.037	.119	-.005	.121	.003	.085	-.012	.094
Visual													
Prefeedback	Small	-.022	.057	-.015	.057	.006	.062	-.012	.107	.035	.058	.023	.078
	Large	-.031	.046	-.023	.043	-.023	.081	-.052	.138	.027	.062	.027	.082
Feedback	Small	.012	.061	.005	.059	.025	.047	.043	.068	.018	.069	.019	.085
	Large	.003	.076	-.005	.082	.013	.053	.019	.064	.004	.109	-.003	.104
Postfeedback	Small	-.028	.052	-.038	.056	.066	.142	.051	.156	.005	.119	-.045	.183
	Large	-.035	.045	-.046	.063	.071	.173	.057	.180	.029	.118	-.038	.206
Audiovisual													
Prefeedback	Small	-.036	.071	-.033	.069	-.006	.063	-.027	.059	.005	.067	-.001	.061
	Large	-.032	.039	-.027	.046	-.012	.045	-.037	.041	.001	.058	-.009	.052
Feedback	Small	-.049	.059	-.049	.047	-.003	.053	-.041	.053	.002	.054	-.001	.061
	Large	-.049	.059	-.055	.061	.012	.051	-.026	.033	.021	.060	.013	.051
Postfeedback	Small	-.008	.124	-.025	.122	-.025	.082	-.042	.154	-.033	.112	-.036	.093
	Large	-.042	.105	-.057	.089	-.052	.125	-.060	.186	-.073	.122	-.066	.124
Combined													
Prefeedback	Small	-.038	.056	-.032	.054	-.018	.056	-.037	.073	.002	.061	-.008	.073
	Large	-.041	.120	-.035	.038	-.034	.056	-.055	.081	-.004	.057	-.013	.068
Feedback	Small	-.027	.053	-.030	.054	-.008	.047	-.020	.059	-.003	.062	-.002	.068
	Large	-.034	.060	-.041	.073	-.017	.048	-.034	.050	-.010	.072	-.014	.068
Postfeedback	Small	-.014	.071	-.024	.070	.029	.104	.003	.130	-.003	.096	-.029	.114
	Large	-.032	.062	-.043	.074	.019	.139	-.003	.162	-.014	.108	-.039	.141

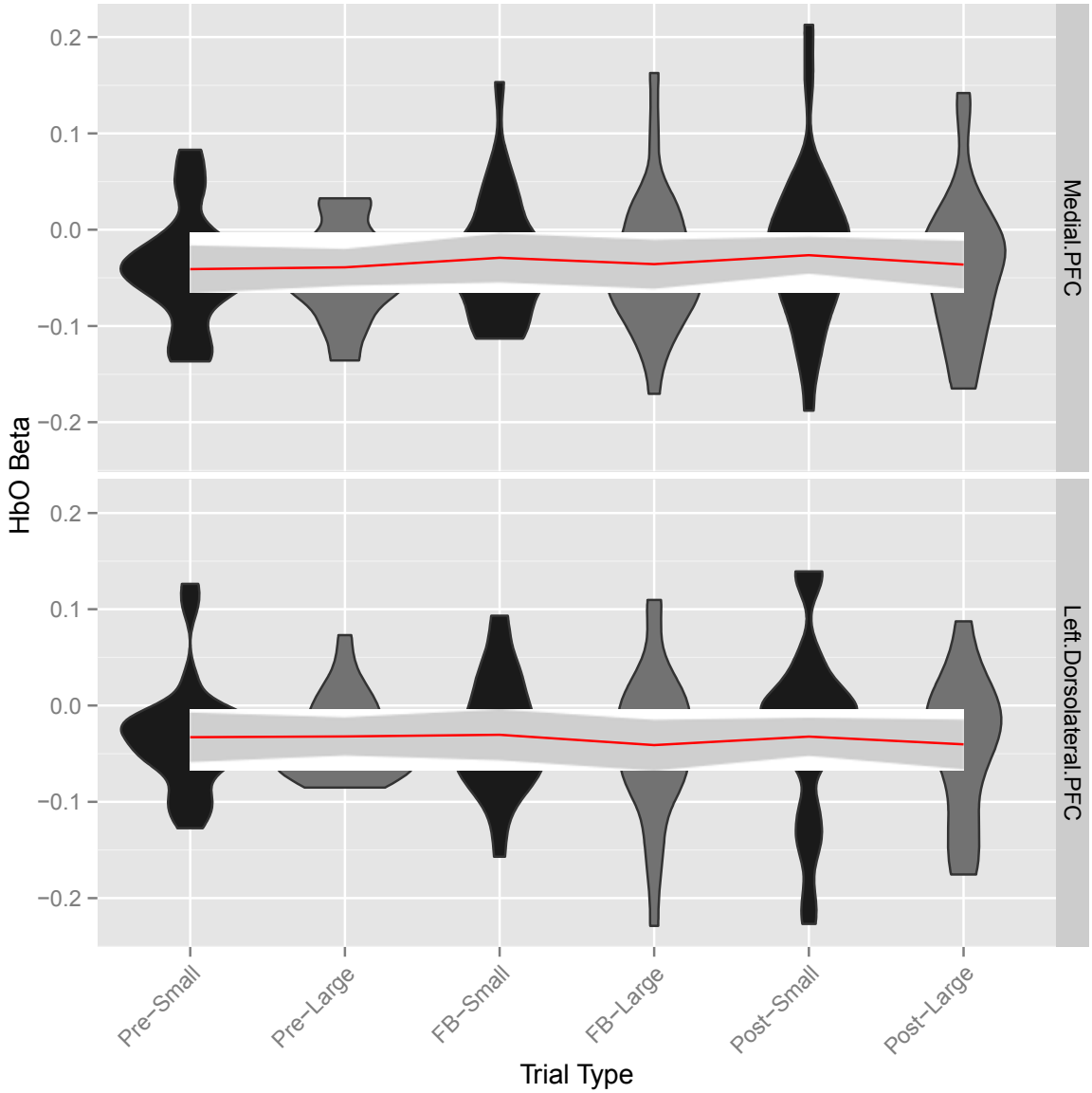

Regions of interest can be seen along each row of the plot above. Trial types are shown along the x-axis. The height of each violin provides an indicator of the distribution of beta values along the y-axis. The width of each plot provides an indicator of the count of beta weights at each point along the y-axis. That is, any portion of the plots that is fatter than another indicates that more beta values occurred at that point on the y-axis compared to a skinnier section. Small-scale estimations are shown in black.

Figure 6. Activation patterns in the adults' prefrontal fROIs.

Table 6

Breakdown of Adults' Medial Prefrontal Beta Value Comparisons

Variable	*df*	Sum of squares	Mean square	*F* ratio	*p* value	Partial eta-squared
Block	1.665	.008	.005	.656	.497	.027
Block x condition	3.331	.036	.011	1.518	.222	.112
Scale	1	.003	.003	9.398	.005[a]	.281
Scale x condition	2	.00003	.00001	.045	.956	.004
Block x scale	2	.002	.001	1.209	.307	.048
Block x scale x condition	4	.002	.001	.787	.539	.062
Condition	2	.017	.008	.909	.416	.070

aSignificantly greater response to small- compared to large-scale estimations.

Table 7

Breakdown of Adults' Left Dorsolateral Prefrontal Beta Value Comparisons

Variable	*df*	Sum of squares	Mean square	*F* ratio	*p* value	Partial eta-squared
Block	1.846	.007	.004	.554	.565	.023
Block x condition	3.692	.04	.011	1.670	.178	.122
Scale	1	.004	.004	12.00	.002[a]	.333
Scale x condition	2	.000	.00007	.212	.811	.017
Block x scale	2	.001	.001	.983	.382	.039
Block x scale x condition	4	.002	.000	.670	.616	.053
Condition	2	.023	.012	1.000	.383	.077

[a]Significantly greater response to small- compared to large-scale estimations.

estimations. No other comparisons within the prefrontal cortex were significant.

Parietal fROI Analyses

See Figure 7 for adult parietal fROI activation patterns. Within the left IPS, a 3 x 2 x 3 repeated measures ANOVA identified a significant main effect of *scale, F*(1, 24) = 9.153, *MSE* = .005, *H-F p* = .006, *partial* η^2 = .276, driven by a significant increase in

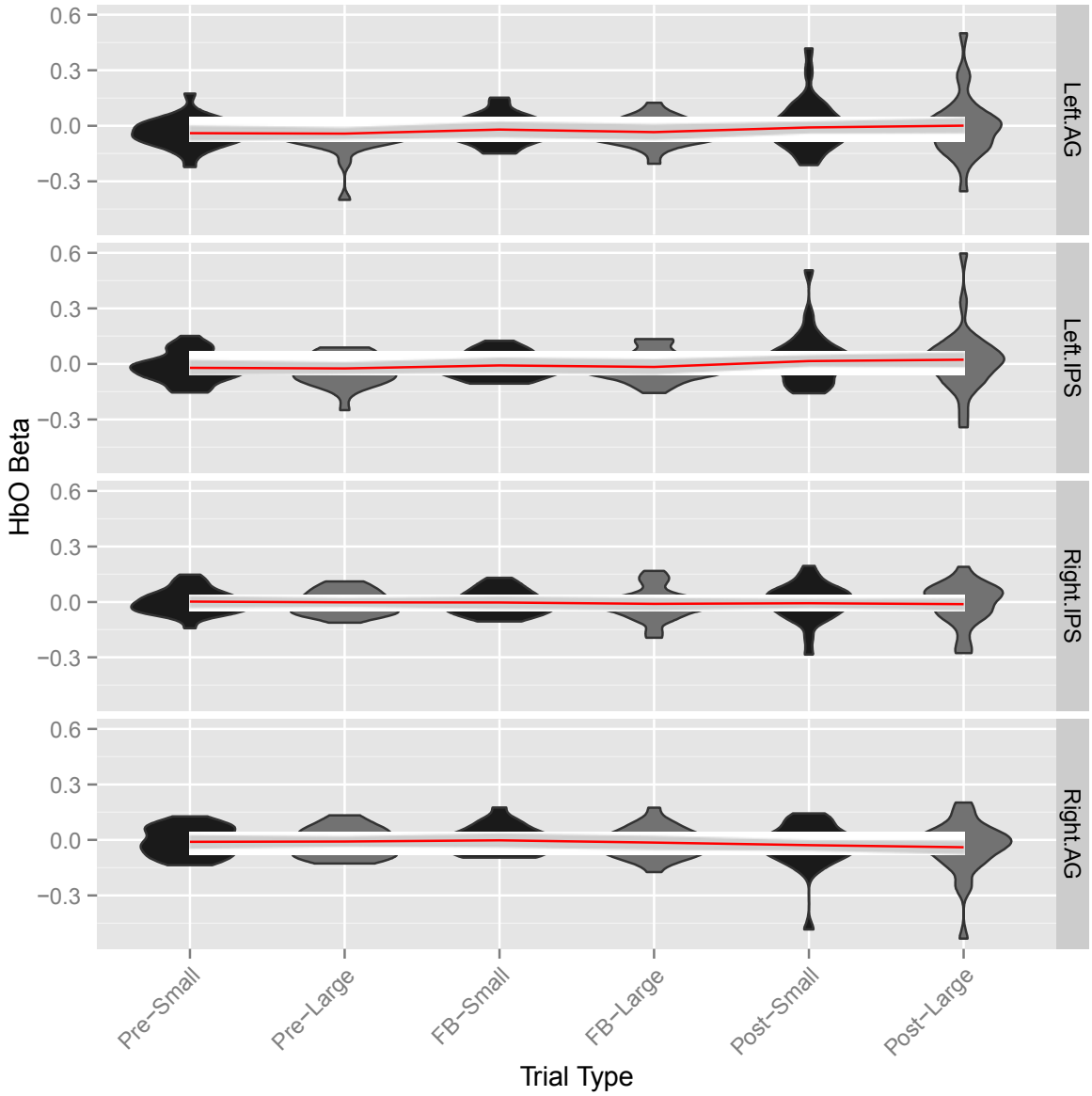

Note. Regions of interest can be seen along each row of the plot above. Trial types are shown along the x-axis. The height of each violin provides an indicator of the distribution of beta values along the y-axis. The width of each plot provides an indicator of the count of beta weights at each point along the y-axis. That is, any portion of the plots that is fatter than another indicates that more beta values occurred at that point on the y-axis compared to a skinnier section. Small-scale estimations are shown in black.

Figure 7. Activation patterns within adults' parietal fROIs.

activation during small scale estimations. Also, while a postfeedback increase in neural activation was present, the effect of block only trended towards significance, $F(1.521, 36.043) = 2.877$, $MSE = .048$, $H\text{-}F\ p = .082$, $partial\ \eta^2 = .107$. Within the left angular gyrus, an identical effect of scale was also identified, $F(1, 24) = 5.099$, $MSE = .007$, $H\text{-}F\ p = .033$, $partial\ \eta^2 = .175$. However, unlike the left IPS, a significant main effect of condition was also identified, $F(2, 24) = 3.424$, $MSE = .073$, $p = .049$, $partial\ \eta^2 = .222$, which was driven by greater overall activation in response to auditory feedback. Next, a significant main effect of scale was identified in the right angular gyrus, $F(1, 24) = 6.137$, $MSE = .003$, $H\text{-}F\ p = .021$, $partial\ \eta^2 = .204$, which was similarly driven by greater neural activation in response to small scale estimations. No other comparison was significant (see Tables 8-11 for breakdown of adult's parietal fROI beta value comparisons).

Table 8

Breakdown of Adults' Left Intraparietal Sulcus Beta Value Comparisons

Variable	*df*	Sum of squares	Mean square	*F* ratio	*p* value	Partial eta-squared
Block	1.521	.074	.048	2.877	.082	.107
Block x condition	3.043	.128	.042	2.508	.073	.173
Scale	1	.005	.005	9.153	.006[a]	.276
Scale x condition	2	.001	.000	.715	.499	.056
Block x scale	1.884	.000	.000	.152	.848	.006
Block x scale x condition	3.767	.008	.002	1.497	.221	.111
Condition	2	.085	.043	2.972	.070	.198

[a]Significantly greater activation for small- compared to large-scale estimations.

Table 9

Breakdown of Adults' Left Angular Gyrus Beta Value Comparisons

Variable	*df*	Sum of squares	Mean square	*F* ratio	*p* value	Partial eta-squared
Block	1.457	.058	.040	1.151	.244	.057
Block x condition	2.914	.082	.028	1.026	.391	.079
Scale	1	.007	.007	5.099	.033[a]	.175
Scale x condition	2	.002	.001	.594	.560	.047
Block x scale	1.632	.001	.001	.321	.683	.013
Block x scale x condition	3.264	.009	.003	1.386	.260	.104
Condition	2	.147	.073	3.424	.049[b]	.222

[a]Significantly greater activation for small- compared to large-scale estimations.
[b]Significantly greater activation within the auditory feedback condition.

Table 10

Breakdown of Adults' Right Intraparietal Sulcus Beta Value Comparisons

Variable	*df*	Sum of squares	Mean square	*F* ratio	*p* value	Partial eta-squared
Block	2	.002	.001	.093	.912	.004
Block x condition	4	.078	.20	2.104	.095	.149
Scale	1	.002	.002	3.830	.062	.138
Scale x condition	2	.002	.001	1.432	.258	.107
Block x scale	2	.000	.00007	.004	.957	.002
Block x scale x condition	4	.013	.003	1.777	.149	.129
Condition	2	.055	.028	1.671	.209	.122

Table 11

Breakdown of Adults' Right Angular Gyrus Beta Value Comparisons

Variable	*df*	Sum of squares	Mean square	*F* ratio	*p* value	Partial eta-squared
Block	1.762	.022	.013	.693	.488	.028
Block x condition	3.524	.072	.020	1.113	.359	.085
Scale	1	.003	.003	6.137	.021[a]	.204
Scale x condition	2	.001	.000	.894	.422	.069
Block x scale	1.974	.001	.000	.198	.818	.008
Block x scale x condition	3.949	.008	.002	1.426	.240	.106
Condition	2	.024	.012	.526	.598	.042

[a]Significantly greater activation for small- compared to large-scale estimations.

Discussion

The behavioral results from Experiment 1 indicate that, despite restricting adults' response time and subjecting them to extremely large-scale estimations, adults performed very accurately and exhibited estimation performance that was better fit by a linear than logarithmic function (see Figure 4). Thus, these results corroborate the claims of past researchers, which suggest that adults perform linearly on number line estimation tasks despite the scale magnitude. Furthermore, the significant increase in accuracy between the prefeedback and feedback blocks, along with the lack of an effect of condition or a block x condition interaction, indicates that each feedback condition was equally beneficial in improving adults' number line estimation performance. Interestingly, adults consistently overestimated the location of the lowest values on each scale (e.g., the values that lay on the far left side of the number line), while slightly underestimating the location of larger values along each scale. This can be seen in Figure 4 by the trend line of each subplot rising above the checkered black line with a intercept of zero and a slope of one (i.e., perfect performance) on the far left end of each line. Conversely, nearly all of the adults estimations of values that lied within the middle and far right side of the line were slightly underestimated, which can be seen by the trend line dipping slightly below the checkered line. Furthermore, the linear nature of each block x scale estimation is apparent in Figure 4.

The response time main effect of block indicated that, while learning in response to this feedback or learning over time in this task, adults are capable of maintaining high levels of accuracy while decreasing their overall response time. As was seen in Figure 5,

the median values for the small-scale estimations (i.e., black box-and-whisker plots) were consistently lower than the large-scale estimations. Furthermore, the height of the each box consistently decreased from pre- to postfeedback, highlighting the block main effect.

Based on findings reported in previous research (see Arsalidou & Taylor, 2011) suggesting that PFC activity is increased when numerical problems increase in difficulty, it was hypothesized that large-scale estimations would elicit greater PFC activity. In contrast to this hypothesis, current results show that small-scale estimations elicited greater activity in each of the regions of interest within the PFC (see Figure 6). Because this increased activity coincided with faster response times to small- compared to large-scale estimations, these results may reflect greater post-estimation thought processes following small-scale estimations, as participants had a greater amount of time to reflect on their estimation performance on such trials. Thus, one possibility for our divergent results is that the PFC may not have been contributing significantly to the estimation process per se.

Apparent in Figure 6 is the fact that some participants exhibited large fluctuations in their prefrontal fROIs in the feedback and postfeedback conditions. This pattern can be seen in the large shift along the y-axis of each violin plot following the prefeedback condition. Conversely, the prefeedback violins are much shorter, which indicates that the neural activation patterns in the prefeedback conditions were more homogenous than within the feedback and postfeedback blocks. The main effect of scale can be seen in Figure 6 by the trend line rising slightly within each small-scale (i.e., black) violin plot.

The significant effect of scale within the left IPS corroborates previous findings that identify similar activation in response to other numerical processing in adults

(Arsalidou & Taylor, 2011; Dehaene et al., 2003; Delazer et al., 2005). Furthermore, greater left IPS response to small- compared to large-scale estimations supports my hypothesis that parietal activation will be increased for "easy" scale estimations. A similar effect of scale within the left angular gyrus indicates that greater amounts of verbal numerical reasoning may have been occurring as adults negotiated small-scale estimations (Arsalidiou & Taylor, 2011). Further, the effect of condition within the left angular gyrus indicates that such verbal numerical reasoning was greatest in the visual feedback condition, although this effect was nearly insignificant ($p = .049$).

Given the significant involvement of the right angular gyrus in visuospatial attention and fact retrieval (Arsalidou & Taylor, 2011; Zenon, Filali, Duhamel, & Oliver, 2010), the significant effect of scale on this region suggests that adults may have been engaging in greater amounts of visuospatial processing as scales rose in magnitude. Previous findings suggest that humans possess an "eye-centered" spatial viewpoint of their mental number lines (Dehaene et al., 1993). Therefore, these results suggest that adults' mental number lines may be extended due to scale increases, and as such, greater visuospatial processing may be needed to navigate such large-scale mental number lines. Interestingly, this result coincides with a slowing of response times to large compared to small scale estimations, which is expected if adults truly are navigating a larger mental number line. This explanation is supported elsewhere, such as within Kosslyn, Ball, and Reiser (1978), and Finke and Pinker (1982) tests of mental imagery scanning. Here, adults memorized a visual scene. When asked to generate a mental image of the scene and to scan across to specific locations, response times were linearly related to the actual distance between locations on the map (Finke & Pinker, 1982; Kosslyn et al., 1978).

Perhaps most apparent in the visualization of the parietal activation patterns (see Figure 7) is the large amount of postfeedback fluctuation that occurs in each fROI. For example, the final two violins in the top two rows of Figure 7 (i.e., left IPS and AG, respectively) both exhibit a large positive up-shoot in their shape, indicating that the neural responses for a subset of participants was markedly positively increased. Conversely, a nearly identical negative down-shoot can be seen in the shape of the violins relating to both right parietal fROIs, indicating that a subset of participants exhibited significant decreases right parietal regions following feedback.

CHAPTER III

EXPERIMENT 2

The Effect of Intersensory Redundancy on Number Line Estimation Accuracy and Hemodynamic Response Patterns in Children

As discussed above, accurate number line estimations correlate highly with standardized assessments of mathematics aptitude (Seigler & Booth, 2004). Accurate performance on this task is arguably most important within the second- and third-grade years, as these are the years when children truly begin formal mathematics education (Siegler & Booth, 2004). Positive results in children of this age group on the current task could ultimately have implications for mathematics teachers who struggle with facilitating linear estimations in their students. Previous attempts to facilitate accurate number line estimations in children involve extensive material preparation and intensive training on the part of the instructor and student (Thompson & Opfer, 2010). A simpler method could be to employ intersensory redundancy within virtual number line teaching tools, which may enhance children's psychophysical representations of number and number line estimation abilities. Here, the effect of intersensory redundancy on facilitating number line estimation accuracy in children is tested. Moreover, concurrent neurological observation provided by NIRS will highlight the neurological activity that relates to number line estimations in typically developing children.

Participants

Twenty-three second- and third-grade students (second grade = 9, third grade = 14, female = 16) participated in the study.[2] Two additional children were recruited but did not finish the session due to illness and an unwillingness to wear the NIRS cap, respectively, and are therefore not included. The majority of children were recruited by way of their affiliation with Dr. Kerry Jordan's Multisensory Cognition Lab (MCL). That is, as infant and child participants are recruited for studies within the MCL, records are generated regarding the children's age, number and age of siblings, and the parents' willingness to bring their children in again in the future. These records are then added to a large database of past participants. For the current experiment, a subset of this database was generated that contained only children within the target age range and who expressed a willingness to come back into the lab. The parents of these children were then contacted directly. Following participation, each of these participants was then asked if they had friends who may also want to participate, and if so, to contact Joseph Baker by email or telephone. Another subset of participants was told of the study by other researchers who were actively involved in other research with children within the target age range. Similar to the procedure described above, the parents of these children were told to contact Joseph Baker by email or telephone if they were interested in having their child participate in the study. Each child was given a gift certificate to Aggie Ice Cream for his/her participation. All participants were typically developing, of normal intelligence,

[2] Because a significant main effect of scale on estimation accuracy was identified with 23 participants, and the original power analysis was geared towards this effect, it was determined that such a sample size was sufficient for the current study.

had normal hearing and normal or corrected to normal vision and were native English speakers.

Setting and Apparatus

All settings and apparati were identical to those in Experiment 1. The only difference between Experiments 1 and 2 were the scales within which the children estimated ("one hundred" and "one hundred thousand" instead of those used with adults). Similarly, the same NIRS optode arrangement and neurological areas of interest as used in Experiment 1 were used for Experiment 2.

Localization of NIRS Probe Sets and Functional Regions of Interest

All localization procedures were identical to those described for adults above. Furthermore, all regions of interest were identical.

Experimental Design and Procedure

See Figure 3 for trial structure schematic. The design and procedure used in Experiment 2 were identical to those used in Experiment 1, save for an extra second of estimation statement presentation to allow the children more time to read. A pilot study of these procedures prior to NIRS scanning was used to determine the appropriateness of this time length. This decision was made because the children in the pilot study were able to complete the task with very few no-response trials, as well as producing consistent (i.e., nonrandom) data. Therefore, each trial within the pre- and postfeedback blocks of the task lasted exactly 8 seconds, and the feedback block lasted exactly 10 seconds. See

Appendix B for child trial structure.

Behavioral Data Analysis and Outcomes

The behavioral data analyses techniques used in Experiment 2 were identical to those conducted in Experiment 1, except that all analyses also included a "grade" variable to identify main effects and interactions across children of different grades (Rosenberg-Lee et al., 2011).

First, a 3 (block) x 2 (scale) x 3 (feedback condition) x 2 (grade) repeated measures ANOVA was used to assess number line estimation accuracy (see Table 12 for accuracy means and standard deviations). This analysis revealed a significant effect of block on number line estimations, $F(2, 34) = 11.711$, $MSE = 151.769$, $H\text{-}F\ p < .001$,

Table 12

Children's Estimation Accuracy Means and Standard Deviations

		Prefeedback		Feedback		Postfeedback	
Variables		Mean	*SD*	Mean	*SD*	Mean	*SD*
Second grade							
Auditory	One hundred	91.605	6.431	91.373	5.331	93.315	4.063
	One hundred thousand	79.250	22.093	88.778	17.164	92.500	4.647
Visual	One hundred	90.337	8.176	90.176	9.938	91.143	9.133
	One hundred thousand	78.410	21.112	86.064	19.936	88.718	12.098
Audiovisual	One hundred	87.920	11.434	88.106	13.388	85.051	16.006
	One hundred thousand	82.167	15.589	86.050	14.742	76.906	21.466
Third grade							
Auditory	One hundred	88.300	10.540	89.506	12.536	90.239	8.818
	One hundred thousand	79.129	22.695	85.079	18.072	82.946	21.021
Visual	One hundred	93.297	5.310	93.710	9.818	94.634	4.500
	One hundred thousand	83.660	18.029	89.347	14.833	89.030	13.839
Audiovisual	One hundred	91.506	7.721	91.919	7.742	92.165	6.756
	One hundred thousand	81.826	16.468	90.792	8.915	90.431	11.087
Combined	One hundred	90.494	8.269	90.798	9.792	91.091	8.213
	One hundred thousand	80.740	19.331	87.685	15.610	86.755	14.026

partial η^2 = .408, which resulted from an increase in estimation accuracy as the task progressed (see Figure 8). Follow-up pairwise comparisons with Bonferroni corrections indicated that the prefeedback block accuracy was significantly lower than the feedback block ($p < .001$), as well as the postfeedback block ($p = .003$). The feedback and postfeedback blocks did not differ in accuracy ($p > .05$). Moreover, repeated measures ANOVA revealed a significant effect of scale, $F(1, 34) = 7.20$, $MSE = 968.229$, *H-F* $p = .016$, *partial* $\eta^2 = .298$, driven by significantly lower accuracy on large compared to small estimation scales. Furthermore, a significant block x scale interaction was identified, $F(2, 34) = 11.379$, $MSE = 112.127$, *H-F* $p < .001$, *partial* $\eta^2 = .401$, which resulted from particularly poor estimation performance on large scales in the prefeedback block. Next, a significant three-way block x condition x grade interaction, $F(4, 34) = 3.877$, $MSE = 50.247$, *H-F* $p = .001$, *partial* $\eta^2 = .313$, was driven by significantly greater prefeedback accuracy in the auditory feedback condition. This effect was exacerbated for small-scale estimations, leading to a significant four-way block x condition x grade x scale interaction, $F(4, 34) = 2.766$, $MSE = 27.255$, *H-F* $p = .043$, *partial* $\eta^2 = .246$. No other main effects or interactions were significant (see Table 13 for a breakdown of children's estimation accuracy comparisons).

See Table 14 for children's response time means and standard deviations. An identical 3 x 2 x 3 x 2 repeated measures ANOVA of response times revealed a significant effect of block, $F(2, 34) = 3.544$, $MSE = 269506.273$, *H-F* $p = .040$, *partial* $\eta^2 = .173$, which was driven by an overall decrease in reaction times as the task progressed (see Figure 9). Individual pairwise comparisons with Bonferroni corrections indicated

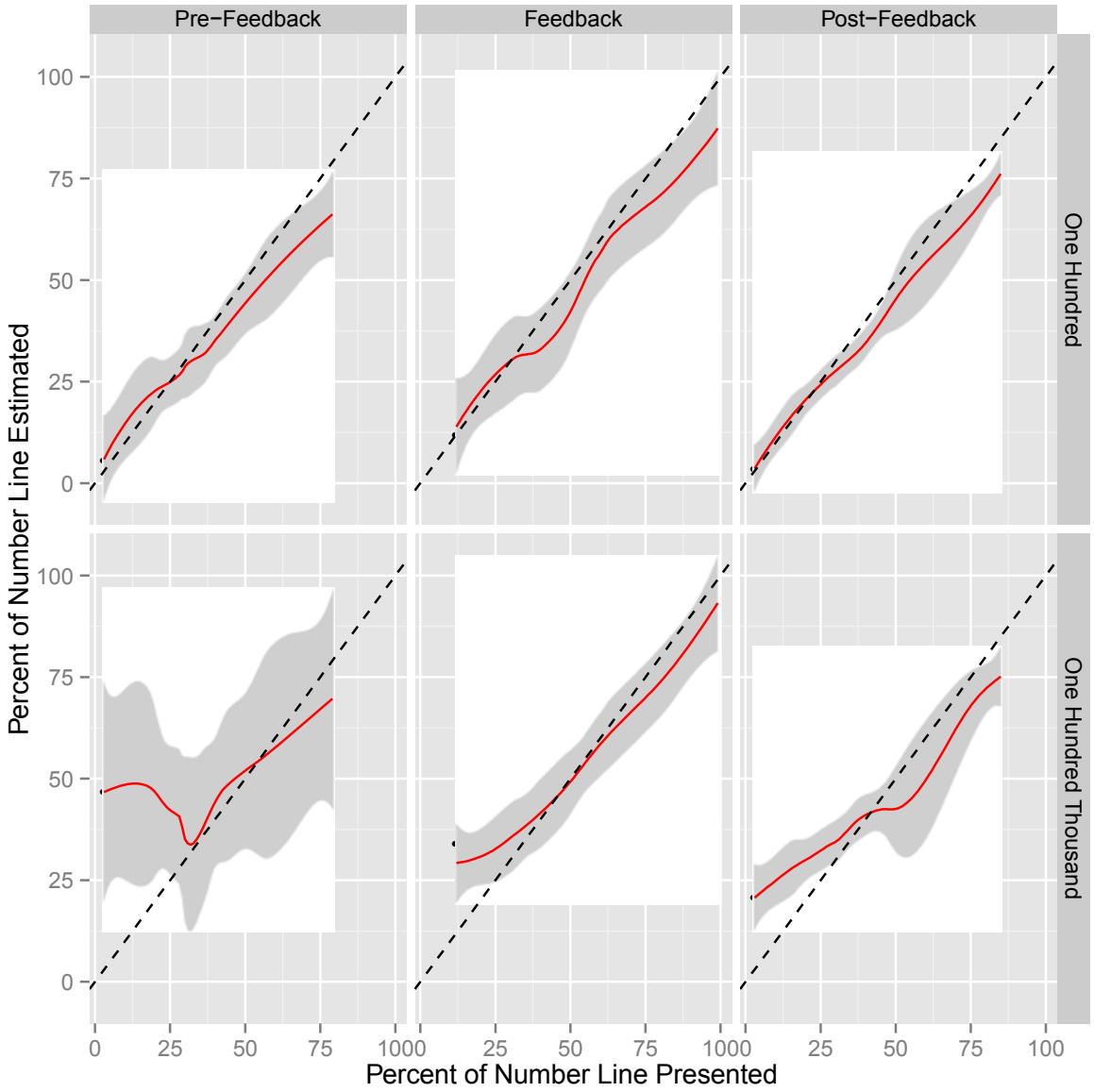

Note. Perfect performance is seen within each subplot by the checkered line with an intercept of 0 and a slope of 1. Each dot represents the average estimation location (y-axis) for each estimation value (x-axis) within each block x scale condition. A trend line has been overlaid to highlight the average overall performance and standard error (shaded area surrounding each trend line) within each condition. A trend line that lies below the perfect performance line indicates a tendency to underestimate the correct location on the line.

Figure 8. Children's block x scale estimation performance.

Table 13

Breakdown of Children's Estimation Accuracy Comparisons

Variable	*df*	Sum of squares	Mean square	*F* ratio	*p* value	Partial eta-squared
Block	2	303.538	151.769	11.711	.000[a]	.408
Block x condition	4	104.795	26.199	2.022	.113	.192
Block x grade	2	1.289	.645	.050	.952	.003
Block x condition x grade	4	200.987	50.247	3.877	.011[b]	.313
Scale	1	968.229	968.229	7.200	.016[c]	.298
Scale x condition	2	19.362	9.681	.072	.931	.008
Scale x grade	1	.092	.092	.001	.979	.000
Scale x condition x grade	2	4.862	2.431	.018	.982	.002
Block x scale	2	224.254	112.127	11.379	.000[d]	.401
Block x scale x condition	4	20.038	5.009	.508	.730	.056
Block x scale x grade	2	6.431	3.216	.326	.724	.019
Block x scale x condition x grade	4	109.021	27.255	2.766	.043[e]	.246
Condition	2	81.490	40.745	.121	.887	.007
Grade	1	86.104	86.104	.256	.619	.004
Condition x grade	2	355.651	177.825	.528	.599	.008

[a]Estimation accuracy improved from pre- to postfeedback.
[b]Prefeedback accuracy in second-grade children was greatest in the audiovisual feedback condition.
[c]Estimation accuracy was significantly greater for small- compared to large-scale estimations.
[d]Driven by very poor performance in for large-scale estimations in the prefeedback condition.
[e]The 3-way interaction found in ^{2} was exacerbated in small-scale estimations.

Table 14

Children's Estimation Response Time Means and Standard Deviations

		Prefeedback		Feedback		Postfeedback	
Variables		Mean	*SD*	Mean	*SD*	Mean	*SD*
Second grade							
Auditory	One hundred	1822.200	703.775	1752.421	660.942	1782.842	659.007
	One hundred thousand	1863.600	745.027	1801.000	676.168	1934.750	575.573
Visual	One hundred	1882.550	491.142	1872.447	622.9827	2016.077	699.984
	One hundred thousand	2079.950	569.2129	2223.513	625.3426	1975.368	754.700
Audiovisual	One hundred	2002.500	880.769	1872.567	779.226	1739.414	819.456
	One hundred thousand	2119.857	789.354	1970.300	861.534	1779.448	731.036
Third grade							
Auditory	One hundred	1938.040	589.406	1871.460	665.426	1717.812	618.704
	One hundred thousand	2052.182	714.131	1875.125	541.399	1817.653	693.492
Visual	One hundred	2479.051	619.219	2123.351	622.980	2150.429	584.510
	One hundred thousand	2379.868	667.5627	2306.083	599.1616	2285.718	703.599
Audiovisual	One hundred	2221.717	582.444	2294.787	566.259	1957.714	567.778
	One hundred thousand	2481.587	603.630	2442.310	671.134	2291.104	611.692
Combined	One hundred	2057.676	644.459	1964.506	652.969	1894.048	658.240
	One hundred thousand	2162.841	681.486	2103.055	662.457	2014.007	678.349

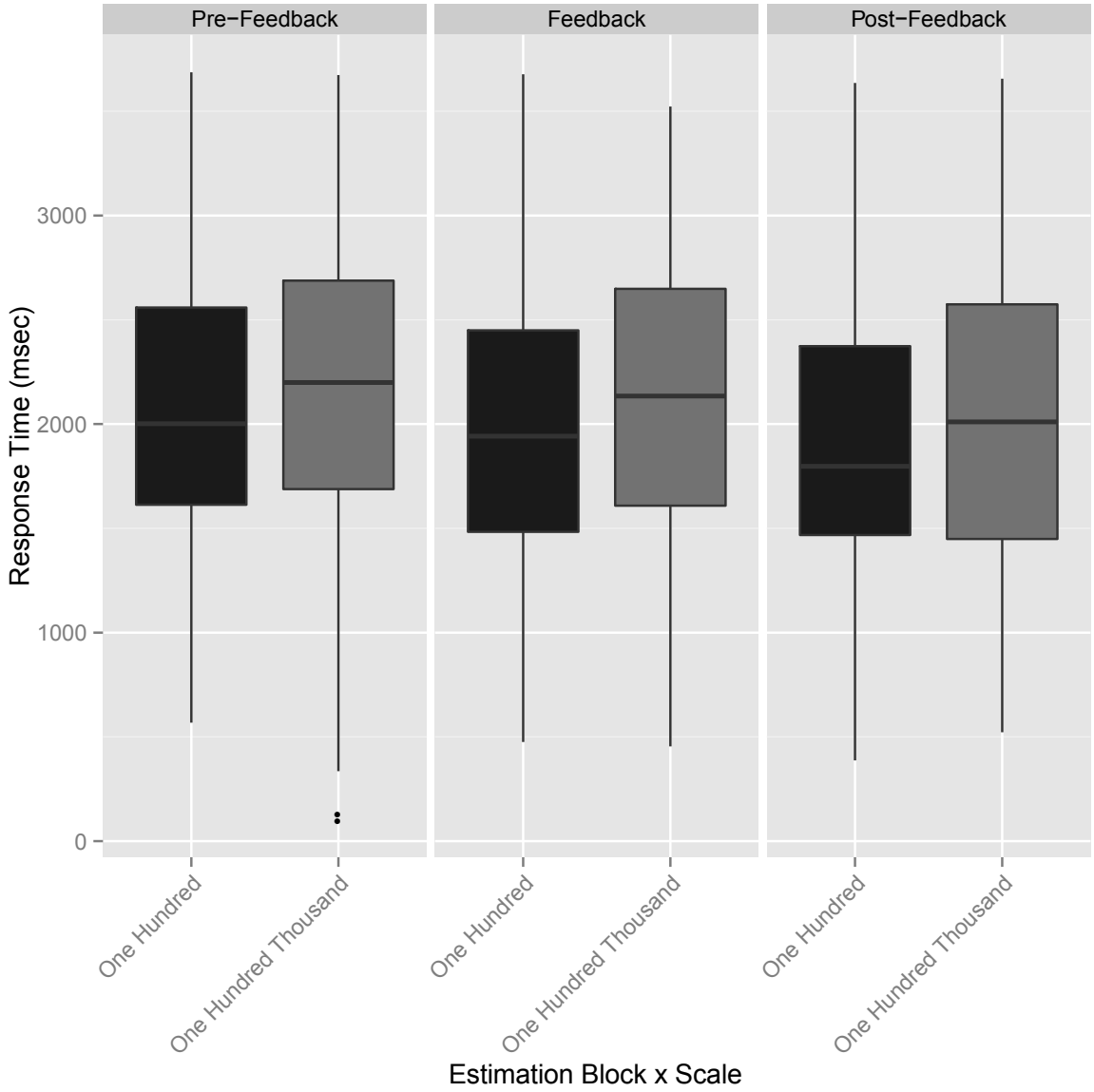

Note. The bold line in the middle of each boxplot represents the median response time for each scale. Seventy-five percent of response time values fall below the top line of each box, while 25% fall below the bottom line of each box. The lines extending from each box (e.g., whiskers) provide an indicator of the range of values along the y-axis.

Figure 9. Children's response times across each block x scale interaction.

that postfeedback response times were nearly significantly faster than prefeedback response times (p = .074). No other pairwise comparison approached significance. Next, a significant main effect of scale was also identified, $F(1, 17) = 8.812$, MSE = 478162.616, $H\text{-}F\ p$ = .009, $partial\ \eta^2$ = .341, which resulted from significantly longer response times for large scale estimations compared to small scale estimations (see Table 15 for a breakdown of children's response times comparisons).

Next, in order to identify whether a linear or logarithmic function best fit the correlation between estimation accuracy and scale across each experimental condition and grade level, a combination of linear and non-linear regression analyses were conducted for each scale x block x grade possibility. Consistent with previous studies (Siegler & Opfer, 2003; Thompson & Opfer, 2008, 2010), median values were used to reduce impact of outliers at group level (although similar logarithmic and linear fits were obtained with mean values). Similar to the estimation results in adults, a linear function best fit each scale x block pair for both second grade (small scale x prefeedback: linear R^2 = .878 > logarithmic R^2 = .880; small scale x feedback: linear R^2 = .957 > logarithmic R^2 = .823; small scale x postfeedback: linear R^2 = .989 > .711; large scale x prefeedback: linear R^2 = .071 > logarithmic R^2 = .017; large scale x feedback: linear R^2 = .948 > logarithmic R^2 = .797; large scale x postfeedback: linear R^2 = .951 > logarithmic R^2 = .598) and third grade (small scale x prefeedback: linear R^2 = .963 > logarithmic R^2 = .688; small scale x feedback: linear R^2 = .965 > logarithmic R^2 = .881; small scale x postfeedback: linear R^2 = .991 > .708; large scale x prefeedback: linear R^2 = .602 > logarithmic R^2 = .282; large scale x feedback: linear R^2 = .972 > logarithmic R^2 = .858; large scale x postfeedback: linear R^2 = .977 > logarithmic R^2 = .654).

Table 15

Breakdown of Children's Estimation Response Time Comparisons

Variable	*df*	Sum of squares	Mean square	*F* ratio	*p* value	Partial eta-squared
Block	2	539012.545	269506.273	3.544	.040[a]	.173
Block x condition	4	180363.026	45090.757	.593	.670	.065
Block x grade	2	106277.072	53138.536	.699	.504	.039
Block x condition x grade	4	230337.207	57584.302	.757	.560	.082
Scale	1	478162.616	478162.616	8.812	.009[b]	.341
Scale x condition	2	39909.024	18854.512	.347	.711	.039
Scale x grade	1	1357.831	1357.831	.025	.876	.001
Scale x condition x grade	2	97085.023	48542.511	.895	.427	.095
Block x scale	1.920	3932.497	2048.574	.053	.943	.003
Block x scale x condition	3.839	121886.353	31747.415	.826	.514	.089
Block x scale x grade	1.920	49874.282	25981.244	.676	.510	.038
Block x scale x condition x grade	3839	84082.571	21900.764	.570	.680	.063
Condition	2	1861432.148	930716.074	1.200	.325	.082
Grade	1	1730007.567	1730007.567	2.231	.154	.092
Condition x grade	2	481530.948	240765.474	.311	.737	.038

[a]Response times increased from pre- to postfeedback.
[b]Response times were faster for small- compared to large-scale estimation.

NIRS Data Analysis and Outcomes

All NIRS data were processed and treated in the exact same manner as reported in Experiment 1 above. Moreover, all fROIs were identical as those in Experiment 1. Finally, all statistical analyses were identical to those in Experiment 1, save for the addition of a grade factor that was introduced to capture any influence of educational development on neurological responses to number line estimations.

Prefrontal fROI Analyses

See Tables 16 and 17 for children's fROIs beta value means and standard deviations within second- and third-grade children, respectively. First, a 3 (block) x 2

Table 16

Second-Grade Children's fROI Beta Means and Standard Deviations

		Frontal ROIs				Parietal ROIs							
		Medial PFC		Left DLPFC		Left IPS		Left AG		Right IPS		Right AG	
Variable	Size	Beta	*SD*	Beta	*SD*	Beta	*SD*	Beta	*SD*	Beta	*SD*	Beta	*SD*
Auditory													
Prefeedback	Small	-4.933	11.935	-.366	5.589	-.124	13.087	4.653	6.700	-3.948	11.603	-4.953	6.770
	Large	-.663	8.824	.823	4.885	2.361	11.562	7.636	5.452	2.100	7.989	-.258	3.724
Feedback	Small	6.860	1.882	6.564	2.184	10.815	1.743	16.449	4.422	20.925	9.423	14.768	7.791
	Large	8.325	3.836	7.369	3.685	11.238	1.744	19.780	5.661	24.438	11.937	23.726	19.274
Postfeedback	Small	-6.253	5.944	-3.311	2.371	6.830	10.348	6.109	9.497	-8.541	11.646	-13.350	18.675
	Large	-6.251	5.390	-3.257	2.650	7.446	13.499	7.076	14.688	-5.608	4.376	-7.522	9.064
Visual													
Prefeedback	Small	-3.374	1.831	-2.807	1.732	.303	1.579	-.104	3.049	-.713	4.967	3.857	11.338
	Large	-1.927	1.742	-2.059	2.531	1.585	1.404	2.404	3.831	1.530	4.471	5.945	8.466
Feedback	Small	-.634	1.922	-1.195	3.245	.403	10.351	2.504	6.762	8.013	1.695	7.282	2.302
	Large	-1.201	3.836	-1.645	5.353	-.890	6.638	3.867	5.599	7.114	6.694	5.018	6.587
Postfeedback	Small	-1.066	2.339	-1.195	3.603	.631	4.743	4.829	6.184	.175	6.100	1.832	4.067
	Large	-1.074	3.148	-.930	2.116	2.602	5.776	5.257	7.643	2.983	2.436	3.979	3.519
Audiovisual													
Prefeedback	Small	1.193	3.802	-1.426	5.516	2.765	4.995	2.856	8.436	-.829	4.300	2.659	5.506
	Large	2.387	3.129	-1.311	4.914	5.125	3.909	3.510	6.859	1.234	5.680	3.848	7.704
Feedback	Small	-4.963	1.383	-2.808	2.224	2.286	3.047	3.938	7.165	.923	2.548	5.046	7.163
	Large	-1.96	1.401	-1.127	2.557	4.506	3.276	5.155	5.089	1.570	3.533	5.018	6.587
Postfeedback	Small	2.415	6.234	1.943	3.064	3.223	6.054	6.469	5.316	3.751	4.362	3.233	7.705
	Large	-.279	5.003	.695	2.005	4.711	7.726	8.329	8.926	8.061	6.212	9.904	9.037
Combined													
Prefeedback	Small	-2.371	5.856	-1.533	4.279	0.981	6.554	2.468	6.062	-1.830	6.957	0.521	7.871
	Large	-0.068	4.565	-0.849	4.110	3.024	5.625	4.517	5.381	1.621	6.047	3.178	6.631
Feedback	Small	0.421	1.729	0.854	2.551	4.501	5.047	7.630	6.116	9.954	4.555	9.032	5.752
	Large	1.721	3.024	1.532	3.865	4.951	3.886	9.601	5.450	11.041	7.388	11.254	10.816
Postfeedback	Small	-1.635	4.839	-0.854	3.013	3.561	7.048	5.802	6.999	-1.538	7.369	-2.762	10.149
	Large	-2.535	4.514	-1.164	2.257	4.920	9.000	6.887	10.419	1.812	4.341	2.120	7.207

Table 17

Third-Grade Children's fROI Beta Means and Standard Deviations

		Frontal ROIs				Parietal ROIs							
		Medial PFC		Left DLPFC		Left IPS		Left AG		Right IPS		Right AG	
Variable	Size	Beta	*SD*	Beta	*SD*	Beta	*SD*	Beta	*SD*	Beta	*SD*	Beta	*SD*
Auditory													
Prefeedback	Small	-4.423	2.935	-4.506	.968	-2.972	5.224	-1.072	9.392	-1.097	9.324	-4.038	9.411
	Large	-3.833	2.927	-3.574	.965	-1.448	3.346	-.321	6.267	.287	6.582	-1.520	6.193
Feedback	Small	-.111	2.981	2.478	1.703	1.229	5.963	.628	11.149	4.990	6.175	2.631	6.218
	Large	-6.24	1.558	1.861	1.151	1.997	5.475	2.474	10.253	6.648	6.117	5.206	9.362
Postfeedback	Small	1.784	6.244	-.705	2.698	.277	5.577	-.417	10.395	1.290	6.257	.619	11.856
	Large	1.062	6.640	.072	5.103	-1.287	4.517	.052	5.763	.337	6.683	.463	7.017
Visual													
Prefeedback	Small	.932	7.733	.563	3.33	1.975	5.638	2.717	2.416	2.215	3.416	1.845	2.218
	Large	2.441	7.892	.946	3.098	2.727	2.627	3.314	2.985	.783	3.607	3.364	3.843
Feedback	Small	-1.095	3.324	-1.470	2.549	2.033	1.334	-.259	4.201	1.423	3.392	4.740	6.368
	Large	.957	3.756	.064	4.231	2.617	2.115	-.013	3.166	4.112	3.229	6.188	6.443
Postfeedback	Small	-.764	6.244	2.110	9.674	6.995	10.786	3.009	7.319	7.046	7.562	9.519	6.142
	Large	1.607	5.032	3.458	7.421	8.657	8.044	4.835	5.564	7.276	8.200	10.735	9.732
Audiovisual													
Prefeedback	Small	-1.956	4.717	-3.673	1.389	.029	4.221	-5.650	7.159	-5.029	6.670	-5.826	4.152
	Large	-1.404	2.883	-2.333	1.827	.690	5.743	-2.998	6.667	-2.328	9.889	-3.518	5.290
Feedback	Small	2.301	4.871	2.576	4.717	-1.015	5.980	-2.994	4.863	.9592	5.810	-1.1469	6.953
	Large	-.278	2.315	-.121	3.087	-1.052	3.688	-3.854	5.529	-.319	4.731	-2.071	8.666
Postfeedback	Small	-1.711	2.561	-2.859	3.691	-4.307	5.958	-5.409	7.327	-2.157	7.929	-5.854	8.698
	Large	-1.082	3.100	-1.546	3.630	-2.117	5.040	-1.786	4.475	-.939	6.748	-3.479	6.504
Combined													
Prefeedback	Small	-1.816	5.128	-2.539	1.896	-0.323	5.028	-1.335	6.322	-1.304	6.470	-2.673	5.260
	Large	-0.932	4.567	-1.654	1.963	0.656	3.905	-0.002	5.306	-0.419	6.693	-0.558	5.109
Feedback	Small	0.365	3.725	1.195	2.990	0.749	4.426	-0.875	6.738	2.457	5.126	2.075	6.513
	Large	-1.854	2.543	0.601	2.823	1.187	3.759	-0.464	6.316	3.480	4.692	3.108	8.157
Postfeedback	Small	-0.230	5.016	-0.485	5.354	0.988	7.440	-0.939	8.347	2.060	7.249	1.428	8.899
	Large	0.529	4.924	0.661	5.385	1.751	5.867	1.034	5.267	2.225	7.210	2.573	7.751

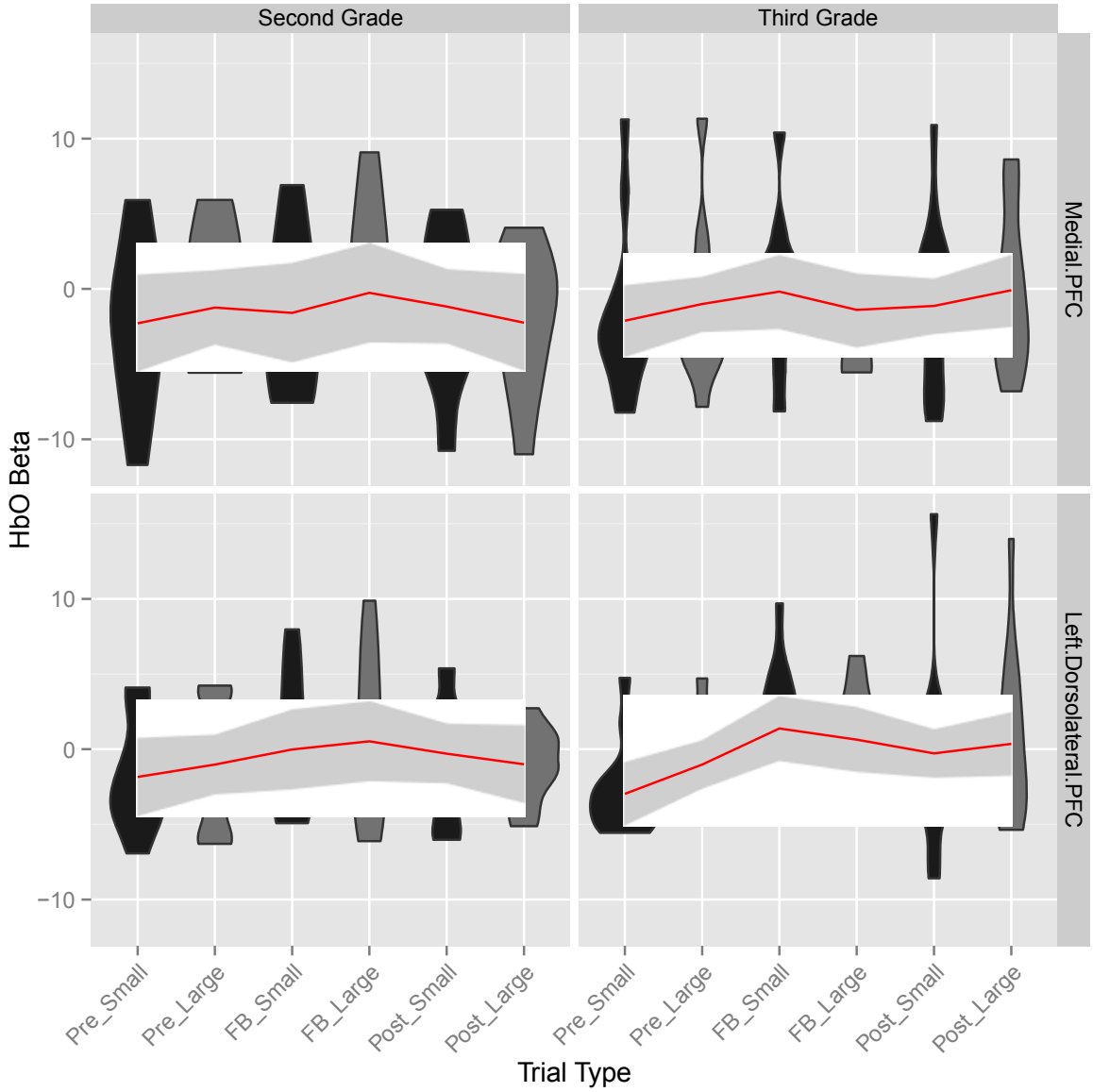

Note. Regions of interest can be seen along each row of the plot above, while grade can be seen within the columns. Trial types are shown along the x-axis. The height of each violin provides an indicator of the distribution of beta values along the y-axis. The width of each plot provides an indicator of the count of beta weights at each point along the y-axis. That is, any portion of the plots that is fatter than another indicates that more beta values occurred at that point on the y-axis compared to a skinnier section. Small-scale estimations are shown in black.

Figure 10. Activation patterns within the children's prefrontal fROIs.

(scale) x 3 (feedback condition) x 2 (grade) repeated measures ANOVA of O_2Hb response patterns in children's medial PFC identified a significant block x scale interaction, $F(2, 34) = 4.373$, $MSE = 8.455$, $H\text{-}F\ p = .020$, $partial\ \eta^2 = .205$, which was driven by significantly greater activation for large- compared to small-scale estimations within the prefeedback block of the task ($p < .001$), followed by comparable activation for both scales following the prefeedback block. Furthermore, a significant three-way block x condition x grade interaction, $F(4, 34) = 3.379$, $MSE = 125.361$, $H\text{-}F\ p = .020$, $partial\ \eta^2 = .284$, indicated that activation within second-grade children during auditory feedback was significantly greater than the pre- ($p = .039$) or postfeedback ($p = .011$) blocks. Similarly, a significant block x scale x grade interaction, $F(2, 34) = 5.763$, $MSE = 11.144$, $H\text{-}F\ p = .007$, $partial\ \eta^2 = .253$, indicated that both second and third-grade children demonstrated significantly greater activation for large scale estimations within the prefeedback block of the task ($p < .05$). Next, within the dorsolateral PFC, repeated measures ANOVA revealed a significant effect of block, $F(2, 34) = 3.594$, $MSE = 75.567$, $H\text{-}F\ p = .038$, $partial\ \eta^2 = .175$. Pairwise comparisons with Bonferroni corrections indicated that activation increased significantly from the prefeedback block to the feedback block ($p = .027$), indicating that neural activation within the dorsolateral PFC increased when feedback was provided. Moreover, a significant block x condition interaction, $F(4, 34) = 3.190$, $MSE = 67.071$, $H\text{-}F\ p = .025$, $partial\ \eta^2 = .273$, indicated that the increase in neural activation within the feedback block was greatest in the auditory feedback condition. No other comparisons within the dorsolateral were significant (see Tables 18 and 19 for breakdown of prefrontal ROI beta value comparisons; see Figure 10 for activation patterns within children's prefrontal fROIs).

Table 18

Breakdown of Children's Medial Prefrontal Beta Value Comparisons

Variable	*df*	Sum of squares	Mean square	*F* ratio	*p* value	Partial eta-squared
Block	2	73.441	36.720	.990	.382	.055
Block x condition	4	313.108	78.277	2.110	.101	.199
Block x grade	2	64.288	32.144	.866	.430	.048
Block x condition x grade	4	501.445	125.361	3.379	.020[a]	.284
Scale	1	9.763	9.763	2.917	.106	.146
Scale x condition	2	4.817	2.408	.720	.501	.078
Scale x grade	1	3.613	3.613	1.080	.313	.060
Scale x condition x grade	2	13.478	6.739	2.014	.164	.192
Block x scale	2	16.910	8.455	4.373	.020[b]	.205
Block x scale x condition	4	9.930	2.482	1.284	.296	.131
Block x scale x grade	2	22.289	11.144	5.763	.007[c]	.253
Block x scale x condition x grade	4	18.998	4.750	2.456	.064	.224
Condition	2	1.872	.936	.026	.974	.003
Grade	1	2.699	2.699	.076	.786	.004
Condition x grade	2	43.626	21.813	.615	.552	.067

[a] Increased activation during feedback was greatest in second-grade children within the auditory feedback condition.
[b] Driven by significantly greater activation during large- compared to small-scale estimations during the prefeedback condition.
[c] The block x scale interaction above was exacerbated within second- compared to third-grade children.

Parietal fROI Analyses

See Figure 11 for activation patterns within children's parietal fROIs. Within the left IPS, identical repeated measures ANOVA of O_2Hb beta weights revealed a significant effect of scale, $F(1, 17) = 5.939$, $MSE = 31.798$, *H-F* $p = .026$, *partial* $\eta^2 = .259$, caused by significantly higher activation during large scale estimations compared to small scale estimations. A significant effect of grade was also identified, $F(1, 17) = 4.955$, $MSE = 248.907$, $p = .04$, *partial* $\eta^2 = .226$, driven by significantly greater activation within second compared to third-grade children. Finally, a significant grade x condition interaction was identified, $F(2, 17) = 6.430$, $MSE = 323.043$, $p = .008$, *partial* $\eta^2 = .431$, which was caused by significantly greater activation for second compared to

Table 19

Breakdown of Children's Left Dorsolateral Prefrontal Beta Value Comparisons

Variable	*df*	Sum of squares	Mean square	*F* ratio	*p* value	Partial eta-squared
Block	2	151.134	75.567	3.594	.038[a]	.175
Block x condition	4	268.283	67.071	3.190	.025[b]	.273
Block x grade	2	21.909	10.955	.521	.599	.030
Block x condition x grade	4	206.825	51.706	2.459	.064	.224
Scale	1	5.391	5.391	1.780	.200	.095
Scale x condition	2	1.950	.975	.322	.729	.037
Scale x grade	1	.135	.135	.045	.835	.003
Scale x condition x grade	2	2.513	1.257	.415	.667	.047
Block x scale	2	2.832	1.416	.630	.538	.036
Block x scale x condition	4	1.815	.454	.202	.936	.023
Block x scale x grade	2	9.650	4.825	2.148	.132	.112
Block x scale x condition x grade	4	20.357	5.089	2.265	.082	.210
Condition	2	32.450	16.225	.462	.637	.052
Grade	1	.032	.032	.001	.976	.000
Condition x grade	2	119.304	59.652	1.700	.212	.167

[a]Activation was greatest during the feedback block of the task.
[b]Increased activation during feedback was greatest in the audiovisual feedback condition.

third-grade children within the auditory and audiovisual feedback conditions, as well as significantly greater activation for third compared to second-grade children within the visual feedback condition. Within the left angular gyrus, effects of scale, $F(1, 17) = 12.475$, $MSE = 67.330$, *H-F* $p = .003$, *partial* $\eta^2 = .423$, and grade, $F(1, 17) = 3.068$, $MSE = 273.737$, $p = .001$, *partial* $\eta^2 = .471$, were present, although no effect of grade x condition was identified (*H-F* $p = .073$; see Tables 20 and 21 for breakdown of beta value comparisons in children's left IPS and left angular gyrus, respectively).

Activation patterns in the right IPS differed from that of the left parietal cortex. The effect of scale was present, $F(1, 17) = 17.769$, $MSE = 85.807$, *H-F* $p = .001$, *partial* $\eta^2 = .511$, although the other effects identified within the left parietal cortex were not.

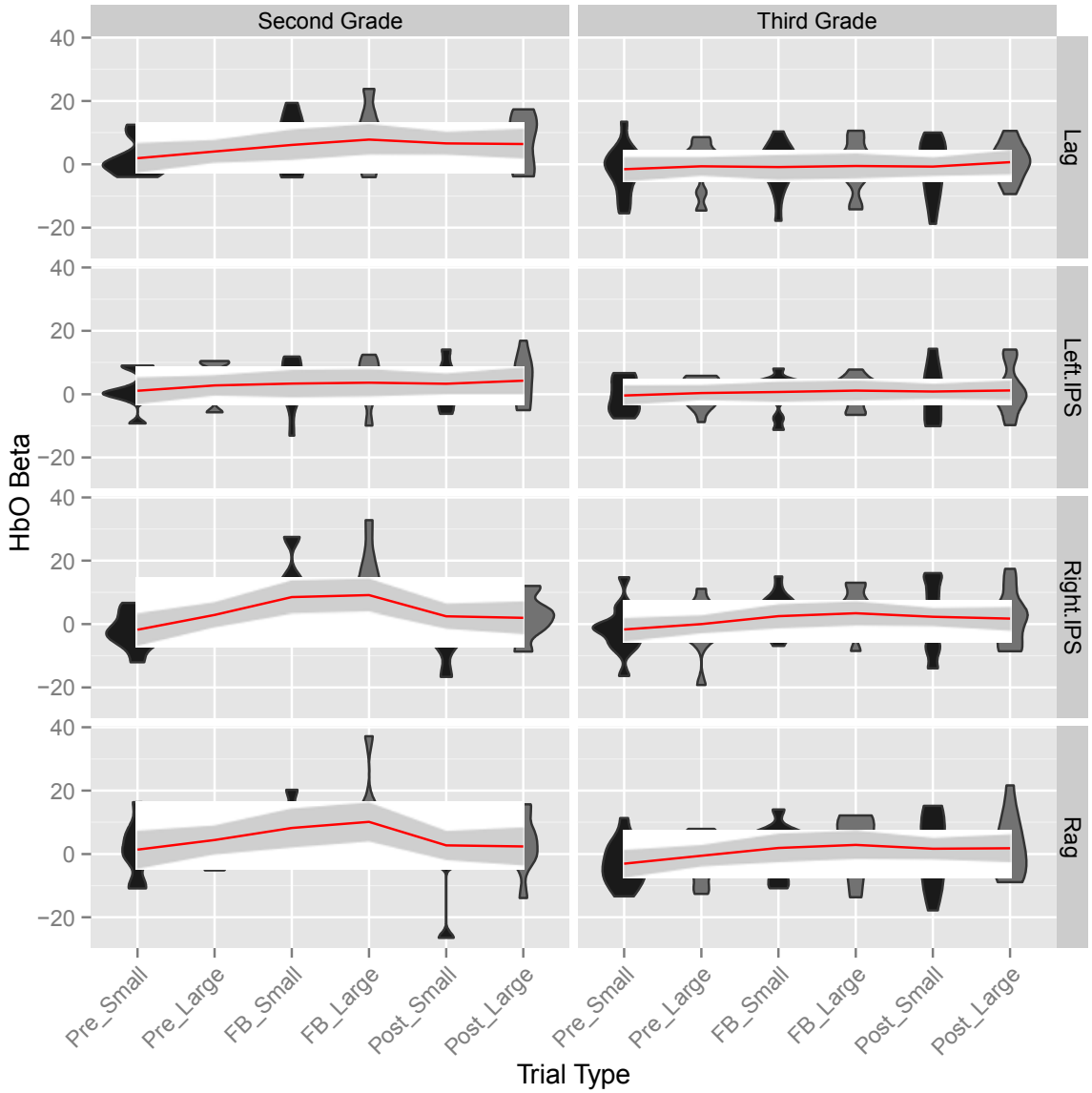

Note. Regions of interest can be seen along each row of the plot above, while grade can be seen within the columns. Trial types are shown along the x-axis. The height of each violin provides an indicator of the distribution of beta values along the y-axis. The width of each plot provides an indicator of the count of beta weights at each point along the y-axis. That is, any portion of the plots that is fatter than another indicates that more beta values occurred at that point on the y-axis compared to a skinnier section. Small-scale estimations are shown in black.

Figure 11. Activation patterns within children's parietal fROIs.

Table 20

Breakdown of Children's Left Intraparietal Sulcus Beta Value Comparisons

Variable	*df*	Sum of squares	Mean square	*F* ratio	*p* value	Partial eta-squared
Block	2	83.638	41.819	.612	.548	.035
Block x condition	4	358.585	89.646	1.311	.285	.134
Block x grade	2	19.241	9.620	.141	.869	.008
Block x condition x grade	4	119.612	29.903	.437	.781	.049
Scale	1	31.798	31.798	5.939	.026[a]	.259
Scale x condition	2	3.584	1.792	.335	.720	.038
Scale x grade	1	2.324	2.324	.434	.519	.025
Scale x condition x grade	2	3.683	1.841	.344	.714	.039
Block x scale	2	5.988	2.994	.459	.636	.026
Block x scale x condition	4	13.547	3.387	.519	.722	.058
Block x scale x grade	2	1.436	.718	.110	.896	.006
Block x scale x condition x grade	4	8.821	2.205	.338	.851	.038
Condition	2	68.589	34.295	.683	.519	.074
Grade	1	248.907	248.907	4.955	.040[b]	.226
Condition x grade	2	646.086	323.043	6.430	.008[c]	.431

[a] Activation was greater in large- compared to small-scale estimations.
[b] Driven by greater activation within second- compared to third-grade children.
[c] Driven by significantly greater activation within second- compared to third-grade children within the auditory and audiovisual feedback conditions, as well as by significantly greater activation within third- compared to second-grade children within the visual feedback condition.

Instead, a significant scale x grade interaction was identified, $F(1, 17) = 6.043$, $MSE = 29.185$, *H-F* $p = .025$, *partial* $\eta^2 = .262$, driven by significantly greater activation during large scale estimations for second-grade children ($p = .001$), but not for third-grade children ($p = .170$). Next, an effect of block, $F(2, 34) = 8.390$, $MSE = 595.432$, *H-F* $p < .001$, *partial* $\eta^2 = .330$, was identified, which was caused by a significant increase in activation during the feedback block of the task. Pairwise comparisons with Bonferroni corrections identified that activation levels in the feedback block were significantly greater than both the prefeedback ($p < .001$) and postfeedback conditions ($p = .021$). Moreover, a significant block x condition interaction, $F(4, 34) = 4.794$, $MSE = 340.199$,

Table 21

Breakdown of Children's Left Angular Gyrus Beta Value Comparisons

Variable	*df*	Sum of squares	Mean square	*F* ratio	*p* value	Partial eta-squared
Block	2	143.235	71.617	.802	.457	.045
Block x condition	4	371.080	92.770	1.039	.405	.109
Block x grade	2	137.613	68.807	.770	.471	.043
Block x condition x grade	4	143.342	35.835	.401	.806	.045
Scale	1	67.330	67.330	12.475	.003[a]	.423
Scale x condition	2	1.706	.853	.158	.855	.018
Scale x grade	1	1.664	1.664	.308	.586	.018
Scale x condition x grade	2	4.825	2.412	.447	.647	.050
Block x scale	2	1.354	.677	.089	.915	.005
Block x scale x condition	4	16.315	4.079	.536	.710	.059
Block x scale x grade	2	8.021	4.010	.527	.595	.030
Block x scale x condition x grade	4	7.886	1.972	.259	.902	.030
Condition	2	416.129	208.065	2.332	.127	.215
Grade	1	1349.480	1349.480	15.126	.001[b]	.471
Condition x grade	2	547.473	279.739	3.068	.073	2.65

[a]Activation was greater in large- compared to small-scale estimations.
[b]Driven by greater activation within second- compared to third-grade children.

H-F p = .004, *partial* η^2 = .361, highlighted a large rise in activation within the feedback block for the auditory compared to the visual (p = .002) and audiovisual (p < .001) conditions. Furthermore, a significant block x grade interaction, $F(2, 34) = 3.522$, *MSE* = 249.960, *H-F p* = .041, *partial* η^2 = .172, indicated greater activation in response to feedback for second compared to third-grade children (p = .004). Finally, a significant three-way block x condition x grade interaction, $F(4, 34) = 2.944$, *MSE* = 208.932, *H-F p* = .034, *partial* η^2 = .257, reinforced the results above suggesting that the rise in activation during feedback was greater for second compared to third-grade children.

An effect of scale was also significant within the right angular gyrus, $F(1, 17) = 17.615$, *MSE* = 188.822, *H-F p* = .001, *partial* η^2 = .509. Similarly, results within the

right angular gyrus indicated a significant effect of block, $F(2, 34) = 4.924$, $MSE = 515.296$, *H-F p* = .013, *partial* $\eta^2 = .225$, as well as a significant block x condition interaction $F(4, 34) = 2.823$, $MSE = 295.467$, *H-F p*= .040, *partial* $\eta^2 = .249$, the causes of which were identical to the right IPS effects reported above. No other main effects or interactions were significant (see Tables 22 and 23 for breakdown of beta value comparions in children's right IPS and right angular gyrus, respectively; see Figure 11 for activation patterns within children's parietal fROIs).

Table 22

Breakdown of Children's Right Intraparietal Sulcus Beta Value Comparisons

Variable	*df*	Sum of squares	Mean square	*F* ratio	*p* value	Partial eta-squared
Block	2	1190.865	595.432	8.390	.001[a]	.330
Block x condition	4	1360.796	340.199	4.794	.004[b]	.361
Block x grade	2	499.919	249.960	3.522	.041[c]	.172
Block x condition x grade	4	835.730	208.932	2.944	.034[d]	.257
Scale	1	85.807	85.807	17.769	.001[e]	.511
Scale x condition	2	11.196	5.598	1.159	.337	.120
Scale x grade	1	29.185	29.185	6.043	.025[f]	.262
Scale x condition x grade	2	8.790	4.395	.910	.421	.097
Block x scale	2	6.584	3.292	.443	.646	.025
Block x scale x condition	4	27.253	6.813	.917	.465	.097
Block x scale x grade	2	14.119	7.059	.951	.397	.053
Block x scale x condition x grade	4	24.593	6.148	.828	.517	.089
Condition	2	276.385	138.193	1.435	.266	.144
Grade	1	1.36.456	136.456	1.417	.250	.077
Condition x grade	2	137.704	68.852	.715	.503	.078

[a] Activation was significantly greater in the feedback block of the task.
[b] Increased activation during feedback was significantly greater in the auditory compared to visual and audiovisual feedback conditions.
[c] Increased activation during feedback was greater in second- compared to third-grade children.
[d] Increased activation during auditory feedback was exacerbated in second- compared to third-grade children.
[e] Activation was significantly greater for large- compared to small-scale estimations.
[f] Increased activation for large- compared to small-scale estimations was exacerbated in second- compared to third-grade children.

Table 23

Breakdown of Children's Right Angular Gyrus Beta Value Comparisons

Variable	*df*	Sum of squares	Mean square	*F* ratio	*p* value	Partial eta-squared
Block	2	1030.593	515.296	4.924	.013[a]	.225
Block x condition	4	1181.869	295.467	2.823	.040[b]	.249
Block x grade	2	547.362	273.681	2.615	.088	.133
Block x condition x grade	4	844.517	211.129	2.017	.114	.192
Scale	1	188.822	188.822	17.615	.001[c]	.509
Scale x condition	2	38.439	19.219	1.793	.197	.174
Scale x grade	1	33.261	33.261	3.103	.096	.154
Scale x condition x grade	2	30.247	15.123	1.411	.271	.142
Block x scale	2	5.570	2.785	.300	.743	.017
Block x scale x condition	4	53.513	13.378	1.441	.242	.145
Block x scale x grade	2	13.325	6.663	.718	.495	.041
Block x scale x condition x grade	4	12.285	3.071	.331	.855	.037
Condition	2	641.444	320.722	2.761	.092	.245
Grade	1	284.258	284.258	2.447	.136	.126
Condition x grade	2	568.575	284.288	2.447	.116	.224

[a] Activation was significantly greater in the feedback block of the task.
[b] Increased activation during feedback was significantly greater in the auditory compared to visual and audiovisual feedback conditions.
[c] Activation was significantly greater for large- compared to small-scale estimations.

Discussion

As expected, children's estimation accuracy improved throughout the task. However, similar to the findings in adults, the lack of a main effect of condition or a block x condition interaction indicates that each type of feedback equally benefitted children's estimation performance. Curiously, the only condition related effects related to children's estimation performance was driven by particularly high prefeedback accuracy, which was greatest for small-scales in particular. While each child was exposed to a small amount of their respective feedback condition prior to beginning the test trials (6 pre-test practice trials with feedback), it is unlikely that this exposure significantly

improved the accuracy of children randomly assigned to this feedback condition. It is likely that this effect was due to chance. Moreover, as predicted, children performed significantly worse on large- compared to small-scale estimations. As is apparent within Figure 8, and consistent with the adults' performance, children also tended to overestimate the estimated location of values on the small end of each scale, while typically underestimating the location on the large end. This tendency is much larger in the large-scale estimation, and is particularly noticeable within the large-scale prefeedback condition.

In contrast with previous studies (Opfer & Seigler, 2007; Siegler & Booth, 2004; Thompson & Opfer, 2010) demonstrating a similar effect of scale on children's estimation performance in response to increases in scale, this decrease in accuracy was not accompanied by an overall better logarithmic rather than linear fit to children's data. Instead, a linear function was shown to be a better fit for all of the children's estimations, despite scale or grade level. The linear fit was greater in each block x scale comparison, and accounted for a significant amount of variance in all but the prefeedback large-scale condition. As was seen in Figure 8, children's performance in this condition was very poor, as children tended to greatly overestimation estimation locations at the low end of the scale, and greatly underestimate locations at the high end. Moreover, the shaded area surrounding the trend line in the prefeedback large-scale subplot in Figure 8 suggests that there was significant variation between participants within this condition.

Moreover, the response time effects in children are in line with those of adults, such that children's estimation speed increased throughout the task, but was significantly slower for large- compared to small-scale estimations. As seen in Figure 9, children's

median response times were consistently lower for small (i.e., black boxplots) compared to large-scale estimations. Furthermore, the small-scale estimation boxplots are consistently shorter for small-compared to large-scale estimations, suggesting that children demonstrated less overall variance in response times for small-scale estimations. This is also apparent in the standard deviation values that were reported in Table 14.

Taken together, these data indicate that, although children were slower to respond to large-scale estimations, their accuracy for large-scale estimations did improve. Conversely, children were both faster and more accurate on small-scale estimations. Similarly, the lack of an effect of grade indicates that second and third-grade children performed similarly on the task regardless of the change in scale.

Despite similar behavioral performance between second and third-grade children, neurological data highlight significant differences in children's response patterns throughout the task. Most striking are the differences in activation within the right IPS. Previous research has implicated the right IPS in numerical processes such as numerical deviance discrimination (Ansari, 2007; Arsalidou & Taylor, 2011) such that greater right IPS activation is reported when greater numerical distance exists between two numerical stimuli. In the current task, as estimation scales increase in magnitude, so too does the numerical distance between the target value and the scale. Thus, greater right IPS activity within children that results from an increase in scale magnitude may be indicative of increased numerical deviance discrimination processes. However, these data do not rule out the possibility that this increase in activation is also driven by other concurrent processes (e.g., attention, spatial processing, etc.) that occur in similar regions of the brain.

Right IPS activation increased during the feedback portion of the task (see Figure 11) with particularly large rises within the auditory feedback condition. A similar pattern of activation was shown to occur within children's dorsolateral PFC, which has been shown to be involved in calculation tasks, particularly when externally generated information about number needs to be monitored and manipulated (Arsalidou & Taylor, 2011; Christoff & Gabrieli, 2000; Curtis & D'Esposito, 2003; Owen, McMillan, Laird, & Bullmore, 2005). Within the auditory feedback condition, though, the response tone must be kept in working memory, and must then be compared to the feedback tone that follows it. Thus, greater amounts of working memory may be needed to assess differences in feedback within the auditory condition. This increase in working memory processing may alternatively be driving the increased dorsolateral PFC activation identified here. Further, the dorsolateral PFC has also been implicated in the integration of crossmodal stimuli, especially when such information is essentially arbitrary (Banati et al., 2000; Bushara et al., 2001; Callan et al., 2001; Calvert, 2001; Calvert et al., 2000; Giard & Peronnet, 1999; Gonzalo et al., 2000; Lewis et al., 2000; Raij et al., 2000). In the current experiment, the auditory feedback tone could have been difficult to interpret if it was similar to the magnitude (i.e., volume) of the participant's estimation tone. Thus, the coincident increase in right IPS and dorsolateral PFC activation in response to auditory feedback may be indicative of concurrent numerical deviance discrimination of essentially arbitrary crossmodal stimuli.

Similar to adults, children exhibited differential neural activation within the right angular gyrus in response to changes in scale magnitude, suggesting that children may engage in increased visuospatial navigation throughout large- compared to small-scale

estimation. The similar presence of increased right angular gyrus activation within the feedback portion of the task indicates that this visuospatial navigation may have been greatest when feedback was provided. Furthermore, this increased activation coincided with a slowing of estimation response times, as well as a decrease in estimation accuracy.

The significant increase in activation within the left IPS and left angular gyrus are expected, given the involvement of in number processing and calculation (Arsalidou & Taylor, 2011; Dehaene et al., 2003). However, overall activation in both areas was greater in second compared to third-grade children, which can be seen within Figure 11 by the consistently higher trend line for second- compared to third-grade children. This pattern of results indicates that young children may be engaging in greater amounts of verbal numerical processing compared to older children—although this increased activation does not affect young children's behavioral performance. Moreover, the fact that this activation is greatest in young children within the auditory feedback condition supports similar findings reported herein that auditory feedback results in neurological activation increases within prefrontal and parietal cortices that are not present during other feedback conditions.

Children's neurological activation patterns in the prefrontal cortex (Figure 10) differed greatly from those of adults. Most notable is the lack of an effect of scale within any prefrontal fROI, which suggests that children recruited similar levels of prefrontal activation no matter the scale magnitude. This result is surprising, given that children responded less accurately on large-scale estimations. That is, within adults each ROI within the PFC has been shown previously to increase in activation as numerical calculations become more difficult (for review see Arsalidou & Taylor, 2011). As

discussed above, increases in dorsolateral PFC activation were observed during the feedback portion of the task, and within the auditory feedback condition in particular. This pattern of results may be indicative of greater working memory processes required within the auditory feedback condition because the estimation and feedback tones are presented sequentially. Thus, the estimation tone must be kept in working memory before it is compared with the correct response tone. Within the visual and audiovisual feedback conditions, the visual elements of the feedback are always presented together simultaneously, so less working memory is needed. Alternatively, this finding may suggest that auditory feedback presented in isolation may have been ambiguous in the sense that its spatial representation was difficult to interpret (Banati et al., 2000; Bushara et al., 2001; Callan et al., 2001; Calvert, 2001; Calvert et al., 2000; Giard & Peronnet, 1999; Gonzalo et al., 2000; Lewis et al., 2000; Raij et al., 2000).

CHAPTER IV

EXPERIMENT 3

Direct Comparison of Neurological Response Patterns Between Children and Adults

Prefrontal fROI Analyses

In order to test for a main effect of age, as well as interactions between each factor (i.e., block, scale, and feedback condition) and age of the participant, an additional 3 x 2 x 3 x 2 repeated measures ANOVA was conducted for each previously defined fROI, and included age (age; 2 groups) as a between-subject condition. Post-hoc tests were performed by Bonferroni corrected two-tailed *t* tests.

Within the medial PFC, repeated measures ANOVA revealed a significant block x scale interaction, $F(1.827, 80.367) = 3.395$, $MSE = 4.607$, $H\text{-}F\ p = .043$, $partial\ \eta^2 = .072$, caused by significantly higher overall activation for large scale estimations in the prefeedback block ($p < .001$). This effect was further extended by the presence of a three-way block x scale x age interaction, $F(1, 827, 80.367) = 3.318$, $MSE = 4.502$, $H\text{-}F\ p = .045$, $partial\ \eta^2 = .07$), which highlighted that children's neurological activation was significantly greater for large compared to small scales within the prefeedback block ($p = .031$), whereas adults' activation levels did not differ ($p > .05$). No other comparisons were significant within the medial PFC (see Table 24 for breakdown of combined medial prefrontal fROI beta value comparisons).

Within the dorsolateral PFC, a significant effect of block, $F(2, 88) = 4.77$, $MSE = 50.735$, $H\text{-}F\ p = .011$, $partial\ \eta^2 = .098$, indicated that activation increased during the

Table 24

Breakdown of Combined Medial Prefrontal Comparisons

Variable	*df*	Sum of squares	Mean square	*F* ratio	*p* value	Partial eta-squared
Block	2	33.874	16.937	.830	.439	.019
Block x condition	4	98.521	24.630	1.208	.313	.052
Block x age	2	32.971	16.485	.808	.449	.018
Block x condition x age	4	98.846	24.711	1.212	.312	.052
Scale	1	2.388	2.388	.145	.235	.032
Scale x condition	2	2.708	1.354	.821	.446	.036
Scale x age	1	2.641	2.641	1.602	.212	.035
Scale x condition x age	2	2.684	1.342	.814	.450	.036
Block x scale	1.827	8.414	4.607	3.395	.043[a]	.072
Block x scale x condition	3.653	2.782	.761	.561	.676	.025
Block x scale x age	1.827	8.223	45.020	3.318	.045[b]	.070
Block x scale x condition x age	3.653	2.689	.736	.542	.689	.024
Condition	2	1.864	.932	.063	.939	.003
Age	1	29.100	29.100	1.963	.168	.043
Condition x age	2	1.664	.832	.056	.946	.003

[a] Significantly greater prefeedback activation for large- compared to small-scale estimations.
[b] Children's neurological activation was significantly greater for large-scale estimations within the prefeedback condition.

feedback portion of the task. A significant block x condition interaction, $F(4, 88) = 2.77$, $MSE = 29.414$, *H-F* $p = .032$, *partial* $\eta^2 = .112$, indicated that participants in the auditory feedback condition experienced significantly greater increases in activation than the visual ($p = .013$), while the increase in activation for the auditory compared to audiovisual feedback conditions trended towards significance ($p = .075$). Moreover, a significant block x age interaction, $F(2, 88) = 4.79$, $MSE = 50.876$, *H-F* $p = .011$, *partial* $\eta^2 = .098$, was driven by significantly greater activation in the prefeedback condition within children compared to adults ($p = .001$). Also, children's neural activation increased significantly from the prefeedback to the feedback condition ($p < .001$). These interactions gave rise to a significant three-way block x condition x age interaction, $F(4,$

88) = 2.853, *MSE* = 30.295, *H-F p* = .028, *partial* η^2 = .115. No other comparisons were significant within the dorsolateral PFC (see Table 25 for breakdown of combined dorsolateral prefrontal fROI beta value comparisons).

Parietal fROI Analyses

Next, identical 3 x 2 x 3 x 2 repeated measures ANOVA were conducted for each of the fROIs identified within the parietal cortex. Here, an effect of scale caused by greater neural response to large scale estimations was significant within each fROI (left IPS: $F(1, 44) = 6.658$, *MSE* = 14.623, *H-F p* = .013, *partial* η^2 = .131; left angular gyrus: $F(1, 44) = 15.942$, *MSE* = 35.492, *H-F p* < .001, *partial* η^2 = .266; right IPS: $F(1, 44) =$

Table 25

Breakdown of Combined Left Dorsolateral Prefrontal Beta Value Comparisons

Variable	*df*	Sum of squares	Mean square	*F* ratio	*p* value	Partial eta-squared
Block	2	101.471	50.735	4.777	.011[a]	.098
Block x condition	4	117.656	29.414	2.770	.032[b]	.112
Block x age	2	101.751	50.876	4.790	.011[c]	.098
Block x condition x age	4	121.178	30.295	2.853	.028[d]	.115
Scale	1	2.609	2.609	2.115	.153	.046
Scale x condition	2	1.129	.564	.457	.636	.020
Scale x age	1	2.913	2.913	2.362	.131	.051
Scale x condition x age	2	1.117	.558	.453	.639	.020
Block x scale	1.742	3.813	2.190	1.578	.215	.035
Block x scale x condition	3.483	2.063	.592	.427	.763	.019
Block x scale x age	1.742	3.764	2.162	1.557	.219	.034
Block x scale x condition x age	3.483	2.013	.587	.423	.766	.019
Condition	2	12.222	6.111	.375	.690	.017
Age	1	17.908	17.908	1.098	.300	.024
Condition x age	2	11.817	5.908	.362	.698	.016

[a]Significantly greater activation during the feedback block of the task.
[b]Increased activation during feedback was greatest in the auditory feedback condition.
[c]Children's activation was significantly greater than adults within the prefeedback block of the task.
[d]Increased feedback activation within the auditory condition was exacerbated within children compared to adults.

12.709, *MSE* = 33.555, *H-F p* = .001, *partial* η^2 = .224; right angular gyrus: *F*(1, 44) = 11.843, *MSE* = 76.625, *H-F p* = .001, *partial* η^2 = .238). Similarly, a significant scale x age interaction was identified within the left IPS, *F*(1, 44) = 7.010, *MSE* = 15.396, *H-F p* = .011, *partial* η^2 = .137, the left angular gyrus, *F*(1, 44) = 16.533, *MSE* = 36.742, *H-F p* < .001, *partial* η^2 = .273, and the right IPS, *F*(1, 44) = 13.005, *MSE* = 34.336, *H-F p* = .001, *partial* η^2 = .228, but not within the right angular gyrus (*p* > .05). This interaction indicated that children experienced greater activation in response to large-scale estimations compared to adults. Moreover, both the left IPS, *F*(1, 44) = 4.703, *MSE* = 179.098, *p* = .036, *partial* η^2 = .097, and the right IPS, *F*(1, 44) = 7.570, *MSE* = 326.653, *p* = .009, *partial* η^2 = .147, indicated a significant effect of age, driven by greater overall activation throughout all blocks of the task for children compared to adults. Furhtermore, within the right IPS, a significant effect of block, *F*(2, 88) = 5.792, *MSE* = 239.124, *H-F p* = .004, *partial* η^2 = .116, and block x age interaction, *F*(2, 88) = 5.811, *MSE* = 239.925, *H-F p* = .004, *partial* η^2 = .117) indicated that overall activation levels increased during the feedback block of the task, and that this increase was greater in children compared to adults. Finally, a significant block x condition x age interaction within the right angular gyrus was driven by greater activation during the auditory feedback condition within children compared to adults, *F*(4, 76) = 3.295, *MSE* = 200.246, *H-F p* = .015, *partial* η^2 = .148; see Tables 26-29 for breakdown of combined parietal fROI beta value comparisons).

Table 26

Breakdown of Combined Left Intraparietal Sulcus Beta Value Comparisons

Variable	*df*	Sum of squares	Mean square	*F* ratio	*p* value	Partial eta-squared
Block	1.960	28.161	14.367	.504	.602	.011
Block x condition	3.920	185.745	47.381	1.664	.167	.070
Block x age	1.960	25.542	13.031	.458	.630	.010
Block x condition x age	3.920	182.442	46.539	1.634	.174	.069
Scale	1	14.623	14.623	6.658	.013[a]	.131
Scale x condition	2	2.235	1.117	.509	.605	.023
Scale x age	1	15.396	15.396	7.010	.011[b]	.137
Scale x condition x age	2	2.119	1.059	.482	.621	.021
Block x scale	1.726	3.064	1.775	.580	.538	.013
Block x scale x condition	3.453	10.974	3.178	1.039	.387	.045
Block x scale x age	1.726	3.155	1.827	.598	.529	.013
Block x scale x condition x age	3.453	11.008	3.188	1.042	.385	.045
Condition	2	45.815	22.908	.602	.552	.027
Age	1	179.098	179.098	4.703	.036[c]	.097
Condition x age	2	42.011	21.006	.552	.580	.024

[a]Greater activation during large- compared to small-scale estimations.
[b]Increased large-scale activation was greater in children compared to adults.
[c]Children demonstrated greater overall activity compared to adults.

Table 27

Breakdown of Combined Left Angular Gyrus Beta Value Comparisons

Variable	*df*	Sum of squares	Mean square	*F* ratio	*p* value	Partial eta-squared
Block	1.857	52.624	28.333	.702	.498	.016
Block x condition	3.715	128.687	34.643	.858	.486	.038
Block x age	1.857	49.128	26.451	.655	.511	.015
Block x condition x age	3.715	133.645	35.978	.891	.467	.039
Scale	1	35.429	35.429	15.942	.000[a]	.266
Scale x condition	2	.645	.322	.145	.865	.007
Scale x age	1	36.742	36.742	16.533	.000[b]	.273
Scale x condition x age	2	.565	.283	.127	.881	.006
Block x scale	1.949	1.465	.752	.234	.755	.005
Block x scale x condition	3.898	11.377	2.919	.908	.461	.040
Block x scale x age	1.949	1.453	.746	.232	.788	.005
Block x scale x condition x age	3.898	12.098	3.104	.965	.429	.042
Condition	2	193.301	96.650	1.301	.283	.056
Age	1	240.499	240.499	3.236	.079	.069
Condition x age	2	189.360	94.680	1.274	.290	.055

[a]Greater activation during large- compared to small-scale estimations.
[b]Increased large-scale activation was greater in children compared to adults.

Table 28

Breakdown of Combined Right Intraparietal Sulcus Beta Value Comparisons

Variable	*df*	Sum of squares	Mean square	*F* ratio	*p* value	Partial eta-squared
Block	2	478.247	239.124	5.792	.004[a]	.116
Block x condition	4	394.791	98.698	2.391	.057	.098
Block x age	2	479.850	239.925	5.811	.004[b]	.117
Block x condition x age	4	405.352	101.338	2.455	.052	.100
Scale	1	33.555	33.555	12.709	.001[c]	.224
Scale x condition	2	1.727	.864	.327	.723	.015
Scale x age	1	34.336	34.336	13.005	.001[d]	.228
Scale x condition x age	2	1.880	.940	.356	.702	.016
Block x scale	2	3.231	1.616	.485	.617	.011
Block x scale x condition	4	17.399	4.350	1.306	.274	.056
Block x scale x age	2	3.212	1.606	.482	.619	.011
Block x scale x condition x age	4	17.891	4.473	1.343	.260	.058
Condition	2	189.134	94.567	2.191	.124	.091
Age	1	3.26.653	326.653	7.570	.009	.147
Condition x age	2	185.062	92.531	2.144	.129	.089

[a]Activation increased significantly within the feedback block of the task.
[b]Increased activation during feedback was greater in children compared to adults.
[c]Greater activation during large- compared to small-scale estimations.
[d]Increased large-scale activation was greater in children compared to adults.

Table 29

Breakdown of Combined Right Angular Gyrus Beta Value Comparisons

Variable	*df*	Sum of squares	Mean square	*F* ratio	*p* value	Partial eta-squared
Block	2	296.257	148.128	2.438	.094	.060
Block x condition	4	115.710	28.927	.476	.753	.024
Block x age	2	61.548	30.774	.506	.605	.013
Block x condition x age	4	800.984	200.246	3.295	.015[a]	.148
Scale	1	76.625	76.625	11.843	.001[b]	.238
Scale x condition	2	24.417	12.209	1.887	.165	.090
Scale x age	1	3.484	3.484	.539	.468	.014
Scale x condition x age	2	39.236	19.618	3.032	.060	.138
Block x scale	2	8.928	4.464	1.033	.361	.026
Block x scale x condition	4	23.809	5.952	1.377	.250	.068
Block x scale x age	2	22.711	11.355	2.626	.079	.065
Block x scale x condition x age	4	29.518	7.380	1.707	.157	.082
Condition	2	256.086	128.043	1.459	.245	.071
Age	1	290.521	290.521	3.311	.077	.080
Condition x age	2	306.419	153.209	1.746	.188	.084

[a]Activation during feedback was significantly greater within children in the auditory feedback condition.
[b]Greater activation during large- compared to small-scale estimations.

Discussion

In line with the individual age group results presented above, the combined age group analysis indicates that parietal activation is similarly affected by changes in scale within both children and adults. However, significant scale x age interactions throughout each of the parietal fROIs indicated that children elicited greater overall activation in response to an increase in scale than adults. Similarly, children elicited greater overall activation compared to adults within the right IPS. Given children's reliance on the right parietal cortex when processing numerical stimuli (Cantlon et al., 2006), this effect is expected and suggests that children may have been eliciting greater amounts of nonverbal numerical processing and numerical deviance discriminations than adults. Moreover, similar to the effects seen in children in regards to increased activation in the dorsolateral PFC throughout the feedback block of the task, results of the combined analysis also indicate a significant main effect of block within the dorsolateral PFC. As discussed above, these results may indicate that greater working memory processes are needed to compare the tones within auditory feedback, or that this region is heavily implicated in interpreting feedback in general. Nevertheless, the interaction with age indicates that children relied more heavily on the dorsolateral PFC compared to adults. Thus, adults may not require as much working memory to compare feedback, regardless of feedback condition. Alternatively, adults may have found the auditory feedback to be less ambiguous than children.

CHAPTER V

GENERAL DISCUSSION

The results reported above indicate that, as hypothesized, increases in scale within a number line estimation task influence behavioral and neurological response patterns in both adults and children. As adults' accuracy on this task seems to be fixed despite increases in scale, significantly faster response times to small- compared to large-scale estimations suggests that greater amounts of decision-making processes may be needed to produce such accurate estimations during large-scale trials. As hypothesized, adults' neurological activity within the prefrontal cortex differed as a function of scale, although the direction of this activation was not as predicted. Specifically, given Delazer and colleagues' (2005) interpretation that greater PFC activity occurs as a result of difficult math problems, the current results showing greater PFC activity resulting from smaller scale (i.e., easier) number line trials were not predicted in adults. Alternatively, this increase in PFC activation may indicate greater metacognitive monitoring that occurs for small- compared to large-scale estimations. That is, during small-scale estimations adults may have been assessing current estimations based on previous estimations, thus eliciting greater activation in areas known to be associated with metacognitive monitoring (Dobbins, Simons, & Schacter, 2004). In contrast, children did demonstrate the predicted significant behavioral (i.e., accuracy and response time) fluctuations as a result of changes in scale, and their prefrontal activation was also modulated in the direction of change as hypothesized. Specifically, children exhibited greater medial PFC activation for large compared to small-scale estimations, while also responding more slowly and

less accurately to large scale estimations. Moreover, this pattern was exacerbated within second compared to third-grade children. These results suggest that, within children, Delazer and colleagues' (2005) prediction applies, in that increased activation in the PFC occurs in response to more difficult estimation trials. However, the lack an effect of scale within children's dorsolateral PFC suggests that multiple processes outside of numerical judgments are occurring within the PFC throughout the task. Therefore, areas of the PFC that were not targeted as regions of interest may have contributed to these decisions.

Both adults and children demonstrated the greatest amount of prefrontal activation during the feedback block of the task. Moreover, while a general increase in task accuracy and neural activity was apparent for all feedback types, the greatest neural response occurred within the auditory feedback condition. As both fROIs identified within the PFC are known to be associated with working memory, this pattern of results may suggest that the greatest working memory processing occurred throughout the feedback portion of the task, when participants were required to make a similarity comparison between their estimation and the correct estimation location. It is likely that such working memory processes would have been greatest during the auditory feedback condition, as this was the only condition in which visual feedback was not concurrently displayed. That is, participants were required to hold their response tone volume in working memory, and subsequently compare that memory with the feedback tone. While the audiovisual feedback condition also provided similar auditory feedback, the concurrent visual feedback may have decreased the working memory load. Alternatively, participants may have simply ignored the auditory feedback within the audiovisual feedback condition.

However, as noted above, it is hypothesized that high levels of dorsolateral PFC activation may be recruited when newly acquired crossmodal cues are essentially arbitrary (Banati et al., 2000; Bushara et al., 2001; Callan et al., 2001; Calvert, 2001; Calvert et al., 2000; Giard & Peronnet, 1999; Gonzalo et al., 2000; Lewis et al., 2000; Raij et al., 2000). Thus, this pattern of activation may be an indicator that participants found the auditory feedback harder to interpret compared to the visual and audiovisual feedback conditions, although this arbitrariness did not negatively affect estimation performance. Alternatively, visual feedback, which was present in both the visual and audiovisual feedback conditions, was likely easier to assess, resulting in less ambiguity, and thus less overall dorsolateral PFC activation.

In any case, contrary to my hypotheses regarding multisensory feedback, there was no evidence either behaviorally or neurologically that audiovisual feedback was superior to either type of unisensory feedback. The reason for a lack of effect of feedback condition may stem from many sources: For example, it may be that a specific condition relevant feedback was interpreted differently across participants. For example, auditory feedback may have provided numerical information to some participants, while providing information about volume or spatial location to others. In this example, the neurological regions that respond to these properties may differ slightly. Given the spatial overlap inherent in NIRS recording channels, these disparate regions may have overlapped with the fROIs, resulting in smaller changes in activation than would be expected if each region were targeted directly. Thus, the activation changes in response to feedback within the ROI's were not large enough to yield statistical significance. Future studies should investigate this further, perhaps by presenting each feedback condition as a within

subjects factor. In this manner, it would be possible to identify whether participants' neural activation patterns differ across each feedback type. Moreover, it may be that there exist more optional feedback types than the three used here for number line estimations. For example, a combination of visual and tactile feedback (e.g., line and vibration) may elicit greater differences in response activation, and may thus drive a significant effect of feedback. Alternatively, intrasensory redundancy (e.g., multiple sources of information within the same sensory modality) may elicit stronger effects, as cross-modal integration of each feedback stimulus would not have to be made.

Overall, children elicited greater levels of bilateral activation in the parietal cortex compared to adults. Most apparent is the total lack of significant differences in activation identified within adults' right IPS. That is, these results indicate that the pattern of activation within adults' right IPS remained constant despite changes in block or scale, both of which had measurable effects within other areas of the adult brain, including the left IPS. As previous studies have indicated that infants and children elicit lateralized right IPS activity in response to abstract number comparisons (Cantlon et al., 2006; Hyde, Boas, Blair, & Carey, 2010), whereas adults elicit bilateral activation (Cantlon et al., 2006), these results may demonstrate that patterns of lateralization between children and adults is task dependent. Alternatively, as many right parietal areas are highly involved in spatial reasoning (Arsalidou & Taylor, 2011), these results may be indicative of greater spatial analyses during this task in children compared to adults. The fact that significant fluctuations in activation were only observed in adults' left IPS, on the other hand, may be indicative of their greater reliance on verbal numerical processing, which is has been shown to be largely isolated to the left parietal lobule (Arsalidou & Taylor, 2011;

Dehaene et al., 2003, Delazer et al., 2005).

Adults' patterns of neural response within the parietal cortex support my hypothesis that greater parietal activation would be observed in small-scale, rather than large-scale, estimations. However, this increase in parietal activation occurred concurrently with an increase in PFC activation. Therefore, a "shift" in neural activation between the PFC and intraparietal regions, as reported by Rosenberg-Lee and colleagues (2011) within a test of symbolic addition, was not documented. Interestingly, within children, greater activation within the PFC and parietal regions occurred during large- compared to small-scale estimations. Therefore, the current results suggest that adults' and children's neurological response patterns to small and large-scale estimations can occur in opposite directions.

The fact that these response patterns occurred in opposite directions between children and adults indicates that the two groups may have been engaging in the same task in functionally different manners. Moreover, this difference may have arisen because of the estimation scales used. Specifically, even though second-grade children have not yet been formally introduced to "one hundred thousand" scales in their mathematics classrooms, the written description of the value could be easily relatable to known values such as "one hundred" simply because the term "one hundred" appears in the number "one hundred thousand." Thus, when encountered within large scale estimations, the easy identification of "one hundred thousand" as a number that is larger than "one hundred" may have elicited greater number related processes in the parietal regions. Similarly, such an understanding may have concurrently elicited frontal working memory processes in children so that such large numbers could be remembered. This increase on working

memory processes may have also contributed to the decline in estimation accuracy as well as increased response times. Future studies may account for this increased working memory load by, for example, making the estimation scales visible throughout each trial. Thus, children would not have to commit such large scales to working memory.

Alternatively, adults read the scale values "one billion" and "one quadrillion," neither of which are easily relatable to common numerical values such as "one hundred." Moreover, despite knowing that "one quadrillion" is a value that is larger than "one billion," the "quadrillion" scale may have been so foreign that it failed to evoke an association with number at all. Thus, the "quadrillion" scale estimations may have functionally been completed as purely spatial estimations without much numerical processing occurring at all. The "billion" scale, on the other hand, is perhaps more familiar, and thus elicited "number related" responses in the left IPS while the "quadrillion" scale did not. In any case, behavioral performance of both scales was equal, suggesting that either both scales were processed similarly (i.e., both purely spatially), or that accuracy in response to disparate stimulus properties (e.g., number and space) is similar.

Finally, these data support recent findings regarding the neurological correlates of fraction representations, which indicate that many of the same neurological areas responsible for processing of whole numbers are also implicated in the processing of proportions (Jacob & Nieder, 2009; Jacob et al., 2012). Because number line estimations are essentially a proportional reasoning task in that one must represent the numerical proportion of the scale value accounted for by the estimation value, it comes as no surprise that similar neurological areas were implicated here and in the findings reported

by Jacob and Nieder (2009) and Jacob and colleagues (2012). However, as the neurological representation of fractions has only recently been reported, very few sources are available to corroborate such findings. Moreover, the results reported here are the first to identify such neurological responding to fraction related material in children. Therefore, my findings may provide much needed evidence to further elucidate the neurological locations associated with fraction representations in children and adults.

A striking result of this study is the lack of replication of number line estimation studies in children that demonstrate a linear to logarithmic "shift" coinciding with an increase in scale (e.g., Opfer & Siegler, 2007; Siegler & Booth, 2004; Thompson & Opfer, 2010). Here, results demonstrate that, although children do become more error prone as the estimation scale rises, a linear fit to the data is consistently best. This may be a function of the speeded nature of the task employed herein. That is, each of the other number line studies reported above allowed children time to think about their estimations, and in many cases even allowed them to modify their estimation. While it remains untested, logarithmic functions in response to large-scale estimations may be attributed to correction errors that only occur when children are given time to "overthink" their estimation. Conversely, in the method reported here children were required to make their estimation quickly, which would force them to provide their initial instinctual response. Therefore, the results reported herein may provide a more accurate depiction of children's internal representation of the spatial layout of number than previous studies which provide children with more time to respond.

Alternatively, overlapping waves theory (Siegler, 1996) suggests that children possess multiple strategies to complete math-related problems, including number line

estimations. According to the theory, children at any age know and use a variety of approaches (i.e., strategies, rules, or representations) that compete with one another for use, with each approach being more or less adaptive depending on the problem and situation (Siegler, 1996). Early in their introduction to mathematics, children rely heavily on their logarithmic wave (i.e., representation), which results in typical logarithmic functions emerging on all number line estimations. As the children age they learn that other waves (e.g., linear representation) are more appropriate for familiar scale estimations. However, as scale rises, they revert back to their logarithmic wave, thus resulting in the logarithmic function that is common as estimation scales rise. It is possible that the timed number line estimation procedure used here facilitated use of children's "linear" wave representation. For example, throughout number line tasks, children may cycle through multiple representations before making their estimation. Given unlimited time to provide such estimations, children may prefer logarithmic representations, and thus demonstrate logarithmic estimation functions. However, children may evoke their linear representation first, before cycling through to their logarithmic representation. Given the timed nature of this task, children may have been "forced" to use their initial representation, and were not able to evoke alternative representations before making their estimations. However, as no previous task has employed a timed estimation design, it is not known whether such results will consistently emerge. Thus, it will be important for multiple comparisons to be made in the future: First, speeded number line estimations, such as those used here, should be used on a separate group of age-matched children to determine if similar linear functions are produced. Next, it will be important to directly replicate previous methods (i.e.,

untimed estimations) that have been shown to elicit a significant linear-to-logarithmic shift. Importantly, both the speeded number line replication, as well as the more typical untimed procedure should be conducted within the NIRS imaging environment. Thus, these comparisons will allow us to determine if significant log-to-linear shifts result in different neurological response patterns compared to those identified here.

Finally, the consistently linear performance by the children within this study may have resulted from an even simpler alternative: children knew they were engaging in a task that was important enough to warrant the imaging of their brains, which may have encouraged them to try harder and perform better than they would if they were in a typical classroom environment in which the same pressures were not present. Moreover, the small amount of feedback given prior to the task may have encouraged or primed subsequent linear performance in the task itself. Nevertheless, these results suggest that providing children with multiple trials of a speeded number line estimation task with any type of accuracy feedback will successfully enhance their number line estimation accuracy. This is important for applied educational settings in which the facilitation of linear number line estimations is crucial for children's mathematics education.

CHAPTER VI

LIMITATIONS AND FUTURE DIRECTIONS

One aspect of the results reported above that is not addressed with the current methodological design is whether feedback of any sort is necessary to enhance estimation performance within a computer-based speeded number line estimation task. That is, the lack of a group of participants who were not given any feedback about estimation accuracy was not included here. The inclusion of such a condition would allow for a general feedback versus no-feedback comparison. However, the increase in estimation accuracy from the prefeedback to the feedback block indicates that feedback did improve estimation performance. I hypothesize that little to no benefit to number line estimation accuracy would arise without some sort of performance feedback, although such a claim cannot be made without first carrying out this new control condition. Data within this condition are currently being collected so that these and other comparisons can be made.

Another aspect of the current study that deserves recognition, and that may inhibit the identification of statistical differences in both the behavioral and neurological components of the project is the sample size used. It is important to note that the target sample size for experiments 1 and 2 were identified based on a power analysis geared towards identifying a statistically significant effect in the behavioral component of the task (i.e., estimation accuracy). In both experiments 1 and 2, results from this analysis indicated that a sample size of 27 would be sufficient to identify such an effect, although within experiment 2 this effect was identified with only 23 participants. However, within experiment 2 in particular, the experimental design yields 36 comparison cells (e.g.,

grade (2) x feedback condition (3) x estimation scale (2) x experimental block (3) = 36 comparison cells). Thus, given only 23 participants, an insufficient sample size may have resulted in Type II error (i.e., false negative) effectively occluding effects that may emerge if a larger sample size were collected. Future studies that replicate this and other similar methodological designs should strive for a larger sample size so that such concerns over Type II error may be alleviated.

As discussed above, the fact that the well-established "linear to log shift" coinciding with an increase in estimation scale was not identified is somewhat disconcerting and represents a limitation to the current study. While the theoretical explanations described above may explain why this effect did not emerge, the fact remains that the novel experimental design may have effectively provided a task in which such an effect should not be expected. That is, while certain elements of the task such as estimation values and scales were consistent with past studies, never before has a speeded number line estimation procedure been conducted. Thus, the expected results of such a task are unknown. While a pilot study did indicate that adults' estimation accuracy was affected by increases in scale, the procedure of the pilot study (e.g., untimed paper and pencil method) was not identical to that used in the current experiment. Future studies should directly replicate past methods that have been shown to elicit a "linear to log shift" within the NIRS imaging environment so that neurological correlates to such a shift may be observed. Moreover, it will be important to replicate the methods used here, perhaps alongside the more common methods in a within subject design, so that expected behavioral and neurological responses to both methods may be further established.

Importantly, the data reported above may hold more information than the

particular analysis approach used herein has revealed. That is, similar to many fields both in and outside of cognitive neuroimaging, many different approaches to data analysis exist. Regarding NIRS, the GLM approach currently holds favor because of its relationship to fMRI analysis, the fact that it provides standardized and thus easily interpretable beta values, and because it allows for event related methodological designs. However, drawbacks to the GLM approach surely exist: For example, the hemodynamic response functions from which the standardized beta values are estimated are not linear, and thus a linear modeling approach may not be most appropriate. With GLM, such non-linear hemodynamic response functions are forced onto a linear model. Therefore, the standardized beta weights that are intended to describe neurological fluctuations may oversimplify the brains true response patterns as being either positive or negative in response to a stimulus, where in actuality the response pattern may be a more complex interplay of positive and negative fluctuations. Such fluctuations may be very important, but are lost throughout the GLM approach. Instead, non-linear methods of beta estimations such as multilevel modeling or growth curve analyses may provide a more accurate assessment of the brains true response patterns. In short, these and other non-linear regression or latent trait analyses would allow for estimations that capture the brains true non-linear response patterns and may thus provide a more complete picture of the brains true response.

Moreover, it is important to note that the elements of the task that were modeled for each participant herein (i.e., each **X** variable described in the NIRS Data Analysis and Outcomes section of experiment 1 above) do not represent an exhaustive list of each element that could be modeled. This is important because the explanatory strength of a

general linear model is enhanced by the inclusion of every possible source of variance affecting the outcome variable of interest. Thus, it may be prudent to include in such models separate **X** variables to capture the hemodynamic fluctuations that occur throughout periods of the task in which the participant was not engaged in the dependent task directly. For example, in the current experimental design, inter-trial intervals that were jittered between 2, 4, 6, or 8 seconds separated each estimations trial, and a 30 second rest period separated each block of the task. Such elements (e.g., ITI and rest) may be modeled as separate **X** variables, and may thus improve the explanatory power of the GLM itself. Moreover, inclusion of such variables would allow for important analyses, such as whether a change in neurological activation occurs between rest and task completion, or the degree to which a particular type of rest reduces overall activation in particular fROIs. Finally, given these and other drawbacks to inferential statistical analyses, it may be useful to also approach these data from a purely visual point of view, such that neural activation patterns, regions of interest, and overall significance are all derived from basic visualizations of obtained hemodynamic response functions.

Another limiting aspect of this and every neuroimaging project is the inherent limitations of the imaging device being used. While NIRS affords many benefits relative to other devices such as fMRI and EEG (e.g., liberal tolerance of movement, ease of use, etc.) there are no doubt drawbacks as well. For example, NIRS is limited to cortical level measurements of the brain. Because NIRS is an optical topography system, the physical dispersion of photons throughout such substrate as the skull and brain limits its imaging capabilities to roughly 3cm below the scalp. Moreover, because the near-infrared light projected by NIRS must travel through various levels of superfluous substrate (e.g., scalp,

skull, etc.) that all absorb light, a considerable amount of signal degradation is to be expected. While the signal to noise ratio has been shown to be similar to that of other imaging techniques such as fMRI (Cui, Bray, Bryant, Glover, & Reiss, 2011), it nevertheless poses a limitation to NIRS based studies. That is, certain neurological responses occurring at levels of the cortex that are identifiable by NIRS may still be obscured due to degradation of the light source as it passes through each substrate. This combined with a finite number of optodes to be placed on the head severely restrict the amount of the brain that can be imaged. Thus, there is no doubt that many important neurological processes may be missed. Moreover, because NIRS observes hemodynamic fluctuations that are restricted by cardiovascular factors such as heart rate, which may differ across individuals, the periods of observation inherent in the design of the experiment (e.g., individual estimation trials) will likely affect the magnitude of responses observed. For example, an individual period of observation that is too short may not capture the hemodynamic fluctuation at all, whereas a period that is too long may be obscured by fluctuations that result from nontarget stimuli.

Finally, while results exist which support HbO as the best indicator of neurological activity (e.g., Baird et al., 2002; Bortfeld et al., 2009; Grossmann et al., 2008; Minagawa-Kawai et al, 2008; Pena et al., 2003; Wilcox et al., 2008, 2009), the debate continues surrounding whether oxygenated or deoxygenated hemoglobin provides the most complete indicator of neurological activation. It will be important for future studies to compare both sources to each other so that a more definitive answer to this question may be identified.

Despite such outstanding questions and limitations, NIRS provides an ideal

platform for neuroimaging that has the potential to positively impact basic and applied psychological sciences alike. Given the benefits of NIRS described above, it will be important for future studies to map the brains responses to other real-world educational tasks as well. I believe that naturalistic neuroimaging designs that allow for concurrent assessments of neurological and behavioral data, such as that reported herein, have the potential to inform mathematics learning and instruction (Butterworth & Kovas, 2013). Taken together, the data reported here demonstrate typical neurological response patterns to a number line estimation task within typically developing children and adults. These data may prove valuable in helping to triangulate indicators of atypical math learning. For example, based on these data, it is now known that typically developing children recruit areas of the brain known to process number and math calculations when number line estimation tasks increase in difficultly. Similar assessment of number line estimation in poor math performers, individuals with math learning disabilities such as dyscalculia, or within populations who possess a genetic abnormality that leads to deficits in numerical cognition (e.g., Turner Syndrome) may demonstrate observable disparities in behavioral and neurological response patterns compared to typically developing children such as those reported here. Thus, such comparisons may help to identify both typical and atypical neurological responses to naturalistic tasks.

Such widespread application of NIRS may prove to be very useful. For example, it may be possible to employ NIRS to identify atypical math learners long before it is possible to identify them with behavioral measures. In fact, NIRS has already been used to identify math related processing in infants as young as 5½ months old (Hyde et al., 2010). This is very important because methodological restrictions make such

neuroimaging tasks impossible with fMRI, and other approaches such as EEG do not provide the spatial resolution needed to identify deficits in specific neurological regions. Thus, it may be possible to use NIRS to identify math-learning abnormalities well before language is acquired so that intervention techniques may be applied early within development. Importantly, this diagnostic aspect of NIRS is not limited to math and number processing, but may also be employed to detect abnormalities in many education related processes such as reading comprehension, and language production. In fact, albeit not in infants or young children, such diagnostic applications have previously been identified for NIRS for such conditions as schizophrenia (Takeshi, Nemoto, Fumoto, Arita, & Mizuno, 2010) and bipolar disorder (Kameyama et al., 2006).

In conclusion, this study has provided much needed information about the behavioral and neurological correlates of a real-world math-learning activity within typically developing children and adults. Such information is needed to help identify how math is effectively learned in the real world, and may prove useful in establishing a baseline from which atypical math learning signatures may be identified. Furthermore, this study extends the use of NIRS as an effective neuroimaging tool for identifying children's and adults' concurrent behavioral and neurological correlates to real-world learning activities within naturalistic environments.

REFERENCES

Abdellatif, H.R., Cummings, R., & Maddux, C.D. (2008). Factors affecting the development of analogical reasoning in young children: A review of the literature. *Education, 129*, 239-249.

Ansari, D. (2007). Does the parietal cortex distinguish between "10," "ten," and ten dots? *Neuron, 53*, 165-167.

Arsalidou, M., & Taylor, M.J. (2011). Is 2+2=4? Meta-analyses of brain areas needed for numbers and calculations. *Neuroimage, 54*, 2382-2393.

Astafiev, S.V., Shulman, G.L., Stanley, C.M., Snyder, A.Z., Van Essen, D.C., & Corbetta, M. (2003). Functional organization of human intraparietal and frontal cortex for attending, looking, and pointing. *Journal of Neuroscience, 23*, 4689-4699.

Bahrick, L.E., Flom, R., & Lickliter, R. (2002). Intersensory redundancy facilitates discrimination of tempo in 3-month-old infants. *Developmental Psychobiology, 41*, 352-363.

Bahrick, L.E., & Lickliter, R. (2000). Intersensory redundancy guides attentional selectivity and perceptual learning in infancy. *Developmental Psychology, 36*, 190-201.

Bahrick, L.E., Lickliter, R. & Flom, R. (2004). Intersensory redundancy guides the development of selective attention, perception, and cognition in infancy. *Current Directions in Psychological Science, 13*(3), 99-102.

Baird, A.A., Kagen, J., Gaudette, T., Walz, K.A., Hershlag, N., & Boas, D.A. (2002). Frontal lobe activation during object permanence: Data from near-infrared spectroscopy. *NeuroImage, 16*, 1120-1126.

Baker, J.M., & Jordan, K.E. (in press). Multiple visual quantitative cues enhance discrimination in infancy. *Journal of Experimental Child Psychology*.

Banati, R.B., Goerres, G.W., Tjoa, C., Aggleton, J.P., & Grasby, P. (2000). The functional anatomy of visual-tactile integration in man: A study using positron emission tomography. *Neuropsychologia, 38*, 115-124.

Barth, D.S., Goldberg, N., Brett, B., & Di, S. (1995). The spatiotemporal organization of auditory, visual, and auditory-visual evoked potentials in rat cortex. *Brain Research, 678*, 177-190.

Barth, H.C., & Paladino, A.M. (2011). The development of numerical estimation: evidence against a representational shift. *Developmental Science, 14*(1), 125-135.

Ben Hamed, S, Duhamel, J.R., Bremmer, F., & Graf, W. (2001). Representation of the visual field in the lateral intraparital area of macaque monkeys: A quantitative receptive field analysis. *Experimental Brain Research, 140*, 127-144.

Best, C.T., McRoberts, G.W., LaFleur, R., & Silver-Isenstadt, J. (1995). Divergent developmental patterns for infants' perception of two nonnative consonant contrasts. *Infant Behavior & Development, 18*, 339-350.

Binkofski, R., Dohle, C., Posse, S., Stephan, K.M., Hefter, H., Seitz, R.J., & Freund, H.J. (1998). Human anterior intraparietal area subserves prehension. *Neurology, 50*, 1253-1259.

Bonda, E., Petrides, M., Frey, S., & Evans, A. (1995). Neural correlates of mental transformations of the body-in-space. *Proceedings of the National Academy of Science, 92*, 11180-11184.

Booth, J.L., & Siegler, R.S. (2006). Development and individual differences in pure numerical estimation. *Developmental Psychology, 41*, 189-201.

Booth, J.L., & Siegler, R.S. (2008). Numerical magnitude representations influence arithmetic learning. *Child Development, 79*, 1016-1031.

Bortfeld, H., Fava, E., & Boas, D.A. (2009). Identifying cortical lateralization of speech processing in infants using near-infrared spectroscopy. *Developmental Neuropsychology, 34*(1), 52-65.

Bremmer, F., Schlack, A., Duhamel, J. R., Graf, W., & Fink, G. R. (2001a). Space coding in the primate posterior parietal cortex. *Neuroimage, 14*(1), 46-51.

Bremmer, F., Schlack, A., Shah, N.J., Zafiris, O., Kubischick, M., Hoffman, K.P., … Fink, G. (2001b). Polymodal motion processing in posterior parietal and premotor cortex: A human fMRI study strongly implies equivalencies between humans and monkeys. *Neuron, 29*, 287-296.

Buccino, G., Binkofski, F., Fink, G.R., Fadiga, L., Fogassi, L., Gallese, V., … Freund, H.J. (2001). Action observation activates premotor and parietal areas in a somatotopic manner: An fMRI study. *European Journal of Neuroscience, 13*, 400-404.

Bullmore, E., Brammer, M., Williams, S. C., Rabe Hesketh, S., Janot, N., David, A., … Sham, P. (1996). Statistical methods of estimation and inference for functional MR image analysis. *Magnetic Resonance Imaging, 35*, 261-277.

Burbaud, P., Camus, O., Guehl, D., Bioulac, B., Caille, J.M., & Allard, M. (1999). A functional magnetic resonance imaging study of mental subtraction in human subjects. *Neuroscience Letters, 273*, 195-199.

Bushara, K.O., Grafman, J., & Hallett, M. (2001). Neural correlates of auditory-visual stimulus onset asynchrony detection. *Journal of Neuroscience, 21*, 300-304.

Bushara, K.O., Weeks, R.A., Ishii, K., Catalan, M.J., Tian, B., Rauschecker, J.P., & Hallett, M. (1999). Modality-specific frontal and parietal areas for auditory and visual spatial localization in humans. *Nature Neuroscience, 2*, 759-766.

Butterworth, B., & Kovas, Y. (2013). Understanding neurocognitive development disorders can improve education for all. *Science, 340*, 300-305.

Calabria, M., & Rossetti, Y. (2005). Interface between number processing and line bisection: a methodology. *Neuropsychologia, 43*, 779-783.

Callan, D.E., Callan, A.M., & Kroos, C., & Vatlklotis-Bateson, E. (2001). Multimodal contribution to speech perception revealed by independent component analysis: A single-sweep EEG case study. *Cognition & Brain Research, 10*, 349-353.

Calvert, G.A. (2001). Crossmodal processing in the human brain: Insights from functional neuroimaging studies. *Cerebral Cortex, 11*, 1110-1123.

Calvert, G.A., Campbell, R., & Brammer, M.J. (2000). Evidence from functional magnetic resonance imaging of crossmodal binding in human heteromodal cortex. *Current Biology, 10*, 649-657.

Cannon, L., Heal, R., Dorward, J., Duffin, J., & Edwards, L. (2010). *National library of virtual manipulatives* [Software]. retrieved from http://nlvm.usu.edu/en/nav/vlibrary.html

Cantlon, J.F., Brannon, E.M., Carter, E.J., & Pelphrey, K.A. (2006). Functional imaging of numerical processing in adults and 4-year-old children. *PLOS Biology, 4*, 844-854.

Cantlon, J.F., Libertus, M.E., Pinel, P., Dehaene, S., Brannon, E.M., & Pelphrey, K.A. (2009). The neural development of an abstract concept of number. *Journal of Cognitive Neuroscience, 21*, 2217-2229.

Castelli, F., Glaser, D., & Butterworth, B. (2006). Discrete and analogue quantity processing in the parietal lobe: A functional MRI study. *Proceedings of the National Academy of Sciences, 103*, 4603-4608.

Chao, L.L., & Martin, A. (2000). Representation of manipulable man-made objects in the dorsal stream. *Neuroimage, 12*, 478-484.

Cheour, M., Ceponiene, R., Lehtokoski, A., Luuk, A., Allik, J., Kimmo, A., & Naatanen, R. (1998). Development of language-specific phoneme representations in the infant brain. *Nature Neuroscience, 1*, 351-353.

Chiroro, P., & Valentine, T. (1995). An investigation of the contact hypothesis of the own-race bias in face recognition. *Quarterly Journal of Experimental Psychology A: Human Experimental Psychology, 48A*, 879-894.

Chochon, F., Cohen, L., van de Moortele, P.F., & Dehaene, S. (1999). Differential contributions of the left and right inferior parietal lobules to number processing. *Journal of Cognitive Neuroscience, 11*, 617-630.

Christoff, K., & Gabrieli, J.D. (2000). The frontopolar cortex and human cognition: Evidence for a rostrocaudal hierarchical organization within the human prefrontal cortex. *Pscyobiology-Austin, 28*, 168-186.

Cipolotti, L., Butterworth, B., & Denes, G. (1991). A specific deficit for numbers in a case of dense acalculia. *Brain, 114*, 2619-2637.

Cohen, L., & Dehaene, S. (1996). Cerebral networks for number processing: Evidence from a case of posterior callosal lesion. *NeuroCase, 2*, 155-174.

Cohen-Kadosh, R., Cohen-Kadosh, K., & Henik, A. (2008). When brightness counts: The neuronal correlate of numerical-luminance interference. *Cerebral Cortex, 18*, 337-343.

Cohen-Kadosh, R., Cohen-Kadosh, K., Schuhmann, T., Kaas, A., Goebel, R., Henik, A., & Sack, A.T. (2007). Virtual dyscalculia induced by parietal-lobe TMS impairs automatic magnitude processing. *Current Biology, 17*, 689-693.

Cordes, S., Gelman, R., & Gallistel, C.R. (2001). Variability signatures distinguish verbal from nonverbal counting for both large and small numbers. *Psychonomic Bulletin & Reivew, 8*, 698-707.

Cui, X., Bray, S., Bryant, D.M., Glover, G.H., & Reiss, A.L. (2011). A quantitative comparison of NIRS and fMRI across multiple cognitive tasks. *NeuroImage, 54,* 2808-2821.

Culham, J.C., Danckert, S.L., De Souze, J.F., Gati, J.S., Menon, R.S., & Goodale, M.A. (2003). Visually guided grasping produces fMRI activation in dorsal but not ventral stream brain areas. *Experimental Brain Research, 153*, 180-189.

Curtis, C.E., & D'Esposito, M. (2003). Persistent activity in the prefrontal cortex during working memory. *Trends in Cognitive Sciences, 7*(9), 415-423.

Dehaene, S. (1992). Variaties of numerical abilities. *Cognition, 44*, 1-42.

Dehaene, S. (1995). Electrophysiological evidence for category-specific word processing in the normal human brain. *NeuroReport, 6*, 2153-2157.

Dehaene, S. (1996). The organization of brain activations in number comparison: Event-related potentials and the additive-factors methods. *Journal of Cognitive Neuroscience, 8*, 47-68.

Dehaene, S. (1997). *The number sense: How the mind creates mathematics.* New York, NY: Oxford University Press.

Dehaene, S. (2011). *The number sense: How the mind creates mathematics*. New York, NY: Oxford University Press.

Daheane, S., Bossini, S., & Giraux, P. (1993). The mental representation of parity and numerical magnitude. *Journal of Experimental Psychology General, 122*, 371-396.

Dehaene, S., & Cohen, L. (1997). Cerebral pathways for calculation: Double dissociation between rote verbal and quantitative knowledge in arithmetic. *Cortex, 33*, 219-250.

Dehaene, S., Dehaene-Lambertz, G., & Cohen, L. (1998). Abstract representations of numbers in the animal and human brain. *Trends in Neurosciences, 21*(8), 355-361.

Dehaene, S., Izard, V., Spelke, E., & Pica, P. (2008). Log or linear? Distinct intuitions of the number scale in western and Amazonian indigene cultures. *Science, 320*, 1217-1220.

Dehaene, S., & Marques, J.F. (2002). Cognitive euroscience: Scalar variability in price estimation and the cognitive consequences of switching to the euro. *The Quarterly Journal of Experimental Psychology: Section A, 55*(3), 705-731.

Dehaene, S., & Mehler, J. (1992). Cross-linguistic regularities in the frequency of number words. *Cognition, 43*(1), 1-29.

Dehaene, S., Piazza, M., Pinel, P., & Cohen, L. (2003). Three parietal circuits for number processing. *Cognitive Neuropsychology, 20*, 487-506.

Dehaene, S., Spelke, E., Pinel, P., Stanescu, R., & Tsivkin, S. (1999). Sources of mathematical thinking: Behavioral and brain-imaging evidence. *Science, 284*, 970-974.

Delazer, M., Domahs, F., Bartha, L., Brenneis, C., Lochy, A., Trieb, T., & Benke, T. (2003). Learning complex arithmetic—an fMRI study. *Cognitive Brain Research, 18*, 76-88.

Delazer, M., Ischebeck, A., Domahs, F., Zamarian, L., Koppelstaetter, F., Siedentopf, C.M., … Felber, S. (2005). Learning by strategies and learning by drill—evidence from an fMRI study. *NeuroImage, 25*, 838-849.

Denys, K., Vanduffel, W., Fize, D., Nelissen, K., Peuskens, H., Van Essen, D., & Orban, G.A. (2004). The processing of visual shape in the cerebral cortex of human and nonhuman primates: A functional magnetic resonance imaging study. *Journal of Neuroscience, 24*, 2551-2565.

Dobbins, I. G., Simons, J. S., & Schacter, D. L. (2004). fMRI evidence for separable and lateralized prefrontal memory monitoring processes. *Journal of Cognitive Neuroscience, 16*, 908-920.

Duhamel, J.R., Colby, C.I., & Goldberg, M.E. (1991). Congruent representations of visual and somatosensory space in single neurons of monkey ventral intra-parietal cortex (area VIP). InJ. Pallard (Ed.), *Brain and space* (pp. 223-236). New York, NY: Oxford University Press.

Eger, E., Sterzer, P., Russ, M.O., Giraud, A.L., & Kleinschmidt, A.A. (2003). A supramodal number representation in human intraparietal cortex. *Neuron, 37*, 719-725.

Eimer, M. (1999). Can attention be directed to opposite locations in different modalities? An ERP study. *Clinical Neurophysiology, 110*, 1252-1259.

Feigenson, L., Dehaene, S., & Spelke, E. (2004). Core systems of number. *TRENDS in Cognitive Sciences, 8*, 307-314.

Fias, W., Brysbaert, M., Geypens, F., & D'ydewalle, G. (1996). The importance of magnitude information in numerical processing: Evidence from the SNARC effect. *Mathematical Cognition, 2*, 95-110.

Fias, W., Lauwereyns, J., & Lammertyn, J. (2001). Irrelevant digits affect feature-based attention depending on the overlap of neural circuits. *Cognitive Brain Research, 12*, 415-423.

Finke, R. A., & Pinker, S. (1982). Spontaneous imagery scanning in mental exploration. *Journal of Experimental Psychology: Learning, Memory, & Cognition, 8*(2), 142-147.

Fischer, M.H. (2001). Number processing includes spatial performance biases. *Neurology, 57*, 822-826.

Fischer, M.H., Castel, A.D., Dodd, M.D., & Pratt, J. (2003). Perceiving numbers causes spatial shifts of attention. *Nature Neuroscience, 6*, 555-556.

Flom, R., & Bahrick, L.E. (2007). The development of infant discrimination of affect in multimodal and unimodal stimulation: The role of intersensory redundancy. *Developmental Psychology, 43*, 238-252.

Friston, K. J., Holmes, A., Worsley, K., & Poline, J. (1995). Statistical parametric maps in functional imaging: A general linear approach. *Human Brain Mapping, 2*, 189-210.

Galton, F. (1880a). Visualised numerals. *Nature, 21*, 252-256.

Galton, F. (1880b). Visualised numerals. *Nature, 22*, 494-495.

Gentner, D., Lowenstein, J., & Hung, B. (2007). Comparison facilitates children's learning of names for parts. *Journal of Cognition & Development, 8*, 285-307.

Giard, M.H., & Peronnet, F. (1999). Auditory-visual integration during multimodal object recognition in humans: A behavioral and electrophysiological study. *Journal of Cognitive Neuroscience, 11*, 473-490.

Gogate, L.J., & Bahrick, L.E. (1998). Intersensory redundancy facilitates learning of arbitrary relations between vowel sounds and objects in seven-month-old infants. *Journal of Experimental Child Psychology, 69*, 133-149.

Gonzalo, D., Shallice, T., & Dolan, R. (2000). Time-dependent changes in learning audiovisual associations: A single-trial fMRI study. *NeuroImage, 11*, 243-255.

Graziano, M.S., & Gross, C.G. (1998). Spatial maps for the control of movement. *Current Opinions in Neurobiology, 8*, 195-201.

Grefkes, C., Weiss, P.H., Zilles, K., & Fink, G.R. (2002). Crossmodal processing of object features in human anterior intraparietal cortex: An fMRI study implies equivalence between humans and monkeys. *Neuron, 35*, 173-184.

Grossmann, T., Johnson, M.H., Lloyd-Fox, S., Blasi, A., Deligianni, F., Elwell, C., & Csibra, G. (2008). Early cortical specialization for face-to-face communication in human infants. *Proceedings of the Royal Society B: Biological Sciences, 275*, 2803-2811.

Hadjikhani, N., & Roland, P.E. (1998). Cross-modal transfer of information between the tactile and the visual representations in the human brain: A poitron emission tomographic study. *Journal of Neuroscience, 18*, 1072-1084.

Halberda, J., Mazzocco, M.M., & Feigenson, L. (2008). Individual differences in non-verbal number acuity correlate with maths achievement. *Nature, 455*, 665-668.

Hannon, E.E., & Trehub, S.E. (2005a). Metrical categories in infancy and adulthood. *Psychological Science, 16*, 48-55.

Hannon, E.E., & Trehub, S.E. (2005b). Tuning in to musical rhythms: Infants learn more readily than adults. *Proceedings of the National Academy of Science, 102*, 12639-12643.

Hoshi, Y. (2003). Functional near-infrared optical imaging: Utility and limitations in human brain mapping. *Psychophysiology, 40*, 511-520.

Hubbard, E.M., Piazza, M., Pinel, P., & Dehaene, S. (2005). Interactions between number and space in parietal cortex. *Nature Reviews: Neuroscience, 6*, 435-448.

Hyde, D.C., Boas, D.A., Blair, C., & Carey, S. (2010). Near-infrared spectroscopy shows right parietal specialization for number in pre-verbal infants. *NeuroImage, 53*, 647-652.

Issacs, E.B., Edmonds, C.J., Lucas, A., & Gadian, D.G. (2001). Calculation difficulties in children of very low birth weight: A neural correlate. *Brain, 124*, 1701-1707.

Izard, V., Dehaene-Lambertz, G., & Dehaene, S. (2008). Distinct cerebral pathways for object identity and number in human infants. *PLOS Biology, 6*, 275-285.

Jacob, S. N., & Nieder, A. (2009). Notation-independent representation of fractions in the human parietal cortex. *The Journal of Neuroscience, 29*, 4652-4657.

Jacob, S.N., Vallentin, D., & Nieder, A. (2012). Relating magnitudes: The brain's code for proportions. *Trends in Cognitive Sciences, 16*, 157-166.

Jordan, K.E., & Baker, J.M. (2011). Multisensory information boosts numerical matching abilities in young children. *Developmental Science, 14*, 205-213.

Jordan, K.E., Suanda, S.H., & Brannon, E.M. (2008). Intersensory redundancy accelerates preverbal numerical competence. *Cognition, 108*, 210-221.

Kameyama, M., Fukuda, M., Yamagishi, Y., Sato, T., Uehara, T., Ito, M., … Mikuni, M. (2006). Frontal lobe function in bipolar disorder: A multichannel near-infrared spectroscopy study. *NeuroImage, 29*, 172-184.

Kawashima, R., Taira, M., Okita, K., Inoue, K., Tajima, N., Yoshida, H., & Fukuda, H. (2004). A functional MRI study of simple arithmetic—a comparison between children and adults. *Cognition & Brain Research, 18*, 227-233.

Kiefer, M., & Dehaene, S. (1997). The time course of parietal activation in single-digit multiplication: Evidence from event-related potentials. *Mathematical Cognition, 3*(1), 1-30.

Kelly, D.J., Liu, S., Lee, K., Quinn, P.C., Pascalis, O., Slater, A.M., & Ge, L. (2009). Development of the other-race effect during infancy: Evidence toward universality? *Journal of Experimental Child Psychology, 104*, 105-114.

Kelly, D.J., Quinn, P.C., Slater, A.M., Lee, K., Ge, L., & Pascalis, O. (2007). The other-race effect develops during infancy: Evidence of perceptual narrowing. *Psychological Science, 18*, 1084-1089.

Köchel, A., Plichta, M.M., Schäfer, A., Schöngassner, F., Fallgatter, A.J., & Schienle, A. (2011). Auditory symptom provocation in dental phobia: A near-infrared spectroscopy study. *Neuroscience Letters, 503*, 48-51.

Kosslyn, S.M., Ball, T.M., & Reiser, B.J. (1978). Visual images preserve metric spatial information: Evidence from studies of image scanning. *Journal of Experimental Psychology: Human Perception & Performance, 4*(1), 47-60.

Kotovsky, L., & Gentner, D. (1996). Comparison and categorization in the development of relational similarity. *Child Development, 67*, 2797-2822.

Kucian, K., Loenneker, T., Dietrich, T., Dosch, M., Martin, E., & von Aster, M. (2006). Impaired neural networks for approximate calculation in dyscalculic children: A functional MRI study. *Behavioral & Brain Functioning, 2* (31). Retrieved from http://www.behavioralandbrainfunctions.com/content/2/1/31

Kucian, K., von Aster, M., Loenneker, T., Dietrich, T., & Martin, E. (2008). Development of neural networks for exact and approximate calculation: An fMRI study. *Developmental Neuropsychology, 33*, 447-473.

Kuhl, P.K., Williams, K.A., Lacerda, F., Stevens, K.N., & Lindblom, B. (1992). Linguistic experience alters phonetic perception in infants by 6 months of age. *Science, 255*, 606-608.

Kuhl, P.K., Tsao, F.M., & Liu, H.M. (2003). Foreign-language experience in infancy: Effects of short-term exposure and social interaction on phonetic learning. *Proceedings of the National Academy of Sciences, 100*, 9096-9101.

Lammertyn, J., Fias, W., & Lauwereyns, J. (2002). Semantic influences on feature-based attention due to overlap of neural circuits. *Cortex, 38*, 878-882.

Langdon, D.W., & Warrington, E.K. (1997). The abstraction of numerical relations: A role for the right hemisphere in arithmetic? *Journal of International Neuropsychological Society, 3*, 260-268.

Laski, E.V., & Siegler, R.S. (2007). Is 27 a big number? Correlational and causal connections among numerical categorization, number line estimation, and numerical magnitude comparison. *Child Development, 76*, 1723-1743.

Le Clec'H, G., Dehaene, S., Cohen, L., Mehler, J., Dupoux, E., Poline, J.B., … Le Bihan, D. (2000). Distinct cortical areas for names of number and body parts independent of language and input modality. *Neuroimage, 12*, 381-391.

Lee, K.M. (2000). Cortical areas differentially involved in multiplication and subtraction: A functional magnetic resonance imaging study and correlation with a case of selective acalculia. *Annals of Neurology, 48*, 657-661.

Lewis, J.W., Beauchamp, M.S., & DeYoe, E.A. (2000). A comparison of visual and auditory motion processing in human cerebral cortex. *Cerebral Cortex, 10*, 873-888.

Lewkowicz, D.J. (2004). Serial order processing in human infants and the role of multisensory redundancy. *Cognitive Processing, 5*, 113-122.

Lewkowicz, D.J., & Ghazanfar, A.A. (2006). The decline of cross-species intersensory perception in human infants. *Proceedings of the National Academy of Science, 103*, 6771-6774.

Lewkowicz, D.J., & Ghazanfar, A.A. (2009). The emergence of multisensory systems through perceptual narrowing. *TRENDS in Cognitive Psychology, 13*, 470-478.

Lewkowicz, D.J., & Kraebel, K. (2004). The value of multimodal redundancy in the development of intersensory perception. In G. Calvert, C. Spence, & B. Stein (Eds.), *Handbook of multisensory processing* (pp. 655-680). Cambridge, MA: MIT Press.

Lewkowicz, D.J., Leo, I., & Simion, F. (2010). Intersensory perception at birth: Newborns match non-human primate faces & voices. *Infancy, 15*(1), 46-60.

Lewkowicz, D.J., & Lickliter, R. (1994). *Development of intersensory perception: Comparative perspectives*. Hillsdale, NJ: Erlbaum.

Lewkowicz, D.J., Sowinski, R., & Place, S. (2008). The decline of cross-species intersensory perception in human infants: Underlying mechanisms and its developmental persistence. *Brain Research, 1242*, 291-302.

Lewkowicz, D.J., & Turkewitz, G. (1980). Cross-modal equivalence in early infancy: Auditory-visual intensity matching. *Developmental Psychology, 16*, 597-607.

Libertus, M. E., Odic, D., & Halberda, J. (2012). Intuitive sense of number correlates with math scores on college-entrance examination. *Acta Psychologica, 141*, 373-379.

Macaluso, E., Frith, C.D., & Driver, J. (2000). Modulation of human visual cortex by crossmodal spatial attention. *Science, 289*, 1206-1208.

Medendorp, W.P., Goltz, H.C., Crawford, J.D., & Vilis, T. (2005). Integration of target and effector information in human posterior parietal cortex for the planning of action. *Journal of Neurophysiology, 93*, 954-962.

Menon, V., Rivera, S.M., White, C.D., Glover, G.H., & Reiss, A.L. (2000). Dissociating prefrontal and parietal cortex activation during arithmetic processing. *NeuroImage, 12*, 357-365.

Minagawa-Kawai, Y., Mori, K., Hebden, J.C., & Dupoux, E. (2008). Optical imaging of infants' neurocognitive development: Recent advances and perspectives. *Developmental Neurobiology, 68*, 712-728.

Mistlin, A.J., & Perrett, D.I. (1990). Visual and somatosensory precssing in the macaque temporal cortex: The role of 'expectation'. *Experimental Brain Research, 82*, 437-450.

Moyer-Packenham, P., & Westenskow, A. (in press). Effects of virtual manipulatives on student achievement and mathematics learning. *International Journal of Virtual and Personal Learning Environments*.

Muhlau, M., Hermsdorfer, J., Goldenberg, G., Wohlschlager, A.M., Castrop, F., Rottinger, M., … Boecker, H. (2005). Left inferior parietal dominance in gesture imitation: An fMRI study. *Neuropsychologia, 43*, 1086-1098.

Naccache, L., & Dehaene, S. (2001). The priming method: Imaging unconscious repetition priming reveals an abstract representation of number in the parietal lobes. *Cerebral Cortex, 11*, 966-974.

Ni, Y. (2000). How valid is it to use number lines to measure children's conceptual knowledge about rational number? *Educational Psychology, 20*, 139-152.

Nieder, A., Diester, I., & Tudusciuc, O. (2006). Temporal and spatial enumeration processes in the primate parietal cortex. *Science, 313*, 1431-1435.

Nieder, A., Freedman, D.J., & Miller, E.K. (2002). Representations of the quantity of visual items in the primate prefrontal cortex. *Science, 297*, 1708-1711.

Nieder, A., & Miller, E.K. (2004). A parieto-frontal network for visual numerical information in the monkey. *Proceedings of the National Academy of Science, 101*, 7457-7462.

Niedermeyer, E., & da Silva, F.L. (Eds.). (2004). *Electroencephalography: Basic principles, clinical applications, and related fields.* New York, NY: Lippincott Williams & Wilkins.

Obrig, H., & Villringer, A. (2003). Beyond the visible: Imaging the human brain with light. *Journal of Cerebral Blood Flow & Metabolism, 23*(1), 1-18

Okamoto, M., Dan, H., Sakamoto, K., Takeo, K., Shimizu, K., Kohno, S., … Dan, I. (2004). Three-dimensional probabilistic anatomical cranio-cerebral correlation via the international 10-20 system oriented for transcranial functional brain mapping. *NeuroImage, 21*, 99-111.

Opfer, J., & Siegler, R.S. (2007). Representational change and children's numerical estimation. *Cognitive Psychology, 55,* 169-195.

Owen, A.M., McMillan, K.M., Laird, A.R., & Bullmore, E. (2005). N-back working memory paradigm: A meta-analysis of normative functional neuroimaging studies. *Human Brain Mapping, 25*(1), 46-59.

Pascalis, O., de Haan, M., & Nelson, C.A. (2002). Is face processing species-specific during the first year of life? *Science, 296*, 1321-1323.

Pascalis, O., Scott, L.S., Kelly, D.J., Shannon, R.W., Nicholson, E., Coleman, M., & Nelson, C.A. (2005). Plasticity of face processing in infancy. *Proceedings of the National Academy of Science, 102*, 5297-5300.

Peña, M., Maki, A., Kovačić, D., Dehaene-Lambertz, G., Koizumi, H., Bouquet, F., & Mehler, J. (2003). Sounds and silence: An optical topography study of language recognition at birth. *Proceedings of the National Academy of Sciences, 100*, 11702-11705.

Pesenti, M., Thioux, M., Seron, X., & De Volder, A. (2000). Neuroanatomical substrates of Arabic number processing, numerical comparisons, and simple addition: A PET study. *Journal of Cognitive Neuroscience, 12*, 461-479.

Piazza, M., Izard, V., Pinel, P., Le Bihan, D., & Dehaene, S. (2004). Turning curves for approximate numerosity in the human intraparietal sulcus. *Neuron, 44*, 547-555.

Piazza, M., Mechelli, A., Butterworth, B., & Price, C.J. (2002a). Are subitizing and counting implemented as separate or functionally overlapping processes? *Neuroimage, 15*, 435-446.

Piazza, M., Mechelli, A., Price, C.J., & Butterworth, B. (2002a). The quantifying brain: Functional neuroanatomy of numerosity estimation and counting. *Neuron, 44*, 547-555.

Piazza, M., Pinel, P., Le Bihan, D., & Dehaene, S. (2007). A magnitude code common to numerosities and number symbols in human intraparietal cortex. *Neuron, 53*, 293-305.

Pinel, P., Dehaene, S., Riviere, D., & Le Bihan, D. (2001). Modulation of parietal activation by semantic distance in number comparison task. *Neuroimage, 14*, 1013-1026.

Pinel, P., Piazza, M., Le Bihan, D., & Dehaene, S. (2004). Distributed and overlapping cerebral representations of number, size, and luminance during comparative judgments. *Neuron, 41*, 1-20.

Plichta, M.M., Heinzel, S., Ehlis, A.C., Pauli, P., & Fallgatter, A.J. (2007). Model-based analysis of rapid event-related functional near-infrared spectroscopy (NIRS) data: a parametric validation study, *Neuroimage, 35*, 625-634.

Plichta, M.M., Herrmann, M.J., Baehne, C.G., Ehlis, A.–C., Richter, M.M., Pauli, P., & Fallgatter, A. J. (2006). Event-related functional near-infrared spectroscopy (fNIRS): Are the measurements reliable? *NeuroImage*, *31*, 116-124.

Pons, F., Lewkowicz, D.J., Soto-Faraco, S., & Sebastian-Galles, N. (2009). Narrowing of intersensory speech perception in infancy. *Proceedings of the National Academy of Science, 10*, 1073.

Poulin-Dubois, D., Serbin, L.A., Kenyon, B., & Derbyshire, A. (1994). Infants' intermodal knowledge about gender. *Developmental Psychology, 30*, 436-442.

Quinn, P.C., Uttley, L., Lee, K., Gibson, A., Smith, M., Slater, A.M., & Pascalis, O. (2008). Infant preference for female faces occurs for same- but not other –race faces. *Journal of Neuropsychology, 2*, 15-26.

Raij, T., Uutela, K., & Hari, R. (2000). Audiovisual integration of letters in the human brain. *Neuron, 28*, 617-625.

Ramani, G.B., & Siegler, R.S. (2008). Promoting broad and stable improvements in low-income children's numerical knowledge through playing number board games. *Child Development, 79*, 375-394.

Raposo, D., Sheppard, J.P., Schrater, P.R., & Churchland, A.K. (2012). Multisensory decision-making in rats and humans. *The Journal of Neuroscience, 32*, 3726-3735.

Rivera, S.M., Reiss, A.L., Eckert, M.A., & Menon, V. (2005). Developmental changes in mental arithmetic: Evidence for increased functional specialization in the left inferior parietal cortex. *Cerebral Cortex, 15*, 1779-1790.

Rosenberg-Lee, M., Barth, M., & Menon, V. (2011). What difference does a year of schooling make? Maturation of brain response and connectivity between 2nd and 3rd grades during arithmetic problem solving. *NeuroImage, 57*, 769-808.

Rosselli, M., & Ardila, A. (1989). Calculation deficits in patients with right and left hemisphere damage. *Neuropsychologia, 27*, 607-617.

Rotzer, S., Kucian, K., Martin, E., von Aster, M., Klaver, P., & Loenneker, T. (2008). Optimized voxel-based morphometry in children with developmental dyscalculia. *Neuroimage, 39*, 417-422.

Sangrigoli, S., & de Schonen, S. (2004). Recognition of own-race and other-race faces by three-month-old infants. *Journal of Child Psychology & Psychiatry, 45*, 1219-1227.

Schneider, W., Eschman, A., & Zuccolotto, A. (2002a). *E-Prime user's guide*. Pittsburgh, PA: Psychology Software Tools.

Schneider, W., Eschman, A., & Zuccolotto, A. (2002b). *E-Prime reference guide*. Pittsburgh, PA: Psychology Software Tools.

Sereno, M.I., Pitzalis, S., & Martinez, A. (2001). Mapping of contralateral space in retinotopic coordinates by a parietal cortical area in humans. *Science, 294*, 1350-1354.

Seymour, S.E., Reuter-Lorenz, P.A., & Gazzaniga, M.S. (1994). The disconnection syndrome: Basic findings reaffirmed. *Brain, 117*, 105-115.

Shikata, E., Hamzei, F., Glauche, V., Koch, M., Weiller, C., Binkofski, F., & Buchel, C. (2003). Functional properties and interaction of the anterior and posterior intraparietal areas in humans. *European Journal of Neuroscience, 17*, 1105-1110.

Siegler, R.S. (1996). *Emerging minds: The process of change in children's thinking*. New York, NY: Oxford University Press.

Siegler, R.S., & Booth, J.L. (2004). Development of numerical estimation in young children. *Child Development, 75*, 428-444.

Siegler, R.S., & Mu, Y. (2008). Chinese children excel on novel mathematics problems even before elementary school. *Psychological Science, 19*, 759-763.

Siegler, R.S., & Opfer, J. (2003). The development of numerical estimation: Evidence for multiple representations of numerical quantity. *Psychological Science, 14*, 237-243.

Siegler, R.S., & Ramani, G.B. (2008). Playing linear numerical board games promotes low-income children's numerical development. *Developmental Science, 11*, 655-661.

Simon, O., Cohen, L., Mangin, J.F., Le Bihan, D.L., & Dehaene, S. (2002). Topographical layout of hand, eye, calculation and language related areas in the human parietal lobe. *Neuron, 33*, 475-487.

Singh, A.K., Okamoto, M., Dan, H., Jucak, V., & Dan, I. (2005). Spatial registration of multichannel multi-subject fNIRS data to MNI space without MRI. *Neuroimage, 27*, 842-851.

Stanescu-Cosson, R., Pinel, P., Van de Moortele, P.-F., Le Bihan, D.L., Cohen, L., & Dehaene, S. (2000). Cerebral bases of calculation processes: Impact of number size on the cerebral circuits for exact and approximate calculation. *Brain, 123*, 2240-2255.

Stevens, S.S. (1957). On the psychophysical law. *Psychological Review*, *64*(3), 153-181.

Takayama, Y., Sugishita, M., Akiguchi, I., & Kimura, J. (1994). Isolated acalculia due to left parietal lesion. *Archives of Neurology, 51*, 286-291.

Takeshi, K., Nemoto, T., Fumoto, M., Arita, H., & Mizuno, M. (2010). Reduced prefrontal cortex activation during divergent thinking in schizophrenia: A multi-channel NIRS study. *Progress in Neuro-Psychopharmacology & Biological Psychiatry, 34*, 1327-1332.

Temple, E., & Posner, M.I. (1998). Brain mechanisms of quantity are similar in 5-year-olds and adults. *Proceedings of the National Academy of Sciences, 95*, 7836-7841.

Thioux, M., Pesenti, M., De Volder, A., & Seron, X. (2002). Category-specific representation and processing of numbers and animal names across semantic tasks: A PET study. *NeuroImage, 13*, S617.

Thompson, C.A., & Opfer, J.E. (2008). Costs and benefits of representational change: Effects of context on age and sex differences in symbolic magnitude estimation. *Journal of Experimental Child Psychology, 101*(1), 20-51.

Thompson, C.A., & Opfer, J.E. (2010). How 15 hundred is like 15 cherries: Effect of progressive alignment on representation changes in numerical cognition. *Child Development, 81*, 1768-1786.

Tudusciuc, O., & Neider, A. (2007). Neuronal population coding of continuous and discrete quantity in the primate posterior parietal cortex. *Proceedings of the National Academy of Science, 104*, 14513-14518.

Turconi, E. (2002). Dissociation between order and quantity meanings in a patient with Gerstmann syndrome. *Cortex, 38*(5), 911-913.

Wallace, M.T., Meredith, M.A., & Stein, B.E. (1992). Integration of multiple sensory modalities in cat cortex. *Experimental Brain Research, 91*, 484-488.

Walsh, V.A. (2003). A theory of magnitude: Common cortical metrics of time, space, and quantity. *Trends in Cognitive Science, 7*, 483-488.

Warrington, E.K. (1982). The fractionation of arithmetical skills: A single case study. *Quarterly Journal of Experimental Psychology, 34A*, 31-51.

Weikum, W.M., Vouloumanos, A., Navarra, J., Soto-Faraco, S., Sebastian-Galles, N., & Werker, J.F. (2007). Visual language discrimination in infancy. *Science, 316*, 1159.

Werker, J.F., & Tees, R.C. (1984). Cross-language speech perception: Evidence for perceptual reorganization during the first year of life. *Infant Behavior & Development, 7*, 49-63.

Wilcox, T., Bortfeld, H., Woods, R., Wruck, E., & Boas, D.A. (2008). Hemodynamic response to featural changes in the occipital and inferior temporal cortex in infants: A preliminary methodological exploration. *Developmental Science, 11*, 361-370.

Wilcox, T., Bortfeld, H., Woods, R., Wruck, E., Armstrong, J., & Boas, D. (2009). Hemodynamic changes in the infant cortex during the processing of featural and spatiotemporal information. *Neuropsychologia, 47*, 657-662.

Wilkinson, L.K., Meredith, M.A., & Stein, B.E. (1996). The role of anterior ectosylvian cortex in cross-modality orientation and approach behavior. *Experimental Brain Research, 112*, 1-10.

Worsley, K.J., & Friston, K.J. (1995). Analysis of fMRI time-series revisited-again. *Neuroimage, 2*, 173-181.

Ye, J C., Tak, S., Jang, K.E., Jung, J., & Jang, J. (2009). NIRS-SPM: Statistical parametric mapping for near-infrared spectroscopy. *Neuroimage, 44*, 428-447.

Zenon, A., Filali, N., Duhamel, J.R., & Oliver, E. (2010). Salience representation in the parietal and frontal cortex. *Journal of Cognitive Neuroscience, 22*, 918-930.

APPENDICES

Appendix A

Adult Trial Structure

	Block 1: Prefeedback				Block 2: Feedback				Block 3: Postfeedback			
Trial Order	**Scale Size**	**ITI**	**Onset**	**Duration**	**Scale Size**	**ITI**	**Onset**	**Duration**	**Scale Size**	**ITI**	**Onset**	**Duration**
30s pre-scan												
1	Large	4	34	7	Small	4	424	9	Small	4	872	7
2	Small	2	43	7	Large	6	439	9	Small	8	887	7
3	Small	8	58	7	Large	8	456	9	Large	2	896	7
4	Small	8	73	7	Small	8	473	9	Small	4	907	7
5	Large	4	84	7	Large	2	484	9	Large	2	916	7
6	Small	6	97	7	Small	4	497	9	Large	4	927	7
7	Large	4	108	7	Small	2	508	9	Large	6	940	7
8	Large	2	117	7	Large	8	525	9	Small	2	949	7
9	Small	6	130	7	Small	4	538	9	Small	8	964	7
10	Large	4	141	7	Small	4	551	9	Large	6	977	7
11	Large	4	152	7	Large	4	564	9	Small	2	986	7
12	Large	8	167	7	Small	4	577	9	Large	4	997	7
13	Large	2	176	7	Large	4	590	9	Small	6	1010	7
14	Large	6	189	7	Large	8	607	9	Small	4	1021	7
15	Small	8	204	7	Large	8	624	9	Small	2	1030	7
16	Small	4	215	7	Small	6	639	9	Large	8	1045	7
17	Small	6	228	7	Large	2	650	9	Large	8	1060	7
18	Small	8	243	7	Large	6	665	9	Small	4	1071	7
19	Small	4	254	7	Large	6	680	9	Large	4	1082	7
20	Small	2	263	7	Small	6	695	9	Large	6	1095	7
21	Small	4	274	7	Large	2	706	9	Large	4	1106	7
22	Large	6	287	7	Small	2	717	9	Large	2	1115	7
23	Large	6	300	7	Small	8	734	9	Large	6	1128	7
24	Small	6	313	7	Small	4	747	9	Small	2	1137	7
25	Large	8	328	7	Small	6	762	9	Small	6	1150	7
26	Small	2	337	7	Large	2	773	9	Small	8	1165	7
27	Large	2	346	7	Small	2	784	9	Small	8	1180	7
28	Large	8	361	7	Large	8	801	9	Large	6	1193	7
29	Large	2	370	7	Large	6	816	9	Small	2	1202	7
30	Large	4	381	7	Small	2	827	9	Large	8	1217	7
30s post-scan												

Note. All values represent seconds. Each block was separated by a 30-second rest period

Appendix B

Child Trial Structure

Block 1: Prefeedback					Block 2: Feedback				Block 3: Postfeedback			
Trial Order	**Scale Size**	**ITI**	**Onset**	**Duration**	**Scale Size**	**ITI**	**Onset**	**Duration**	**Scale Size**	**ITI**	**Onset**	**Duration**
30s pre-scan												
1	Large	2	32	8	Large	2	322	10	Large	4	654	8
2	Small	8	48	8	Large	4	336	10	Small	6	668	8
3	Large	8	64	8	Small	4	350	10	Small	2	678	8
4	Small	4	76	8	Small	6	366	10	Small	8	694	8
5	Large	6	90	8	Small	8	384	10	Large	4	706	8
6	Large	4	102	8	Large	6	400	10	Large	4	718	8
7	Small	6	116	8	Large	6	416	10	Small	6	732	8
8	Large	8	132	8	Small	2	428	10	Small	8	748	8
9	Small	2	142	8	Large	8	446	10	Small	8	764	8
10	Small	6	156	8	Small	8	464	10	Small	6	778	8
11	Small	6	170	8	Small	6	480	10	Large	2	788	8
12	Small	2	180	8	Large	4	494	10	Large	8	804	8
13	Large	2	190	8	Small	8	512	10	Large	2	814	8
14	Large	2	200	8	Large	2	524	10	Large	6	828	8
15	Small	4	212	8	Small	4	538	10	Large	4	840	8
16	Large	8	228	8	Small	4	552	10	Large	8	856	8
17	Large	6	242	8	Large	6	568	10	Small	2	866	8
18	Large	4	254	8	Large	8	586	10	Small	4	878	8
19	Small	8	270	8	Small	2	598	10	Large	2	888	8
20	Small	4	282	8	Large	2	610	10	Small	6	902	8
30s post-scan												

Note. All values represent seconds. Each block was separated by a 30-second rest period

Appendix C

Prefrontal Cortex Probe Set Functional Region of Interest Schematic

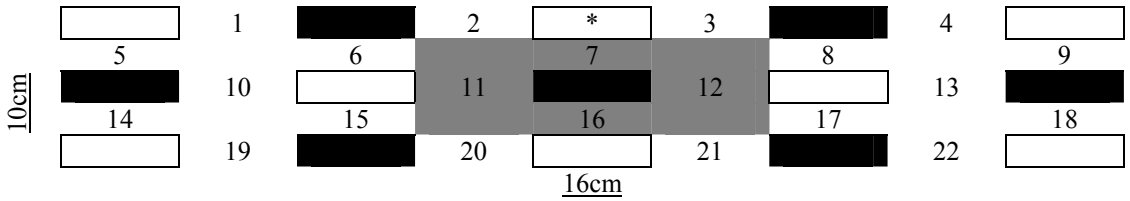

Schematic representation of the medial prefrontal cortex fROI within the 22-channel NIRS probe set placed over the prefrontal cortex. White squares indicate light emitters; black squares indicate light detectors; numbers indicate the measurement channels; grey squares indicate the channels that constitute the *fROI*. The asterisk indicates the light emitter that was located at Fpz

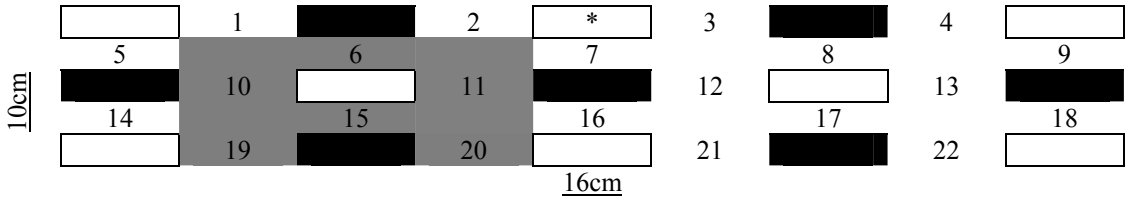

Schematic representation of the left dorsolateral prefrontal cortex fROI within the 22-channel NIRS probe set placed over the prefrontal cortex. White squares indicate light emitters; black squares indicate light detectors; numbers indicate the measurement channels; grey squares indicate the channels that constitute the *fROI*. The asterisk indicates the light emitter that was located at Fpz

Appendix D

Parietal Cortex Probe Set Functional Region of Interest Schematic

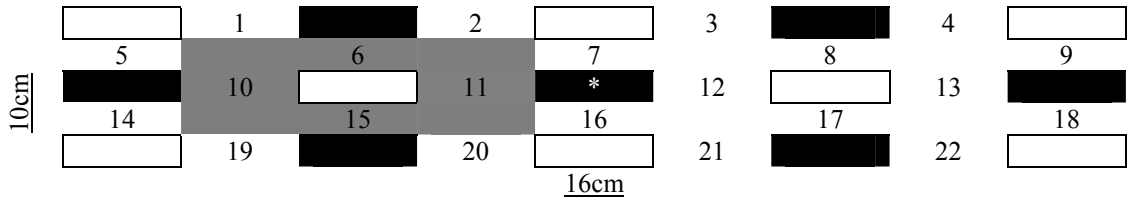

Schematic representation of the left interparietal sulcus within the 22-channel NIRS probe set placed over the parietal cortex. White squares indicate light emitters; black squares indicate light detectors; numbers indicate the measurement channels; grey squares indicate the channels that constitute the *fROI*. The asterisk indicates the light detector that was located at Pz.

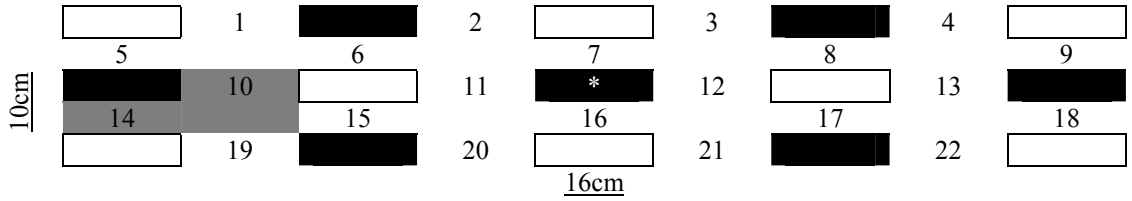

Schematic representation of the left angular gyrus within the 22-channel NIRS probe set placed over the parietal cortex. White squares indicate light emitters; black squares indicate light detectors; numbers indicate the measurement channels; grey squares indicate the channels that constitute the *fROI*. The asterisk indicates the light detector that was located at Pz.

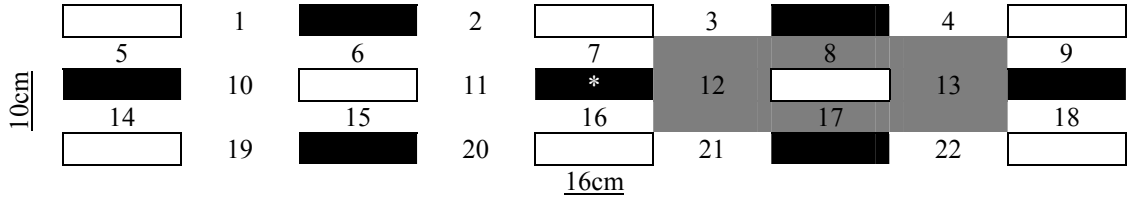

Schematic representation of the right intraparietal sulcus within the 22-channel NIRS probe set placed over the parietal cortex. White squares indicate light emitters; black squares indicate light detectors; numbers indicate the measurement channels; grey squares indicate the channels that constitute the *fROI*. The asterisk indicates the light detector that was located at Pz.

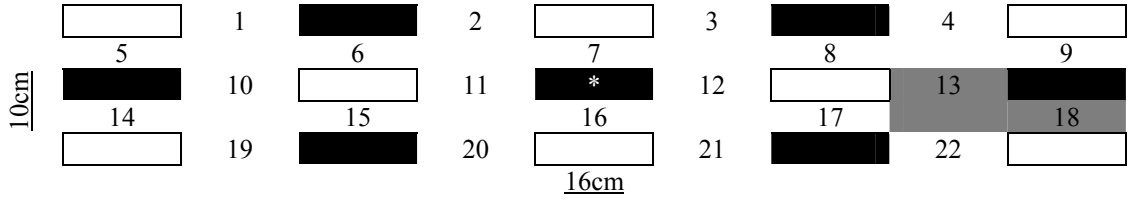

Schematic representation of the right angular gyrus within the 22-channel NIRS probe set placed over the parietal cortex. White squares indicate light emitters; black squares indicate light detectors; numbers indicate the measurement channels; grey squares indicate the channels that constitute the *fROI*. The asterisk indicates the light detector that was located at Pz.

Appendix E

Adult Values and Scales

Value	Scale
eight hundred fifty million	one billion
eight hundred fifty trillion	one quadrillion
five hundred eighty million	one billion
five hundred eighty trillion	one quadrillion
four hundred eighty million	one billion
four hundred eighty trillion	one quadrillion
four hundred thirty million	one billion
four hundred trillion	one quadrillion
nine hundred ninety-nine million	one billion
nine hundred ninety-nine trillion	one quadrillion
one hundred eighty million	one billion
one hundred eighty trillion	one quadrillion
one hundred fifty million	one billion
one hundred twenty trillion	one quadrillion
seven hundred ninety million	one billion
seven hundred ninety trillion	one quadrillion
six hundred million	one billion
six hundred thirty million	one billion
six hundred thirty trillion	one quadrillion
six hundred trillion	one quadrillion
thirty million	one billion
thirty trillion	one quadrillion
three hundred eighty million	one billion
three hundred ninety million	one billion
three hundred ninety trillion	one quadrillion
three hundred ten million	one billion
three hundred ten trillion	one quadrillion
two hundred eighty million	one billion
two hundred eighty trillion	one quadrillion
two hundred thirty trillion	one quadrillion

Appendix F

Child Values and Scales

Value	Scale
eighteen	one hundred
eighteen thousand	one hundred thousand
eighty-five	one hundred
eighty-five thousand	one hundred thousand
fifteen	one hundred
fifteen thousand	one hundred thousand
fifty-eight	one hundred
fifty-eight thousand	one hundred thousand
forty	one hundred
forty thousand	one hundred thousand
forty-eight	one hundred
forty-eight thousand	one hundred thousand
forty-three	one hundred
forty-three thousand	one hundred thousand
ninety-nine	one hundred
ninety-nine thousand	one hundred thousand
seventy-nine	one hundred
seventy-nine thousand	one hundred thousand
sixty	one hundred
sixty thousand	one hundred thousand
sixty-three	one hundred
sixty-three thousand	one hundred thousand
thirty	one hundred
thirty thousand	one hundred thousand
thirty-eight	one hundred
thirty-eight thousand	one hundred thousand
thirty-nine	one hundred
thirty-nine thousand	one hundred thousand
thirty-one	one hundred
thirty-one thousand	one hundred thousand
three	one hundred
three thousand	one hundred thousand
twelve	one hundred
twelve thousand	one hundred thousand
twenty-eight	one hundred
twenty-eight thousand	one hundred thousand
twenty-five	one hundred
twenty-five thousand	one hundred thousand
twenty-three	one hundred
twenty-three thousand	one hundred thousand

CURRICULUM VITAE

JOSEPH M. BAKER, PH.D.

EDUCATION & TRAINING

Stanford University, Stanford, CA
Postdoctoral Fellow, 2013-Present
Faculty Sponsor: Dr. Allan Reiss
Utah State University, Logan, UT
Ph.D., Experimental Psychology, 2013
Dissertation Chair: Dr. Kerry E. Jordan
Middle Tennessee State University, Murfreesboro, TN
Master of Arts in Experimental Psychology, 2008
Thesis Chair: Dr. Stephen Schmidt
New Mexico State University, Las Cruces, NM
Bachelor of Arts in Psychology, 2005

RESEARCH INTERESTS

The development and representation of abstract concepts such as number and the relationship between these representations and education.
The development and mechanisms of inter-sensory perception and its relation to psychophysical discrimination and learning.
Investigation of behavioral and neurological underpinnings of effective learning and achievement in education.
Effective translation of basic cognitive science findings into applied educational settings.

RESEARCH EXPERIENCE

Center for Interdisciplinary Brain Sciences Research, *Postdoctoral Fellow*, Stanford University
Supervisor: Dr. Allan Reiss, 2013-Present
We are currently using NIRS to investigate the neurological signatures of math and number processing in females with Turner Syndrome. Included in this line of research is the development of a NIRS based brain-computer-interface intervention designed to enhance common atypical math and number related processing within this population.

Multisensory Cognition Lab, *Ph.D. Candidate*, Utah State University
Supervisor: Dr. Kerry Jordan, 2008-2013
Using a suite of convergent behavioral and neuroimaging (NIRS) methods, we study

the development and evolution of quantitative cognition in human and non-human animals, as well as the effects of multisensory stimulation on quantitative representations and discrimination. My research also focuses on how to best translate these findings into applied educational settings with the hopes of informing early childhood education.

Learning, Education, Audiology, & Psychology (LEAP) NIRS Brain-imaging Lab, *Research Assistant,* Utah State University
Supervisor: Dr. Ronald Gillam, 2011-2013
We are currently investigating the neurological and behavioral correlates to cognitive processes related to learning and academic achievement in typically developing and learning disabled populations using functional near-infrared spectroscopy.

Virtual Manipulative Research Group, *Research Assistant,* Utah State University
Supervisor: Dr. Patricia Moyer-Packenham, 2009-2013
We investigate the effects of virtual mathematics teaching tools on children's learning and achievement in both school and laboratory settings. Following an initial two-year in-school study, which identified significant influences in children's learning of fraction concepts that are attributable to virtual manipulatives, we are currently designing multiple follow-up studies designed to investigate the neurological correlates to children's use of virtual teaching tools (using NIRS), as well as the effectiveness of such tools when presented on tablet devices.

Active Learning Lab, *Research Assistant,* Utah State University
Supervisor: Dr. Taylor Martin, 2012-2013
Our research team is investigating the effectiveness of emergent technology in facilitating learning and achievement of mathematics in children. Specifically, I am working closely with Dr. Martin to establish a research study designed to map the behavior of children playing the fraction learning game Refraction© onto corresponding neural activation patterns that are recorded by way of NIRS.

Near-Infrared Spectroscopy Team, *Research Assistant*, Stanford University
Supervisors: Drs. Allan Reiss, Xu Cui, and Ning Liu, Summer 2012
I assisted in multiple studies investigating neurological and behavioral correlates to social cognition and decision-making processes using functional near-infrared spectroscopy. Moreover, I gained experience in designing event-related NIRS research studies, as well as conducting NIRS based analyses using a general linear model approach.

Memory and Attention Lab, *Masters of Arts,* Middle Tennessee State University
Supervisor: Dr. Stephen Schmidt, 2005-2008
Studied the effect of taboo stimuli on psychophysical and cognitive processes in humans.

HONORS & AWARDS

2013	Utah State University Open Access Funding Initiative Award ($1,268.45)
2013	NIH Conference on the Evolutionary Precursors and Early Development of Basic Number Processing, Travel Award ($1,000).
2013-2014	Doctoral researcher ($20,000). *Captivated! Young children's learning interactions with iPad mathematics apps*. 2013-14. Utah State University, Vice President for Research RC Funding. Project goal: build theory and knowledge about the nature of young children's ways of thinking and interacting with virtual manipulatives using touch-screen mathematics apps on the iPad (with Principal Investigator Patricia Moyer-Packenham, Co-PI Cathy Maahs-Fladung, and the Virtual Manipulative Research Group). My role: Statistical analysis and visualization of quantitative and qualitative data, conduct iPad-based interviews with participants, observe and code participant actions, and coding of data.
2012-2013	Utah State University Dissertation Fellowship
2011	Intermountain Graduate Research Symposium Lecture Presentation Competition, Second Place
2011-2012	Graduate Research Assistant ($35,000). *Virtual Manipulatives Research Group: Effects of Multiple Visual Modalities of Representation on Rational Number Competence*. 2011-12. Utah State University, Vice President for Research SPARC Funding. Lead PI- Patricia Moyer-Packenham; Collaborating Faculty—Kerry Jordan, Dicky Ng, and Kady Schneiter; My role: Conduct data collection and analysis, participate in research team meetings, collaborate on publications and presentations focusing on using virtual manipulatives to teach rational number concepts.
2010	Conference Travel Fellowship, Utah State University
2010	Intermountain Graduate Research Symposium Lecture Presentation Competition, First Place
2010	Walter R. Borg Scholarship and Research Productivity Award, Utah State University, Department of Psychology

2008	Conference Travel Fellowship, Utah State University
2007	Robert E. Prytulla Scholarship for Excellence in Psychological Studies, Middle Tennessee State University, Department of Psychology
2007	Research Travel Grant, Middle Tennessee State University

PUBLISHED PEER-REVIEWED MANUSCRIPTS

Baker, J. M., Rodzon, K. S., & Jordan, K. E. (In Press). The impact of emotion on visual numerical estimation. *Frontiers in Cognition*.

Moyer-Packenham, P., **Baker, J. M.**, Westenskow, A., Rodzon, K., Anderson, K., Shumway, J., & Jordan, K. (In Press). Achievement performance: A random assignment study in seventeen third- and fourth-grade classrooms comparing virtual manipulatives with other instructional treatments. *Journal of Education*.

Baker, J. M., Morath, J., Rodzon, K. S., & Jordan, K. E. (2012). A shared system of representation governing quantity discrimination in canids. *Frontiers in Psychology, 3*, 387.

Baker, J. M., Shivik, J., & Jordan, K. E. (2011). Tracking of food quantity by coyotes (*Canis Latrans*). *Behavioral Processes, 88*, 72-75

Jordan, K. & **Baker, J.M.** (2011). Multisensory information boosts numerical matching abilities in young children. *Developmental Science,* 14(2), 205-213

PUBLISHED PEER-REVIEWED CONFERENCE PROCEEDINGS

Clark, D., **Baker, J. M.**, & Jordan, K. E. (2013). Salience of race vs. gender to children and adults. Published in the proceedings of the National Conference on Undergraduate Research (NCUR).

Baker, J. M., Feigleson, J. M., & Jordan, K. E. (2010). Multiple visual cues enhance quantitative perception in infancy. Published in the proceedings of the Cognitive Science Society, 2799.

Jordan, K. E., **Baker, J. M.**, & Rodzon, K. S. (2010). Multisensory stimuli improve numerical matching abilities of preschool children. Published in the proceedings of the Cognitive Science Society, 552.

MANUSCRIPTS UNDER REVIEW/REVISION/IN PREPARATION

Baker, J. M., Mahamane, S., & Jordan, K. E. (Under revision). Multiple visual

quantitative cues enhance discrimination in infancy. *Journal of Experimental Child Psychology*, May 2013.

Moyer-Packenham, P., **Baker, J. M.**, Westenskow, A., Anderson, K., Shumway, J. F., Rodzon, K. S., Ng, D., & Jordan, K. E. (Under revision). Virtual manipulatives versus classroom instruction: Hidden predictors of achievement. Submitted to *Computers & Education*, December 2012.

Maclean, E., Addessi, E., Amici, F., Anderson, R., Aureli, F., **Baker, J.M.**, Barnard, A., Boogert, N., Brannon, E., Bray, J., Bray, E., Brent, L., Burkart, J., Call, J., Cantlon, J., Cheke, L., Clayton, N., Delgado, M., Fujita, K., Hiramatsu, C., Jacobs, L., Jordan, K., Moura, A., Nowicki, S., Nunn, C., Ostojić, L., Platt, M., Plotnik, J., Range, F., Reddy, R., Sandel, A., Shaw, R., Su, Y., Takimoto, A., Tan, J., Tao, R., van Schaik, C., Visalberghi, E.,Watanabe, A., Zhao, Y., & Hare, B. (In preparation). Brain size predicts performance on inhibitory control tasks across 33 species.

Baker, J. M., & Schmidt, S. (In preparation). Naughty words: The influence of taboo words on cognition.

Baker, J. M., Rodzon, K. S., Shumway, J., Ng, D., Moyer-Packenham, P., & Jordan, K. (In preparation). Visual vs. symbolic part-whole understanding in fraction learning.

Jordan, K. E., **Baker, J. M.**, & Mitroff, S. (In preparation). The sensitive geek: Enhanced matching of numerosity in videogamers.

PROFESSIONAL PRESENTATIONS & INVITED LECTURES

Baker, J. M., & Jordan, K. E. (2013, May). *Concurrent neurological and behavioral assessment of number line estimation performance in early math learners*. Poster presented at the NIH Conference on the Evolutionary Precursors and Early Development of Basic Number Processing, Washington, D.C.

Baker, J. M., & Jordan, K. E. (2013, April). *NIRS based neurological assessment of number line estimation performance in children and adults.* Talk given at the annual Intermountain Graduate Research Symposium, Logan, UT.

Baker, J. M., Jordan, K. E. (2013, January). *Multiple cues enhance quantitative discrimination in infancy.* Talk given at the annual Interdisciplinary Conference, Jackson Hole, WY.

Baker, J. M. (2012, October). *Data visualization and management techniques: Approaches using Mondrian and Excel*. Invited lecture, Graduate Student Seminar, Department of Special Education, Utah State University.

Baker, J. M., Jenkins, S., Friedel, J., & Jordan, K. E. (2012, April). *The effect of scale on number line estimations*. Talk given at the annual Intermountain Graduate Research Symposium, Logan, UT.

Moyer-Packenham, P., Jordan, K. E., Ng, D., Anderson, K., **Baker, J. M.**, Rodzon, K., Shumway, J., & Westenskow, A. (2011, October). *School mathematics research on virtual manipulatives: A collaborative team approach*. Talk given at the annual meeting of the School Science & Math Association, Colorado Springs, CO.

Baker, J. M., & Jordan, K. E. (2011, October). *The effect of intrasensory stimulation on infants' quantitative discrimination*. Poster presented at the biennial meeting of the Cognitive Development Society, Philadelphia, PA.

Rodzon, K., **Baker, J. M.**, Jordan, K. E. (2011, July). *Impact of emotion on numerical estimation*. Talk given at the annual Cognitive Society Society, Boston, MA.

Baker, J. M., & Jordan, K. E. (2011, June). Investigating the effects of multisensory stimulation on numerical cognition. Invited lecture, Family Consumer and Human Development Honors, USU, Logan, UT.

Baker, J. M., Thrailkill, E., & Shahan, T. (2011, April). *Allocation of unconscious visual attention and the matching law*. Talk given at the annual Intermountain Graduate Research Symposium, Logan, UT.

Baker, J. M., Feigleson, J., & Jordan, K. E. (2010, August). *Multiple visual cues enhance quantitative perception in infancy*. Talk given at the annual conference of the Cognitive Science Society, Portland, OR.

Jordan, K. E., **Baker, J. M.**, & Rodzon, K. S. (2010, August). *Multisensory information boosts numerical matching abilities in young children*. Poster presented at the annual conference of the Cognitive Science Society, Portland, OR.

Jordan, K. E., **Baker, J. M.** (2010, July). *Multisensory stimuli enhance numerical abilities of preschool children*. Poster presented at the annual conference of the International Society for the Study of Behavioral Development, Lusaka, Zambia.

Jordan, K. E., **Baker, J. M.**, & Rodzon, K. S. (2010, May). *Tracking of food quantity by coyotes* (*Canis Latrans*). Poster presented at the annual meeting of the Visual Sciences Society, Naples, FL.

Baker, J. M., Rodzon, K. S., Shivik, J., & Jordan, K. E. (2010, April). *Numerical discrimination abilities in coyotes* (*Canis Latrans*). Talk given at the annual conference of the Utah Academy of Sciences, Arts, and Letters, St. George, UT.

Baker, J. M., & Jordan, K. E. (2010, April). *Multisensory redundancy and numerical*

discrimination abilities in infancy. Invited lecture, Research Methods, USU, Logan, UT.

Baker, J. M., & Jordan, K. E. (2010, March). *Intrasensory cues enhance quantitative perception in infancy*. Talk given at the annual Intermountain Graduate Research Symposium, Logan, UT.

Jordan, K. E., & **Baker, J. M.** (2010, March). *Redundant visual cues amplify preverbal quantitative skills*. Poster presented the Biennial Meeting of the International Society on Infant Studies, Baltimore, MD.

Baker, J. M. (2010, March). *Improving quantitative competence in infancy and early childhood*. Invited lecture, Cognition & Instruction, Utah State University, Logan, UT.

Jordan, K. E., & **Baker, J. M.** (2009, October). *Does multisensory information improve matching of large numerosities in young children?* Poster presented at the Annual Meeting of the Cognitive Development Society, Chicago, IL.

Baker, J. M., & Jordan, K. E. (2009, April). *Multisensory information boosts numerical matching abilities in pre-school children.* Poster presented at the Biannual Meeting of the Society for Research in Child Development, Denver, Co.

Baker, J. M., & Jordan, K. E. (2008, October). *Multisensory information boosts numerical matching abilities in young children.* Round-table discussion presented at the Annual Meeting of the Northern Rocky Mountain Education Research Association, South Lake Tahoe, NV.

Baker, J.M., & Schmidt, S. (2007, November). *A word choice: The effect of emotion on lexical decision and accuracy.* Poster session presented at the Annual Meeting of the Psychonomics Society, Long Beach, CA.

Baker, J.M., & Schmidt, S. (2006, November). *Lexical pop-out: The effect of emotion on automatic attention to words.* Poster session presented at the Annual Meeting of the Psychonomics Society, Houston, TX.

UNDERGRADUATE MENTORING

Zobell, C.J., Anderson, A.J., Snow, J., Cooper, J., Johnson, B., **Baker, J.M.**, & Bates, S.C. (2013, April). Subjective well-being and working memory as predictors for sales success. Poster presented at the Westeron Psychological Association Conference, Reno, NV.

Jenkins, S., **Baker, J. M.**, Friedel, J., & Jordan, K. E. (2012, April). *Incomplete understanding of large scale numbers in adults*. Poster presented at the annual

Intermountain Undergraduate Research Symposium, Logan, UT.

Clark, D., **Baker, J. M.**, & Jordan, K. E. (2012, March). *Salience of race vs. gender to children and adults*. Poster presented at the National Conference for Undergraduate Research, Ogden, UT.

Clark, D., **Baker, J. M.**, & Jordan, K. E. (2012, January). *Salience of race vs. gender to children and adults*. Poster presented at the Research on Capitol Hill Undergraduate Research Conference, Salt Lake City, UT.

Attwood, N., **Baker, J. M.**, & Jordan, K. E. (2011, April). *Attention restorative effects of differing environments*. Poster presented at the annual meeting to the Rocky Mountain Psychological Association, Salt Lake City, UT.

Feigleson, J., **Baker, J. M.**, & Jordan, K. E. (2010, April). *Attention to social categories across infant development*. Poster presented at the Utah Academy of Sciences, Arts, and Letters, St. George, UT.

Feigleson, J., **Baker, J. M.**, & Jordan, K. E. (2010, March). *Attention to social categories in infants*. Poster presented at the Utah State University Undergraduate Research Symposium, Logan, UT.

TEACHING EXPERIENCE

Graduate Level:

Research Design & Analysis (Psy./Educ. 6600), Instructor of Record, USU:
Fall, 2010
Summer, 2010
Spring, 2009
Research Design & Analysis II (Psy./Educ. 7610), Supplemental Instructor, USU:
Spring, 2011
Fall, 2010

Undergraduate Level:

Introduction to Psychology (Psy. 1010), Instructor of Record, USU:
Spring, 2012
Fall, 2011
Fall, 2010
Perception & Psychophysics (Psy. 3450), Instructor of Record, USU:
Spring, 2011 (online)
Fall, 2010 (online)
Summer, 2010 (online)
Spring, 2010 (online)

Fall, 2009
Cognitive Psychology (Psy. 4420), Instructor of Record, USU:
Spring, 2011

SERVICE TO PROFESSION

Reviewer, Cognitive Development Society Annual Conference, 2011-present
Reviewer, Cognitive Science Society Annual Conference, 2010-present

APPOINTED & ELECTED POSITIONS

Virtual manipulative research group NIRS methodologist and statistician, USU, 2011 – present

Experimental & Applied Psychological Sciences Student Representative, USU, 2008 – 2009

Assistant to Chief Compliance Officer, Middle Tennessee State University, 2006 – 2008

Vice President, Psi Chi, NMSU Chapter, 2004

Public Relations Executive, Psi Chi, NMSU Chapter, 2003-2004

PROFESSIONAL AFFILIATIONS

Cognitive Development Society (2011-Present)
Vision Science Society Member (2010-Present)
Sigma Xi Scientific Research Society Member (2010-Present)
APA Student Affiliate (2008-Present)
Society for Research in Child Development, Graduate Student Member (2008-Present)
Psi Chi, New Mexico State University Chapter (2001-Present)

PROGRAMMING AND TECHNICAL PROFICIENCY

Hitachi ETG-4000 Near-Infrared Spectroscopy
E-Prime Psychological Software
Matlab
R
Visual Basic
NIRS-SPM
SPSS
AMOS